Final Technical Report

"*Isotope Analyses of Hair as a Trace Evidence Tool to Reconstruct Human Movements: Establishing the Effects of the "Human Ecosystem" on Strontium and Oxygen Isotope Ratios*"

2013-DN-BX-K009

Grantee:
IsoForensics Inc.
421 Wakara Way, Suite 100
Salt Lake City, UT 84108

Principal Investigator:
Brett J. Tipple
Tel. 801-851-3545

Project Supervisor:
Lesley A. Chesson
Tel. 801-755-7990

Report submitted:
April 26, 2016

Abstract

Critical advances in isotope mass spectrometry technologies, laboratory methodologies, and spatial modeling have allowed for increased application of oxygen ($^{18}O/^{16}O$) and strontium ($^{87}Sr/^{86}Sr$) isotope analysis of human hair to determine an individual's travel histories and probable region-of-origin. We have established that the $^{18}O/^{16}O$ and $^{87}Sr/^{86}Sr$ ratios of human hair relate to geography, where human hair isotope values are primarily influenced by isotope ratios of municipal waters in which an individual imbibes ($^{18}O/^{16}O$) and bathes ($^{87}Sr/^{86}Sr$). Both the $^{18}O/^{16}O$ and $^{87}Sr/^{86}Sr$ ratios of municipal waters are governed by geography and by the water distribution system in a specific locality.

Many major metropolitan areas within the Western United States acquire their municipal waters from a mix of local groundwater and surface waters as well as waters from distant regions (i.e., transported water). Here, we expanded on our initial work relating tap water and hair isotope values by targeting six major metropolitan test areas of the Western United States with diverse water management practices: Los Angeles-Long Beach-Santa Ana (CA), San Francisco-Oakland-Fremont (CA), Riverside-San Bernardino-Ontario (CA), Phoenix-Mesa-Glendale (AZ), San Diego-Carlsbad-San Marcos (CA), and San Jose-Sunnyvale-Santa Clara (CA). In these regions, we collected tap water and hair samples and analyzed the hydrogen, oxygen, and strontium isotope ratios of these materials. The paired water-hair isotope patterns were related to established water management practices. We found that the isotope ratios of tap water corresponded to the stated water sources and management practices for discrete areas in a given metropolitan area. As expected, the spatial isotopic heterogeneities observed in the isotope values of tap water across a specific metropolitan area were apparent in the isotope values of human hair, but not as sharply defined as seen in the isotope values of the water. Nonetheless, the isotope values of hair corresponded to the isotope values of water in the overall metropolitan areas.

We then expanded on the spatial dynamics of the strontium and oxygen isotope values of water and hair in urban systems by integrating a temporal component. Hair and water were collected and analyzed at a high spatial and temporal resolution within one metropolitan area with diverse, but constrained, water management practices and seasonal water sourcing dynamics: Salt Lake City, UT. Here, we again found that the isotope ratios of tap water corresponded to the stated water sources and management practices for water districts within the Salt Lake City metropolitan area. In addition, we observed seasonal variation in the isotope ratios of tap waters, indicative of changes in water source throughout the sampling interval. Similar to the California and Arizona collections, the spatial isotopic heterogeneities observed in the isotope values of tap water in Salt Lake City were apparent; these heterogeneities were not as visibly defined in the isotope values of human hair of individuals sampled in the same area as compared to those of the water samples. Our findings permit the development of coupled O-Sr isotope ratios of modern human hair as a novel forensic tool in urban settings for determining human region-of-origin.

Table of Contents

Executive Summary

PROBLEM: Isotope analysis has proven valuable to law enforcement for establishing the timeline of geographic movements of unidentified decedents and suspects; yet, in urban environments the isotopic relationships between people and places are multifaceted due to modern infrastructure and population dynamics, confounding the interpretation of isotope analysis in these urban environments.

Reconstructing the geographic-movement of individuals has become important to many forensic investigations. Analysis of stable isotopes recorded in human scalp hair at natural abundance levels has shown to be a useful tool to law enforcement to reconstruct the recent geographic-movement histories of individuals.

Our research firm pioneered the use of oxygen (O) and strontium (Sr) isotope ratios as a forensic tool for determining human region-of-origin. While the use of a single stable isotope provides a valuable law enforcement tool for describing geographical spaces where an individual may have originated, the estimated geographical regions can be broad. With previous NIJ support, we demonstrated that a combined O-Sr isotopic approach using human hair refines region-of-origin predictions. *However, in many urban environments the factors controlling the spatial patterns of both O and Sr isotope ratios may be disrupted due to human infrastructure. Thus, both a theoretical understanding of isotopic variation across landscapes and an appreciation for the built environment and the specific management practices impacting that environment are required to apply the O-Sr isotopic approach in densely populated settings.*

PURPOSE: The combination of O isotope values ($\delta^{18}O$) and Sr isotope ratios ($^{87}Sr/^{86}Sr$) of human hair has been shown to further constrain the estimated regions from which an individual originated. There are two major questions this technology can answer for law enforcement and forensic communities:

1) *Is the individual a resident of the region in which the person was found*?
2) *If not, from what regions could the individual have originated?*

The applications of coupled O and Sr isotope analysis of hair are far-reaching considering the ubiquitous occurrence of human hair at many crime scenes. Specifically, the uses of this technology include, but are not limited to, reconstructing travel histories of unidentified murder victims, reconstructing movements of trans-nationals associated with organized crime syndicates and having uncertain origins and travel histories, and investigating the region-of-origin of exploited women and children transported across state and international boundaries.

The objective of the proposed research is to confirm the hypothesis that $\delta^{18}O$ and $^{87}Sr/^{86}Sr$ ratios can be used together to more precisely describe the region-of-origin of humans through chemical analyses of scalp hair. The goals of this proposed research are to (a) test this overarching hypothesis in complex urban environments with understood

spatial and temporal incongruities (b) build a data product and a model product that would further refine and constrain the region-of-origin predictions. We will accomplish these objectives through data collection and analyses to test three specific hypotheses:

Hypothesis 1.
The strontium and oxygen isotope ratios of municipal waters reflect well-described water management practices, reflecting transported and/or local groundwater sources.

Hypothesis 2.
The strontium and oxygen isotope ratios of human hairs record the water management practices of the municipality in which an individual resides.

Hypothesis 3.
Any seasonal variations in water management practices associated with changes in water source will be reflected in the strontium and oxygen isotope ratios of both municipal waters and human hairs.

RESEARCH DESIGN AND FINDINGS: A series of experiments were designed to meet the research objectives and hypothesis of this program of study.

Experiment 1. To test the hypothesis that geographic variation in the $\delta^{18}O$ values and $^{87}Sr/^{86}Sr$ ratios of water reflect the known variations in water management practices within distinct and important major metropolitan areas in the Western United States:

- San Francisco and surrounding cities in the San Francisco Bay Area
- Los Angeles and surrounding cities in Los Angeles, Riverside, and San Bernardino Counties
- San Diego and surrounding cities in San Diego County
- Phoenix and surrounding cities in Maricopa and Pinal Counties.

We found that the sampled areas had water with distinct $^{87}Sr/^{86}Sr$ ratios and $\delta^{18}O$ values within specific regions. In addition, we found that the isotope ratios of tap water corresponded to the stated water sources and management practices for particular regions in a given metropolitan area. This study laid the foundation to move to *Experiments 2* and *3*. Further, these findings support the concept that isoscape development in urban settings should consider the water management practices employed by local communities.

Experiment 2. To test the hypothesis that spatial variation in the $\delta^{18}O$ values and $^{87}Sr/^{86}Sr$ ratios of water driven by water management practices are transferred to individuals living in these areas. Given the known differences in water management practices in the metropolitan areas sampled for *Experiment 1*, we focused our efforts on the Los Angeles-Long Beach-Santa Ana, San Francisco-Oakland-Fremont, Riverside-San Bernardino-Ontario, Phoenix-Mesa-Glendale, San Diego-Carlsbad-San Marcos, and San Jose-Sunnyvale-Santa Clara areas.

We found that the spatial heterogeneities observed in the isotope values of tap water across a specific metropolitan area were also apparent in the isotope values of human

hair. We found that the isotope values of human hair were less sharply defined by water management practice as seen in the isotope values of the water. The lower geographic definition observed in the isotope values of the hair, particularly with the $\delta^{18}O$ values, are possibly due to the combination of the daily movements of the individuals between regions with isotopically distinct tap waters, consumption of beverages produced outside their region of residence, or visitation to hair salons/barbershops outside their region of residence. These factors may contribute to reducing the spatial fidelity of the isotope ratios of human hair. Nonetheless, we found that the isotope values of hair corresponded to the isotope values of water in the overall metropolitan areas and specific regions within the larger metropolitan areas. These findings suggest that additional population and socioeconomic considerations could inform isotope landscape (isoscape) development. By weighting modeled isotope values to known demographic patterns, error envelopes and distribution functions of predicted isotope values could be further refined.

Experiment 3. To test the hypothesis that both spatial and temporal variation in the $\delta^{18}O$ values and $^{87}Sr/^{86}Sr$ ratios of water are transferred to individuals by sampling both tap water and hair from a single metropolitan area with known water management practices through a seasonal cycle. Here, we focused on the Salt Lake City metropolitan area.

We found that the Salt Lake City metropolitan area had water with distinct $\delta^{18}O$ values and $^{87}Sr/^{86}Sr$ ratios within specific regions. Also, we found that the isotope ratios of tap water corresponded to the stated water sources and management practices for particular water management districts within the Salt Lake City metropolitan area. Finally, we noted temporal patterns in the $\delta^{18}O$ values and $^{87}Sr/^{86}Sr$ ratios of water corresponding to seasonal water switching. We found that the isotope values of human hair were less clearly defined by water management practice than those patterns seen in the isotope values of the water. Further, we noted that the isotope values of the hair lagged the temporal dynamics observed in the isotope values of tap water. This could possibly be due to sampling bias or additionally due to the expected lag between environmental exposure and a subsequent signal in hair cut months to years later.

CONCLUSIONS: We collected over 2500 authentic water and hair specimens and carried out over 3000 isotope analyses on these materials (**Table 1**). This program of study confirmed the hypotheses set forth and showed the $\delta^{18}O$ values and $^{87}Sr/^{86}Sr$ ratios of water were related to the water management practices. Further, this program demonstrated the isotope values of hair from individuals living in regions with diverse water management practices reflected the isotope patterns of the water to which they are exposed. Our findings demonstrate the application of coupled O-Sr isotope ratios of modern human hair as a novel forensic tool in urban settings. The prediction of O and Sr isotope ratios of human hair in urban settings has many potential implications with respect to investigations into human movements and forensic cases.

Introduction

The ability to reconstruct the travel pattern and movement of individuals is an essential tool to criminal investigations. Analysis of light stable isotopes (i.e., oxygen, hydrogen) recorded in human hair has assisted in reconstruction of the geographic-movement histories of individuals. While this state-of-the-art tool has proven valuable to law enforcement, the geographical regions predicted from measured isotope values can be spatially large and undefined. A novel and complementary analysis and prediction approach using human hair would help refine these region-of-origin estimates.

Strontium (Sr) isotope, specifically $^{87}Sr/^{86}Sr$, ratios within organic materials reflect the $^{87}Sr/^{86}Sr$ ratios of the environment in which an organism lives and/or migrates through. Thus, $^{87}Sr/^{86}Sr$ ratios are an additional estimator of an organism's geographic region. Environmental $^{87}Sr/^{86}Sr$ ratios vary geographically as a function of age and the Rb/Sr ratio of the rock or soil type, creating a definable and predictable geographic landscape tool for sourcing a specimen (Beard and Johnson 2000). ^{86}Sr (9.87% abundance) is a stable isotope, while ^{87}Sr (7.04%) is radiogenic produced by the beta decay of ^{87}Rb (Faure 1977).

The $^{87}Sr/^{86}Sr$ ratios of biological materials have been successfully applied to many region-of-origin questions in the fields of archaeology (English et al. 2001, Bentley et al. 2002, Reynolds et al. 2005, Price et al. 2007, von Carnap-Bornheim et al. 2007, Perry et al. 2008, Richards et al. 2008, Knudson et al. 2009, Nehlich et al. 2009, Chenery et al. 2010), ecology (Britton et al. 2009, Sellick et al. 2009, Radloff et al. 2010), food science (Franke et al. 2007, Rodrigues et al. 2010, Rosner 2010, Voerkelius et al. 2010), and forensic science (Lewis and Rutty 2003, Montgomery et al. 2006, Rauch et al. 2007, Juarez 2008, West et al. 2009). These studies indicate that the $^{87}Sr/^{86}Sr$ ratios of internal organism tissues reflect the $^{87}Sr/^{86}Sr$ ratios of water and diet during the time period(s) when the biological materials formed. In contrast, exposed tissues (i.e., hair, horns, nails, etc.) record the $^{87}Sr/^{86}Sr$ ratios of contamination from the external environment (i.e., dust and aerosols).

Sr contained within newly formed hair initially reflects water and food sources of the individual; once the hair segment protrudes from the follicle, the hair $^{87}Sr/^{86}Sr$ ratios changes (Gellein et al. 2008). As hair is exposed to the external environment and detached from the animal's metabolism, the Sr concentration within hair increases with exposure time, reflecting continuous inputs of dust and aerosol particles into the external hair matrix (Gellein et al. 2008). This externally-sourced Sr is embedded within the keratin sheets of hair and not easily removed by bathing or washing (Chittleborough 1980).

While the initial results of $^{87}Sr/^{86}Sr$ ratios in human hair as geographic recorders are promising, the use of $^{87}Sr/^{86}Sr$ ratios in hair to reconstruct an individual's travel history presents a unique set of analytical and theoretical challenges as humans significantly modify their "ecosystem" through the use of transported waters. Thus, individuals that drink/bathe with waters transported from distant regions will have isotope values inconsistent with local hydroclimatic and geologic isotopic signals. These geospatial

disconnections imparted on an individual's "ecosystem" are transferred to the individual's hair and invalidate straightforward isotopic relationships and models.

Previous support from NIJ allowed us to establish fundamental linkages between the $\delta^{18}O$ and $^{87}Sr/^{86}Sr$ of tap water and hair ratios for many US cities. However, municipal water management practices strongly affect the $\delta^{18}O$ and $^{87}Sr/^{86}Sr$ of residential water in cities with transported water, which appear to be recorded in human hair. In this study, we sought to understand the impacts of management of municipal waters for the development of strontium isoscapes and refinements to the $\delta^{18}O$ and $^{87}Sr/^{86}Sr$ isoscape projection for the US.

The objective of the proposed research is to test the overarching hypothesis that $\delta^{18}O$ and $^{87}Sr/^{86}Sr$ ratios can be used together as a diagnostic tool to more precisely describe the recent region-of-origin of humans through chemical analyses of scalp hair. The goals of this proposed research are to (a) confirm this hypothesis and (b) build a data product and a model product that would further refine and constrain the region-of-origin predictions based on $\delta^{18}O$ and $^{87}Sr/^{86}Sr$. We will accomplish these objectives through data collection and analyses to test three specific hypotheses:

Hypothesis 1.
The strontium and oxygen isotope ratios of municipal waters reflect well-described water management practices, reflecting transported and/or local groundwater sources.

Hypothesis 2.
The strontium and oxygen isotope ratios of human hairs record the water management practices of the municipality in which an individual resides.

Hypothesis 3.
Any seasonal variations in water management practices associated with changes in water source will be reflected in the strontium and oxygen isotope ratios of both municipal waters and human hairs.

Methods

Experiments

Experiment 1. Investigating the impacts of water distribution networks on the isotope ratio of tap water

To test the isotopic impacts of transported water supplies within managed water distribution systems, tap water samples were collected from six major metropolitan regions with known diverse water supplies. Oxygen, hydrogen, and strontium isotope ratios of tap waters were measured and related to known water management practices.

Experiment 2. Examining the relationship between water and human hair isotopes values in complex urban systems

To assess the linkages between water and hair isotope ratios, hair samples were collected and paired with water samples from six major metropolitan regions with known diverse water supplies. Oxygen and strontium isotope ratios of hair samples were measured and related to the isotope ratios of the measured waters.

Experiment 3. Exploring the temporal dynamics of managed water supplies and the effects on the population

To evaluate the temporal dynamics of transported water supplies on urban populations, tap water and hair samples were collected from a single metropolitan region with known water management practices through a seasonal cycle. The relationships between water and hair isotope signatures through time were evaluated with oxygen and strontium isotope ratios.

Samples

Experiment 1

Water samples were collected from public building taps throughout the Los Angeles-Long Beach-Santa Ana (CA), San Francisco-Oakland-Fremont (CA), Riverside-San Bernardino-Ontario (CA), Phoenix-Mesa-Glendale (AZ), San Diego-Carlsbad-San Marcos (CA), and San Jose-Sunnyvale-Santa Clara (CA) metropolitan areas. A total of one thousand four hundred forty-nine water samples were collected from these six metropolitan areas. Of these, one thousand three hundred seventy-nine and two hundred seventy-three specimens were analyzed for oxygen and hydrogen isotope value and strontium isotope ratio, respectively. Three hundred twenty water samples were measured for oxygen and hydrogen isotopes from the Phoenix-Mesa-Glendale metropolitan area on two trips (Spring 2014 and Fall 2014). Of these Phoenix-Mesa-Glendale samples, forty-seven were analyzed for strontium isotope ratios. Seven hundred twenty-four waters were measured from the San Francisco-Oakland-Fremont and San Jose-Sunnyvale-Santa Clara metropolitan areas on seven trips (Winter 2013/2014, Spring 2014, Summer 2014, Fall 2014, Winter 2014/2015, Spring 2015, and Summer 2015). From the San Francisco-Oakland-Fremont and San Jose-Sunnyvale-Santa Clara metropolitan areas, one hundred fifty-one water samples were analyzed for strontium isotope ratios. One hundred sixty-two water samples were measured for oxygen and hydrogen isotopes from the Los Angeles-Long Beach-Santa Ana and Riverside-San Bernardino-Ontario metropolitan areas on three trips (Winter 2013/2014, Spring 2014 and Fall 2014). Of these Los Angeles-Long Beach-Santa Ana and Riverside-San Bernardino-Ontario samples, forty were analyzed for strontium isotope ratios. Ninety-three waters were measured from the San Diego-Carlsbad-San Marcos metropolitan area on two trips (Winter 2013/2014 and Spring 2014). From the San Diego-Carlsbad-San Marcos metropolitan area, thirty-five samples were analyzed for strontium isotope ratios. During subsequent visits to a metropolitan area, the initial sampling location was revisited and the water sample was collected from the same tap. If an initial sampling location was closed or inaccessible during a subsequent visit, a new nearby location was selected and substituted for the

initial sampling location. On any subsequent sampling trip, waters were sampled from both the initial and any substituted sampling location.

Experiment 2.

We randomly collected discarded hair from the floors of barbershops throughout each metropolitan area. A total of three hundred eighty-two hair samples were collected. Of these, one hundred sixty and one hundred thirty-six hair specimens were analyzed for oxygen isotope value and strontium isotope ratio, respectively. Thirty-five hair samples were measured for oxygen and strontium isotopes from the Phoenix-Mesa-Glendale metropolitan area on two trips (Spring 2014 and Fall 2014). Sixty-nine hair samples were measured for oxygen and strontium isotope values from the San Francisco-Oakland-Fremont and San Jose-Sunnyvale-Santa Clara metropolitan areas on two trips (Winter 2013/2014, Spring 2014). Twenty-six hair samples were measured for oxygen isotopes from the Los Angeles-Long Beach-Santa Ana and Riverside-San Bernardino-Ontario metropolitan areas on two trips (Spring 2014 and Fall 2014). Of these Los Angeles-Long Beach-Santa Ana and Riverside-San Bernardino-Ontario samples, two were analyzed for strontium isotope ratios given lack of spatial coverage. The oxygen and strontium isotope ratios of thirty hair samples were measured from the San Diego-Carlsbad-San Marcos metropolitan area on a single trip (Spring 2014). During subsequent visits to a metropolitan area, the initial sampling location was revisited. If an initial sampling location was closed or inaccessible during a subsequent visit, a new nearby location was selected and substituted for the initial sampling location.

Experiment 3.

Water samples were collected from public building taps throughout the Salt Lake Valley, Utah. Approximately forty water samples were collected from fourteen water districts nine times over 1¾ seasonal cycles to capture temporal variations. Waters from the Salt Lake City metropolitan area were sampled in the Fall 2013, Winter 2013/2014, Spring 2014, Summer 2014, Summer 2014, Fall 2014, Winter 2014/2015, and Spring 2015. A total of four hundred ninety-three water samples were collected. Of these, four hundred seventy-seven water samples were analyzed for oxygen and hydrogen isotopes and three hundred ninety-two were analyzed for strontium isotope ratio, respectively. During subsequent visits to collection location, the initial sampling site was revisited and the water sample was collected from the same tap. If an initial sampling site was closed or inaccessible during a subsequent visit, a new nearby site was selected and substituted for the initial sampling site. On any subsequent sampling trip, waters were sampled from both the initial and any substituted sampling location.

We randomly collected discarded hair from the floors of predominately national chain barbershops throughout the Salt Lake Valley, Utah. Hair samples from the Salt Lake City metropolitan area were sampled in the Winter 2013/2014, Spring 2014, Summer 2014, and Winter 2014/2015. A total of two hundred twenty-seven hair samples were collected. Of these, one hundred thirty hair samples were analyzed for oxygen and hydrogen isotopes and eighty-two were analyzed for strontium isotope ratio, respectively.

Water collections

Experiments 1 and 3.

Water samples were collected in acid-leached low-density polyethylene (LDPE) bottles. Prior to collection, the cold water tap was opened and allowed to run for 10 sec. Samples were sealed and stored in the dark at 10° C prior to analysis.

Hair collections

Experiments 2 and 3.

Hair samples were collected in paper coin envelopes. No information was collected regarding the identification and/or origins of the individuals from which discarded hair samples were obtained. We assumed that these individuals were residents of the city in which the hair sample was collected and that they had no significant dietary differences. Since original collection date, envelopes had been stored at room temperature and in the dark.

Hair cleaning

Experiments 2 and 3.

Hair samples were cleaned in a variety of polar and acidic reagents to remove any external contamination. To remove lipids, residues, and surface contaminates, subsamples (~100 mg) of each hair sample were cleaned using a modified International Atomic Energy Agency (IAEA)-recommended (Druyan et al. 1998) cleaning procedure. Specifically, we followed the modified IAEA hair-washing methodology with an additional wash of 0.1 M HCl. Hair was rinsed successively in acetone, water, again in acetone, and finally 0.1 M HCl for 10 min each. Following each step, the solute was decanted into a centrifuge tube to combine all solutes from each cleaning step. Cleaned hair samples were allowed to dry at room temperature within a laminar flow hood. Subsamples of each hair sample were also collected and left untreated as a control for cleaning methods.

All acetone and hydrochloric acid used in hair cleaning were HPLC grade. The ultrapure water used for sample cleaning and acid dilutions was from a Milli-Q Academic A10® system (EMD Millipore; Billerica, Massachusetts, USA) with a resistivity >18 MΩ.

Sample preparation for hydrogen and oxygen isotope analysis of water

A 500-µl aliquot of water was transferred from the parent container into a clean 2-ml glass autosampler vial. The vial was sealed with an autosampler lid with a Teflon®-lined septum. Water samples were analyzed immediately following placement in autosampler vials.

Hydrogen and oxygen isotope analysis of water

The stable isotope abundances of water samples were analyzed on a Picarro model L1102-i water analyzer. Each sample was analyzed four times (four consecutive replicate injections) alongside a set of three laboratory reference materials, which had previously been calibrated to the VSMOW-SLAP international isotope scale. Sets included two primary laboratory reference materials for slope/intercept normalization and a secondary laboratory reference material for quality assurance and quality control (QA/QC). Using delta notation, stable isotope ratios for oxygen and hydrogen are calculated as: $\delta = [(R_{samp}/R_{std})\text{-}1]$, where R represents the $^{2}H/^{1}H$ or $^{18}O/^{16}O$ abundance ratio, and R_{samp} and R_{std} are the ratios in the sample and standard, respectively. $\delta^{2}H$ and $\delta^{18}O$ values are expressed relative to the standard Vienna Standard Mean Ocean Water (VSMOW) and expressed in parts per thousand (‰).

Sample preparation for hydrogen and oxygen isotope analysis of hair

The hair sample was ground into a homogeneous, fine powder, using a RETSCH MM301 mixer mill. Because there is partial isotopic exchange of H atoms in keratin with water (either in liquid or vapor form), all samples were analyzed together with hair reference materials for which the $\delta^{2}H$ value of nonexchangeable H atoms had been determined. Both reference materials and unknown hairs were allowed to equilibrate with water vapor in the laboratory atmosphere for a minimum of 48 hours before being weighed (150 μg) in silver capsules; weighed samples were stored under vacuum for 5 days before being analyzed. Measured values for the reference materials were then used to determine the nonexchangeable H isotope ratios of the samples from the measured values and isotope mass balance.

Oxygen isotope analysis of hair

The stable oxygen isotope abundances of hair samples were analyzed on a Thermo Finnigan MAT 253 isotope ratio mass spectrometer. Samples were introduced to the instrument via a zero-blank autosampler attached to a high temperature conversion elemental analyzer (TC/EA). Samples were analyzed alongside sets of reference materials for data normalization. Sets included two primary laboratory reference materials for slope/intercept normalization and a secondary laboratory reference material for QA/QC. $\delta^{18}O$ values are expressed relative to the standard VSMOW and expressed in parts per thousand (‰).

Sample preparation for strontium isotope analysis

Hair samples were digested using an Ethos EZ® SK-10 High Pressure Rotor microwave digestion system (Milestone, Inc.; Shelton, Connecticut, USA). Approximately 50-70 mg of hair was weighed into a Teflon® digestion microvessel. Two milliliters of concentrated ultrapure HNO_3 (Aristar® ULTRA; BDH Chemical, Darmstadt, Germany) were added to

the microvessel containing the hair. The microvessel was then sealed and submerged inside a 100-ml Teflon® digestion vessel containing 10 ml of milli-Q water and 50 µl H_2O_2 (30% v/v). The digestion vessel was then placed in the digester rotor segment and tightened to specified torque. Following the principle of identical treatment, two certified reference materials (TORT-2 Lobster Hepatopancreas Reference Material for Trace Metals from the National Research Council Canada and Human Hair No. 13 from the National Institute for Environmental Studies) and a method blank were digested along with the hair samples. The microwave program used for hair digestion was 13.3°C/min ramp to 200°C, followed by an isothermal at 200°C for 15 min with a 60 min cool down to room temperature. The microwave was operated at full power (1500 W) for all heating cycles. Once cooled to room temperature, the hair digests were transferred to acid-leached 2-ml snap-cap centrifuge tubes for strontium isotope analysis. A 100-µl aliquot of the primary hair digest was transferred to a 15-ml tube and the volume was brought to 10 ml with 2.4% ultrapure HNO_3 for strontium abundance analysis.

Strontium abundance and isotope analysis

The strontium elemental abundances were measured via inductively coupled plasma quadrupole-mass spectrometry (ICP-MS) on an Agilent 7500ce instrument (Agilent Technologies; Santa Clara, California, USA) at the ICP-MS Metals Lab in the Department of Geology & Geophysics at the University of Utah, Salt Lake City, Utah, USA. A double-pass spray chamber with perfluoroalcoxy fluorocarbon (PFA) nebulizer (0.1 mL/min), a quartz torch, and nickel cones were used. A calibration solution containing Sr was prepared gravimetrically using a single-element standard (Inorganic Ventures, Inc.; Christiansburg, Virginia, USA). Standard reference solution T-205 (USGS; Reston, Virginia, USA) was measured as an external calibration standard at least five times within each analytical sequence. The long-term reproducibility for T-205 and differences relative to the accepted values indicated that the Sr concentrations were accurate within 10%.

Strontium in hair digests and water samples was isolated with a prepFAST auto-dilution system (Elemental Scientific; Omaha, Nebraska, USA) using an in-line separation column packed with crown ether Sr resin (Eichrom Technologies; Lisle, Illinois, USA). Following isolation, all strontium isotope measurements were made using a Neptune *Plus* multi-collector ICP-MS (ThermoFisher Scientific; Bremen, Germany) housed in the Department of Geology & Geophysics at the University of Utah, Salt Lake City, Utah, USA. The instrument was operated at an RF power of 1200 W with nickel sampling and skimmer cones (1.1 mm and 0.8 mm apertures, respectively). The cool, auxiliary, and sample gas flow rates were optimized daily for signal intensity and stability with a solution containing 20 ppb Sr. For $^{87}Sr/^{86}Sr$ analysis, a static multi-collector routine was used that consisted of 1 block of 170 cycles with an integration time of 1.032 sec per cycle for an individual analysis. Each analysis was followed by a blank to monitor the efficiency of the crown ether Sr resin column. Sr isotope ratios of samples and references were blank- and interference-corrected and then normalized for instrumental mass discrimination using a defined $^{87}Sr/^{86}Sr$ of 0.1194.

Solutions of the international Sr standard reference material SRM 987 (National Institute of Standards and Technology; Gaithersburg, Maryland, USA) were analyzed with samples. The ratio of samples to standards within a single analytical sequence was 5:1. Within-run reproducibility of SRM 987 was 0.71030 ± 0.00004 (2σ, *n* = 92). The long-term mean $^{87}Sr/^{86}Sr$ of SRM 987 analyzed using the automated purification method and MC-ICP-MS at concentrations of hair and leachate measurements was 0.71027 ± 0.00004 (2σ, *n* = 292).

Results

Experiment 1.

We observed ranges in δ^2H, $\delta^{18}O$, and $^{87}Sr/^{86}Sr$ ratios of tap water from all sampling location of between -107 to -9‰, -14.4 to -1.2‰, and 0.70538 to 0.71325, respectively (**Figures 1** and **2**).

Table 2 provides the summary statistics for water analyzed from the Phoenix-Mesa-Glendale metropolitan area (hereafter, PHX metro area). In the PHX metro area, 320 water samples were measured for δ^2H and $\delta^{18}O$ values with an average value of -79‰ and -10.0‰, respectively. δ^2H and $\delta^{18}O$ values of PHX tap waters ranged between -104 to -33‰ and -13.0 to -3.7‰, respectively (**Figure 3**). Of these PHX tap waters, 47 were analyzed for $^{87}Sr/^{86}Sr$ with an average value of 0.71074 and range of 0.70802 to 0.71325 (**Figure 4**). **Figures 5** and **6** display the spatial coverage and variation of the $\delta^{18}O$ values and $^{87}Sr/^{86}Sr$ ratios, respectively, of tap waters measured from the PHX metro area. We observed the most negative $\delta^{18}O$ values in the northern and eastern PHX regions, while the most positive $\delta^{18}O$ values are observed in central PHX (**Figure 5**). In addition, we found the lowest $^{87}Sr/^{86}Sr$ ratios of tap water in the southwestern and western regions and the highest $^{87}Sr/^{86}Sr$ ratios of tap water in the southeastern and southern regions of the PHX metro area (**Figure 6**). **Figure 7** is a cross-plot of the $\delta^{18}O$ and $^{87}Sr/^{86}Sr$ of tap waters from regions within the PHX area. We find that tap waters from specific regions within the PHX have unique combinations of $\delta^{18}O$ and $^{87}Sr/^{86}Sr$ values (**Figure 7**). **Table 3** provides the water sources for the cities within the PHX metro area.

Table 4 provides the summary statistics for water analyzed from the San Francisco-Oakland-Fremont and San Jose-Sunnyvale-Santa Clara metropolitan areas (hereafter, SFB metro area). In the SFB metro area, 724 water samples were measured for δ^2H and $\delta^{18}O$ values with an average value of -69‰ and -9.3‰, respectively. δ^2H and $\delta^{18}O$ values of SFB tap waters ranged between -107 to -9‰ and -14.4 to -1.5‰, respectively (**Figure 8**). Of these SFB tap waters, 151 were analyzed for $^{87}Sr/^{86}Sr$ with an average value of 0.70701 and range of 0.70538 to 0.70882 (**Figure 9**). **Figures 10** and **11** display the spatial coverage and variation of the $\delta^{18}O$ and $^{87}Sr/^{86}Sr$ of tap waters measured from the SFB metro area. We observed the most negative $\delta^{18}O$ values in the City and County of San Francisco and in the Peninsula, while the most positive $\delta^{18}O$ values are observed in Marin County (**Figure 10**). We found the lowest $^{87}Sr/^{86}Sr$ ratios of tap water in Marin County and the highest $^{87}Sr/^{86}Sr$ ratios of tap water in the City and County of San Francisco and in the Peninsula (**Figure 11**). **Figure 12** is a cross-plot of the $\delta^{18}O$ and

$^{87}Sr/^{86}Sr$ of tap waters from regions within the SFB area. We find that tap waters from specific regions within the SFB have somewhat unique combinations of $\delta^{18}O$ and $^{87}Sr/^{86}Sr$ values (**Figure 12**). We find the $\delta^{18}O$ of tap water within the SFB area have more geographic variation than the $^{87}Sr/^{86}Sr$ values. **Tables 5** and **6** provide the water sources for the cities within the SFB metro area.

Table 7 provides the summary statistics for water analyzed from the Los Angeles-Long Beach-Santa Ana and Riverside-San Bernardino-Ontario metropolitan areas (hereafter, LA metro area). In the LA metro area, 242 water samples were measured for $\delta^{2}H$ and $\delta^{18}O$ values with an average value of -66‰ and -9.2‰, respectively. $\delta^{2}H$ and $\delta^{18}O$ values of LA tap waters ranged between -102 to -41‰ and -12.4 to -5.3‰, respectively (**Figure 13**). Of these LA tap waters, 40 were analyzed for $^{87}Sr/^{86}Sr$ with an average value of 0.71071 and range of 0.70758 to 0.71304 (**Figure 14**). **Figures 15** and **16** display the spatial coverage and variation of the $\delta^{18}O$ and $^{87}Sr/^{86}Sr$ of tap waters measured from the LA metro area. We observed the most negative $\delta^{18}O$ values in Los Angeles County, while the most positive $\delta^{18}O$ values are observed in Riverside County (**Figure 15**). We found the lowest $^{87}Sr/^{86}Sr$ ratios of tap water in Los Angeles and San Bernardino Counties and the highest $^{87}Sr/^{86}Sr$ ratios of tap water in Riverside County (**Figure 16**). **Figure 17** is a cross-plot of the $\delta^{18}O$ and $^{87}Sr/^{86}Sr$ of tap waters from regions within the LA area. We find that tap waters from specific regions within the LA have somewhat unique combinations of $\delta^{18}O$ and $^{87}Sr/^{86}Sr$ values (**Figure 17**). **Tables 8** and **9** provide the water sources for the cities within the LA metro area.

Table 10 provides the summary statistics for water analyzed from the San Diego-Carlsbad-San Marcos metropolitan area (hereafter, SD metro area). In the SD metro area, 93 water samples were measured for $\delta^{2}H$ and $\delta^{18}O$ values with an average value of -86‰ and -10.5‰, respectively. $\delta^{2}H$ and $\delta^{18}O$ values of SD tap waters ranged from -97 to -24‰ and from -12.1 to -1.2‰, respectively (**Figure 18**). Of these SD tap waters, 35 were analyzed for $^{87}Sr/^{86}Sr$ with an average value of 0.70989 and range of 0.70613 to 0.71064 (**Figure 19**). **Figures 20** and **21** display the spatial coverage and variation of the $\delta^{18}O$ and $^{87}Sr/^{86}Sr$ of tap waters measured from the SD metro area. We observed the most negative $\delta^{18}O$ values throughout the central, eastern and northern regions of the SD metro area, while the most positive $\delta^{18}O$ values are observed in south San Diego (**Figure 20**). We found the lowest $^{87}Sr/^{86}Sr$ ratios of tap water in the North County of San Diego and the highest $^{87}Sr/^{86}Sr$ ratios of tap water throughout the central, eastern and northern regions of the SD metro area (**Figure 21**). **Figure 22** is a cross-plot of the $\delta^{18}O$ and $^{87}Sr/^{86}Sr$ of tap waters from regions within the SD metro area. **Table 11** provides the water sources for the cities within the SD metro area.

Experiment 2.

Table 12 provides the summary statistics for hair samples analyzed from the PHX metro area. In the PHX metro area, 35 hair samples were measured for $\delta^{18}O$ values with an average value of 12.0‰ (**Figure 23**). $\delta^{18}O$ values of PHX hair ranged from 9.3 to 13.7‰ (**Table 12**). In the PHX metro area, 35 hair samples were analyzed for $^{87}Sr/^{86}Sr$ with an

average value of 0.71080 and range of 0.70849 to 0.71334 (**Figure 24**). **Figures 25** and **26** display the spatial coverage and variation of the $\delta^{18}O$ values and $^{87}Sr/^{86}Sr$ ratios of hair measured from the PHX metro area. We observed the lowest $\delta^{18}O$ values in the northern and western PHX regions, while the highest $\delta^{18}O$ values are observed in central and southeastern PHX (**Figure 25**). In addition, we found the lowest $^{87}Sr/^{86}Sr$ ratios of hair in the southwestern and western regions and the highest $^{87}Sr/^{86}Sr$ ratios of hair in the southeastern and central regions of the PHX metro area (**Figure 26**). **Figure 27** is a cross-plot of the $\delta^{18}O$ and $^{87}Sr/^{86}Sr$ of hair from regions within the PHX area.

Table 13 provides the summary statistics for hair samples analyzed from the SFB metro area. In the SFB metro area, 69 hair samples were measured for $\delta^{18}O$ values with an average value of 11.9‰ (**Figure 23**). $\delta^{18}O$ values of SFB hair samples ranged from 8.3 to 14.8‰ (**Table 13**). All 69 hair samples were analyzed for $^{87}Sr/^{86}Sr$ with an average value of 0.70740 and range of 0.70660 to 0.70923 (**Figure 28**). **Figures 29** and **30** display the spatial coverage and variation of the $\delta^{18}O$ and $^{87}Sr/^{86}Sr$ of hair samples measured from the SFB metro area. We observed the lowest $\delta^{18}O$ values in the City and County of San Francisco and in the Peninsula, while the highest $\delta^{18}O$ values were observed in Marin County (**Figure 29**). We found the lowest $^{87}Sr/^{86}Sr$ ratios of hair in Marin County and the highest $^{87}Sr/^{86}Sr$ ratios of hair in the City and County of San Francisco and in the Peninsula (**Figure 30**). **Figure 31** is a cross-plot of the $\delta^{18}O$ and $^{87}Sr/^{86}Sr$ of hair from regions within the SFB area.

Table 14 provides the summary statistics for hair samples analyzed from the LA metro area. In the LA metro area, 26 hair samples were measured for $\delta^{18}O$ values with an average value of 11.9‰ (**Figure 23**). $\delta^{18}O$ values of LA hair ranged from 9.0 to 16.4‰, respectively (**Table 14**). Of these LA hair samples, two were analyzed for $^{87}Sr/^{86}Sr$ with an average value of 0.70884 (**Figure 32**). **Figure 33** displays the spatial coverage and variation of the $\delta^{18}O$ of hair samples measured from the LA metro area. We observed the lowest $\delta^{18}O$ values in the Riverside County, while the highest $\delta^{18}O$ values are observed in Los Angeles County (**Figure 33**).

Table 15 provides the summary statistics for hair samples analyzed from the SD metro area. In the SD metro area, 30 hair samples were measured for $\delta^{18}O$ values with an average value of 11.9‰ (**Figure 23**). $\delta^{18}O$ values of SD hair samples ranged from 8.6 to 14.0‰, (**Table 15**). All hair samples were analyzed for $^{87}Sr/^{86}Sr$ with an average value of 0.71020 and range of 0.70954 to 0.71039 (**Figure 34**). **Figures 35** and **36** display the spatial coverage and variation of the $\delta^{18}O$ and $^{87}Sr/^{86}Sr$ of human hair measured from the SD metro area. We observed the lowest $\delta^{18}O$ values in central SD, while the highest $\delta^{18}O$ values are observed in south San Diego (**Figure 35**). We found the lowest $^{87}Sr/^{86}Sr$ ratios of hair in East County and the highest $^{87}Sr/^{86}Sr$ ratios of hair throughout the Central San Diego and North County regions of the SD metro area (**Figure 36**). **Figure 37** is a cross-plot of the $\delta^{18}O$ and $^{87}Sr/^{86}Sr$ of hair from regions within the SD metro area.

Experiment 3.

Table 16 provides the summary statistics for water analyzed from the Salt Lake City metropolitan area (hereafter, the SLV metro area). We observed ranges in δ^2H, $\delta^{18}O$, and $^{87}Sr/^{86}Sr$ ratios of tap water of between -130 to -95‰, -17.9 to -11.0‰, and 0.70840 to 0.71573, respectively (**Figures 38** and **39**). In the SLV metro area, 477 water samples were measured for δ^2H and $\delta^{18}O$ values with an average value of -120‰ and -15.8‰, respectively. Of these SLV tap waters, 392 were analyzed for $^{87}Sr/^{86}Sr$ with an average value of 0.71078. **Figure 40** is a series of cross-plots of the $\delta^{18}O$ and $^{87}Sr/^{86}Sr$ of tap waters from regions within the SLV area throughout the sampling interval. **Table 17** provides the water sources for the water districts within the SLV metro area. We observed the most negative $\delta^{18}O$ values in the areas supplied by the Salt Lake City Corporation, while the most positive $\delta^{18}O$ values are observed in areas serviced by Magna Water Improvement District (**Figure 40**). In addition, we found the lowest $^{87}Sr/^{86}Sr$ ratios of tap water in areas supplied by the Salt Lake City Corporation and the highest $^{87}Sr/^{86}Sr$ ratios of tap water in areas supplied by Murray City and Salt Lake City Corporation (**Figure 40**). We find that tap waters from several water districts within the SLV have unique combinations of $\delta^{18}O$ and $^{87}Sr/^{86}Sr$ values (**Figure 40**) and these combinations vary seasonally.

Table 18 provides the summary statistics for hair samples analyzed from the SLV metro area. We observed ranges $\delta^{18}O$, and $^{87}Sr/^{86}Sr$ ratios of hair of 6.0 to 12.7‰, and 0.70941 to 0.71399, respectively. In the SLV metro area, 130 hair samples were measured for $\delta^{18}O$ values with an average value of 9.4‰ (**Figure 41**). In the SLV metro area, 82 hair samples were analyzed for $^{87}Sr/^{86}Sr$ with an average value of 0.71070 (**Figure 42**). **Figure 43** is a series of cross-plots of the $\delta^{18}O$ and $^{87}Sr/^{86}Sr$ of hair samples from regions within the SLV area throughout the sampling interval. We observed the lowest $\delta^{18}O$ values of human hair in the areas with water supplied by the Murray City Water System, while the highest $\delta^{18}O$ values are observed in areas serviced by the Salt Lake City Corporation (**Figure 43**). In addition, we found the lowest $^{87}Sr/^{86}Sr$ ratios of hair in areas with water supplied by the Salt Lake City Corporation and the highest $^{87}Sr/^{86}Sr$ ratios of hair in areas with water supplied by Murray City (**Figure 43**). We find that hair samples from specific regions within the SLV have unique combinations of $\delta^{18}O$ and $^{87}Sr/^{86}Sr$ values (**Figure 43**).

Discussion and Conclusions

Experiment 1.

In *Experiment 1*, we sought to examine tap waters from highly urbanized areas that use diverse and isotopically distinct water supplies. Here, we sampled tap waters from the PHX, SFB, LA, and SD urban regions and measured the δ^2H values, $\delta^{18}O$ values, and $^{87}Sr/^{86}Sr$ ratios of these municipal waters. **Tables 3**, **5**, **6**, **8**, **9**, and **11** show the water sources from these four urban regions comprising of six metropolitan areas. These six metropolitan areas use well-documented combinations of transported waters and local surface and/or groundwater.

Table 3 provides the water sources for the cities within the PHX metro area. The main water sources used in the PHX area include waters from the Colorado River via the Central Arizona Project aqueduct, various groundwater aquifers, and several local rivers. We found PHX tap waters had a relatively large range in the $^{87}Sr/^{86}Sr$ ratios. This large range in $^{87}Sr/^{86}Sr$ ratios of tap waters was observed in regions and cities using exclusively groundwater sources. These include cities in the South, Southeast, and Southwest (**Figure 7**). Further, we observed little variation in $\delta^{2}H$ values, $\delta^{18}O$ values and $^{87}Sr/^{86}Sr$ ratios of tap waters from regions and cities using exclusively or large proportions of Colorado River water. These regions include the Central, Northeast, Northwest, and East (**Figure 7**). These $\delta^{2}H$, $\delta^{18}O$, and $^{87}Sr/^{86}Sr$ values of tap water observed in the PHX area are consistent with the water sources stated in the local municipalities' consumer confidence reports.

Tables 5 and **6** show the water sources for the cities within the SFB metro area. The water sources used in the SFB regions include local groundwater, local surface waters, and transported surface waters from the Coastal and Sierra Nevada Mountains. The major water providers in the SFB area, except those in Marin County, predominately supply waters sourced from several watersheds in the western Sierra Nevada Mountains. Marin County is unique in the region as water providers there predominately supply waters from the Coastal Range and local reservoirs. When compared to the other urban regions in this study, the SFB area had a relatively narrow range of $^{87}Sr/^{86}Sr$ values of tap water (**Figure 12**). This is likely due to similar bedrock lithologies underlying the various Sierra Nevada and Coastal Range watersheds. Given the large difference in watershed elevation and precipitation type, there is a large difference in the $\delta^{2}H$ and $\delta^{18}O$ values of tap water between the regions using predominately Sierra Nevada- vs. Coastal Range-derived waters (**Figure 12**). Regions using predominately Sierra Nevada-derived water include San Francisco and the Peninsula, while Marin County uses Coastal Range-derived waters. The areas of East Bay and South Valley use more diverse water sources and also mix waters from various sources. This is likely the reason for the intermediate $\delta^{2}H$ and $\delta^{18}O$ values of tap waters observed in these areas (**Figure 12**). Nonetheless, the $\delta^{2}H$, $\delta^{18}O$, and $^{87}Sr/^{86}Sr$ values of tap water observed in the SFB area are consistent with the water sources stated in the local municipalities' consumer confidence reports.

The water sources for the three regions in the LA metro area are shown in **Tables 8** and **9**. The main water sources used in the LA area include waters from the Colorado River via the Colorado River Aqueduct, waters from Northern California via the California Aqueduct, waters from the Eastern Sierra Nevadan Owen and Mono Lake watersheds via the Los Angeles Aqueduct, and various local groundwater aquifers. We found LA tap waters had a large range in the $^{87}Sr/^{86}Sr$ ratios, with a similar range to the PHX area (**Figure 17**). Given the large difference in elevation and distance from the coast to watersheds that provide water to the LA area, there is a large difference in the $\delta^{2}H$ and $\delta^{18}O$ values of tap water (**Figure 17**). Further, we observed $\delta^{2}H$, $\delta^{18}O$ and $^{87}Sr/^{86}Sr$ ratios of tap waters from Los Angeles County have similar values as those observed in the PHX area (**Figure 7**). These values are consistent with regions that use large proportions of Colorado River water. These $\delta^{2}H$, $\delta^{18}O$, and $^{87}Sr/^{86}Sr$ values of tap water observed in the

LA area are consistent with the water sources stated in the local municipalities' consumer confidence reports.

Tap water in SD metro area is predominately sourced from the Colorado River via the Colorado River and the San Diego Aqueducts, as well as minor contributions from waters in Northern California via the California Aqueduct, and local groundwater (**Table 11**). The majority of tap waters collected and measured from the SD area have δ^2H, $\delta^{18}O$ and $^{87}Sr/^{86}Sr$ ratios of tap waters (**Figure 22**) similar to those values observed in the PHX and LA areas (**Figures 7** and **17**). All samples collected from Central San Diego have values in this range. In the areas outside of the Central region, more variation in the δ^2H, $\delta^{18}O$ and $^{87}Sr/^{86}Sr$ ratios of tap waters are observed (**Figure 22**). These include a collection of data points indicative of desalinated brackish groundwater in South San Diego and fresh groundwater in North County San Diego (**Figure 22**). These δ^2H, $\delta^{18}O$, and $^{87}Sr/^{86}Sr$ values of tap water observed in the SD area are consistent with the water sources stated in the local municipalities' consumer confidence reports.

Our findings from *Experiment 1* demonstrated that water management practices clearly influence the isotopic composition of tap waters available to urban populations. We found that not only did metropolitan areas studied in *Experiment 1* have δ^2H, $\delta^{18}O$, and $^{87}Sr/^{86}Sr$ values of tap water that corresponded to the water sources known to be used in each metropolitan area, but that discrete regions within these metropolitan areas used only specific waters. These results indicate that specific regions within each of the metropolitan areas have unique combinations of δ^2H, $\delta^{18}O$, and $^{87}Sr/^{86}Sr$ values of tap water. These findings support the hypothesis that the strontium and oxygen isotope ratios of municipal waters reflect well-described water management practices.

Experiment 2.

Here, we sought to relate discrete variations in the $\delta^{18}O$ and $^{87}Sr/^{86}Sr$ values of tap water in urban areas to the $\delta^{18}O$ and $^{87}Sr/^{86}Sr$ values of human hair collected within the same region. We collected and analyzed hair from barbershop floors from the PHX, SFB, LA, and SD urban regions and measured the $\delta^{18}O$ values and $^{87}Sr/^{86}Sr$ ratios of these materials. From these same regions we sampled tap water to directly compare to urban populations. These regions have well-documented combinations of transported waters and local surface and/or ground waters (**Tables 3**, **5**, **6**, **8**, **9**, and **11**) that are reflected in the δ^2H, $\delta^{18}O$, and $^{87}Sr/^{86}Sr$ values of tap water available in these regions (see *Experiment 1*). We hypothesized that these variations in the δ^2H, $\delta^{18}O$, and $^{87}Sr/^{86}Sr$ values of tap water will be recorded in the hair of populations living in these regions.

Within the PHX metro area, we observed large variation in both the $\delta^{18}O$ and $^{87}Sr/^{86}Sr$ values of tap water with both isotope systems varying systematically with water management practice. We found the $\delta^{18}O$ and $^{87}Sr/^{86}Sr$ values of human hair also vary throughout the PHX metro area (**Figure 24**). Specifically, we found the $^{87}Sr/^{86}Sr$ values of human hair had nearly the same absolute range (**Table 12**) as of that observed in the $^{87}Sr/^{86}Sr$ values of tap water (**Table 3**). Further, we observed the predicted $\delta^{18}O$ values of tap water as modeled from the $\delta^{18}O$ values of human hair had a larger range (**Figure 44a**

and **b**). We observed large spatial variation in both the $\delta^{18}O$ and $^{87}Sr/^{86}Sr$ values of hair throughout the PHX area (**Figures 25** and **26**). The overall spatial distribution of the $\delta^{18}O$ and $^{87}Sr/^{86}Sr$ values of human hair analyzed from PHX showed a similar relative relationship to that of the $\delta^{18}O$ and $^{87}Sr/^{86}Sr$ values of tap water (**Figure 7** and **27**). These findings may indicate that the isotope ratios of human hair reflect that of the tap water in the region an individual resides. As an example, the most radiogenic (i.e., highest ratio of $^{87}Sr/^{86}Sr$) human hair and tap water samples were from regions in the Southeast, while the least radiogenic ratios were from the Southwest (**Figure 27**). Further, this linkage between isotopic values of tap water and that of the isotopic values of human hair suggest that the anonymous individuals sampled likely lived in the nearby area.

In the SFB metropolitan area, we observed the $\delta^{18}O$ and $^{87}Sr/^{86}Sr$ values of human hair varied (**Figure 28**). We found the $\delta^{18}O$ and $^{87}Sr/^{86}Sr$ values of human hair had a range (**Table 13**) similar to that observed in the predicted $\delta^{18}O$ and measured $^{87}Sr/^{86}Sr$ values of tap water (**Tables 5** and **6**; **Figure 44c** and **d**). We observed large spatial variation in both the $\delta^{18}O$ and $^{87}Sr/^{86}Sr$ values of hair throughout the SFB area (**Figures 29** and **30**). The overall spatial distribution of the $\delta^{18}O$ and $^{87}Sr/^{86}Sr$ values of human hair analyzed from SFB showed a similar relative relationship to that of the $\delta^{18}O$ and $^{87}Sr/^{86}Sr$ values of tap water (**Figure 12** and **31**). As an example, human hair and tap water samples that were most depleted in the heavy isotope (i.e., most negative $\delta^{18}O$ values) were collected from San Francisco and the Peninsula, while the most enriched in were from Marin County (**Figure 31**).

In LA, we found the $\delta^{18}O$ and $^{87}Sr/^{86}Sr$ values of human hair varied (**Table 14**, **Figure 32**). We observed the $\delta^{18}O$ values of human hair varied spatially (**Figure 33**). We noted the $\delta^{18}O$ values of human hair predicted a much larger range of the $\delta^{18}O$ values of tap water than that of measured $\delta^{18}O$ values of tap water (**Figure 44e** and **f**).

Within the SD metropolitan area, we found the $\delta^{18}O$ and $^{87}Sr/^{86}Sr$ values of human hair varied (**Table 15**, **Figure 34**). We found the $^{87}Sr/^{86}Sr$ values of human hair ranged less than that of the $^{87}Sr/^{86}Sr$ values of tap waters in SD (**Table 15**) and the $\delta^{18}O$ values of tap water predicted from hair had a larger range than that observed in the $\delta^{18}O$ values of tap waters in SD (**Figure 44g** and **h).** We observed large spatial variation in both the $\delta^{18}O$ and $^{87}Sr/^{86}Sr$ values of hair throughout the SD area (**Figures 35** and **36**). The overall spatial distribution of the $\delta^{18}O$ and $^{87}Sr/^{86}Sr$ values of human hair analyzed from SD showed a similar relative relationship to that of the $\delta^{18}O$ and $^{87}Sr/^{86}Sr$ values of tap water (**Figure 22** and **37**).

Overall, these findings suggest the isotope ratios of human hair reflect that of the tap water in the region an individual resides (**Figure 45**). In all populations, we observed the range of predicted $\delta^{18}O$ values of tap waters overlapped with the measured $\delta^{18}O$ values of tap waters (**Figure 44**). Further, we noted the range of $^{87}Sr/^{86}Sr$ ratios of hair overlapped with the range $^{87}Sr/^{86}Sr$ of tap waters in all cities. We found a strong relationship between the $^{87}Sr/^{86}Sr$ of hair and tap water (**Figure 46**).

These data also indicated that the discrete spatial variations observed in the isotope values of tap water were less clearly defined in hair, particularly in the $\delta^{18}O$ values of hair (**Figures 2** and **45**). The lower geographic definition in hair $\delta^{18}O$ values relative to the $^{87}Sr/^{86}Sr$ ratios may be due to individuals moving between regions with isotopically distinct tap waters (i.e., drinking water at work that is isotopically different than water in the home); consuming beverages produced within the metropolitan area, but outside their specific region of residence; or having their hair cut outside their region of residence. These factors would contribute to reducing the spatial fidelity of the oxygen isotope ratios of human hair while preserving the strontium isotope signature, as strontium is predominately incorporated during bathing, which usually takes place at the site of residence. The linkage between $^{87}Sr/^{86}Sr$ ratios of tap water and that of the human hair suggest that the anonymous hair samples collected in this study likely derived from individuals that lived in the nearby area.

Overall, we found that the isotope values of hair corresponded to the isotope values of water in the overall metropolitan areas and specific regions within the larger metropolitan areas. These finding also suggest that additional population and socioeconomic considerations could inform isoscape development in urban regions using diverse water sources. By weighting modeled isotope values to known demographic patterns, error envelopes and distribution functions of predicted isotope values could be further refined.

Experiment 3.

For this component of the research program, we sought to capture any seasonal cycles within the water sources or variations within the delivery of specific water sources to individual communities within a single metropolitan area. In *Experiment 3*, we collected waters from public taps and hair samples from barbershop floors in the SLV metropolitan area. We collected these materials for more than one seasonal cycle (i.e., Fall, Winter, Spring, Summer). We then measured the $\delta^{18}O$ values and $^{87}Sr/^{86}Sr$ ratios of these materials. SLV has well-documented water management practices that include combinations of transported waters and local surface water and/or groundwater (**Table 17**). Previous research has demonstrated that these water management practices are reflected in the $\delta^{2}H$, $\delta^{18}O$, and $^{87}Sr/^{86}Sr$ values of tap water in SLV and vary throughout the season with climate patterns and consumer needs (*NIJ-2011-DN-BX-K544*). We hypothesized that these variations in the $\delta^{2}H$, $\delta^{18}O$, and $^{87}Sr/^{86}Sr$ values of tap water will be recorded in the populations living in these regions.

The main water sources used in the SLV metropolitan area include waters derived from the adjacent Wasatch Mountains, transported water derived from the Uinta Mountains, and groundwater aquifers and springs. We found SLV tap waters had a relatively large range in the $^{87}Sr/^{86}Sr$ ratios of tap waters. The most radiogenic $^{87}Sr/^{86}Sr$ ratios of tap waters were observed in water districts using groundwater sources (**Figure 40**). These include the Murray City Water System, Salt Lake City Corporation Culinary Water, and the Taylorsville-Bennion Water Improvement Districts (**Table 17**). We also observed variation in the $\delta^{2}H$ and $\delta^{18}O$ values and $^{87}Sr/^{86}Sr$ ratios of tap waters from districts using mixtures of water sources (**Figure 40**). These include the Salt Lake City Corporation

Culinary Water and Magna Water Improvement Districts. These δ^2H, $\delta^{18}O$, and $^{87}Sr/^{86}Sr$ values of tap water observed in the SLV area are consistent with the water sources stated in the local municipalities' consumer confidence reports. Nonetheless, we noted seasonal variations in the $^{87}Sr/^{86}Sr$ ratios of tap waters from the Salt Lake City Corporation Culinary Water System, with $^{87}Sr/^{86}Sr$ ratios corresponding to groundwater usage being observed more frequently during the latter portion of 2014 and into Spring 2015 (**Figure 40**). This may have been a response to the low snowpack accumulation in the winter of 2013/2014.

We found that the $\delta^{18}O$ and $^{87}Sr/^{86}Sr$ values of human hair also varied temporally throughout the SLV area (**Figure 43**). In addition, we noted spatial variation in both the $\delta^{18}O$ and $^{87}Sr/^{86}Sr$ values of hair throughout SLV (**Figure 43**). However, the overall distribution of the $\delta^{18}O$ values and $^{87}Sr/^{86}Sr$ ratios of human hair analyzed from SLV was relatively similar to that of the $\delta^{18}O$ values and $^{87}Sr/^{86}Sr$ ratios of tap water (**Figure 40** and **43**). As with the previous two *Experiments*, we found that overall the $^{87}Sr/^{86}Sr$ ratios of hair more directly related to the $^{87}Sr/^{86}Sr$ ratios of water in specific regions than did the $\delta^{18}O$ values of hair and tap water. Further, we noted a possible lag between when specific $^{87}Sr/^{86}Sr$ ratios of water were observed in regions and when correspondent $^{87}Sr/^{86}Sr$ ratios of hair were observed. This can be best demonstrated by comparing the $^{87}Sr/^{86}Sr$ ratios of water and hair collected from the Salt Lake City Corporation Culinary Water System District. Here, we find that during Summer 2014 (**Figure 43c**) $^{87}Sr/^{86}Sr$ ratios of hair from the Salt Lake City Corporation Culinary Water System District is most radiogenic, while the $^{87}Sr/^{86}Sr$ ratios of water from the Salt Lake City Corporation Culinary Water System District during this time are near the lowest ratios observed throughout the entire time series. However, approximately 6 months prior, in Fall 2013 and Winter 2013/2014, we note $^{87}Sr/^{86}Sr$ ratios of water from the Salt Lake City Corporation Culinary Water System District as having ratios similar to those observed in the hair in Summer 2014. This suggests a temporal lag between when a pulse of more radiogenic water is introduced to the water system and when this pulse is observed in hair clippings from the population exposed to that water. An additional explanation could be due to sampling bias (i.e., limited coverage of hair and/or water).

Experiment 3 demonstrated that water management practices influence the isotopic composition of tap waters available to urban populations. In addition, a seasonal isotopic variation in tap water associated with water switching in water districts was noted. In this collection, water switching only occurred in districts that stated they used multiple water sources.

As with the previous two *Experiments* in this research program, the discrete spatial variations observed in the isotope values of tap water were less clearly defined in hair. Nonetheless, the isotope values of hair corresponded to the isotope values of water in the Salt Lake City metropolitan areas and within the specific water districts within the metropolitan area. Finally, we noted a possible lag between when specific $^{87}Sr/^{86}Sr$ ratios of water were observed in regions and when corresponding $^{87}Sr/^{86}Sr$ ratios of hair were observed. This finding suggests that there is a delay of approximately 6 months between when isotopic signals are introduced into a water system and when these signals are

observed in hair clippings of the population, our sampling scheme was biased, or individuals got haircuts outside their region of residence.

In conclusion, the three *Experiments* each confirm the initial hypotheses proposed. Specifically, these *Experiments* demonstrated: 1.) The isotope patterns in municipal waters are a function of water management and management practices vary spatially with coherent isotopic patterns that reflect the stated practices; 2.) The isotope patterns of human hair collected in urban regions with specific water management reflect that of the tap water delivered to that region and the underlying water management practices controlling the isotope ratios of that water; 3.) Spatiotemporal patterns in tap water isotope ratios are apparent and these patterns may be transferred to hair of individuals exposed to these spatial and temporal variations in water isotope ratios.

Description of Deliverables

Progress Reports

Five Semi-Annual Progress Report were delivered via the GMS system for the time periods between:

- Sept 1, 2013-Dec 31, 2013,
- Jan 1, 2014-June 30, 2014,
- July 1, 2014-Dec 31, 2014,
- Jan 1, 2015-June 30, 2015, and
- July 1, 2015-Dec 31, 2015.

Ten Financial Status Reports were also submitted for the time periods between:

- Oct 1, 2013-Dec 31, 2013,
- Jan 1, 2014-Mar 31, 2014,
- April 1, 2014-June 30, 2014,
- July 1, 2014-Sept 30, 2014,
- Oct 1, 2014-Dec 31, 2014,
- Jan 1, 2015-Mar 31, 2015,
- April 1, 2015-June 30, 2015,
- July 1, 2015-Sept 30, 2015,
- Oct 1, 2015-Dec 31, 2015, and
- Jan 1, 2016-Mar 31, 2016.

The PI provided project status reports during nine conference calls with the NIJ project manager on:

- April 15, 2014,
- June 24, 2014,
- August 12, 2014,
- October 14, 2014,
- December 30, 2014,
- April 14, 2015,
- June 30, 2015,

- July 7, 2015, and
- Sept 21, 2015.

Database

All data collected for hair and waters during this work effort have been collated in a relational FileMaker® database. This database includes sample information, collection location, element composition, and a measured stable isotope ratio for the elements H, O, and Sr. The database is stored on IsoForensics' secure fileserver.

Dissemination of Research Findings

Presentations

Oral

Tipple, B.J., Valenzuela, L.O., Chesson, L.A., and Ehleringer, J.R. (Oral), *Strontium isotope ratios of hair for human provenancing*, American Chemical Society, Annual Meeting, Boston, MA (August, 2015).

Tipple, B.J., Chau, T.H., Chesson, L.A., Ehleringer, J.R., Mancuso, C.J., and Valenzuela, L.O. (Oral), *Strontium isotope ratios of hair for human provenancing,* American Academy of Forensic Sciences, Orlando, FL (February, 2015).

Tipple, B.J. (Oral), *Combining strontium and oxygen isotope ratios of hair for human provenancing.* American Academy of Forensic Sciences, Seattle, WA (February, 2014).

Publications

Ehleringer, J.R., Chesson, L.A., Valenzuela, L.O., Tipple, B.J., and Martinelli, L.A., (2015) Humans and Society – Amazing insights from stable isotope biogeochemistry, *Elements*, 11, 4, 259-264.

Ehleringer, J.R., Barnette, J.E., Jameel, Y., Tipple, B.J., and Bowen, G.J. (*In Press*) Urban water – A new frontier in isotope hydrology, *Isotopes in Environmental & Health Studies*.

Jameel, Y., Brewer, S., Good, S.P., Tipple, B.J., Ehleringer, J.R., Bowen, G.J. (*Submitted*) Spatiotemporal variation in the tap water isotope ratios of Salt Lake City: a novel indicator of urban water system structure and dynamics, *Water Resource Research*.

Tipple, B.J., Chau, T.H., Chesson, L.A., Mancuso, C.J., and Ehleringer, J.R. (*In Preparation*) Using isotopes of tap waters to dissect a human ecosystem: A spatial and temporal study of water from the San Francisco Bay Area.

Tipple, B.J., Chau, T.H., Chesson, L.A., and Ehleringer, J.R. (*In Preparation*) Spatial and temporal dynamics of southwestern U.S. municipal water supplies as recorded by isotopes of tap water.

Figures and Tables

Table 1. Tap water and hair samples samples collected and analyzed to meet research objectives outlined in 2013-DN-BX-K009.

Material	Number Collected	Number Analyzed for $\delta^{18}O/\delta^{2}H$	Number Analyzed for $^{87}Sr/^{86}Sr$
Tap Water	1942	1856	665
Human Hair	609	290	218

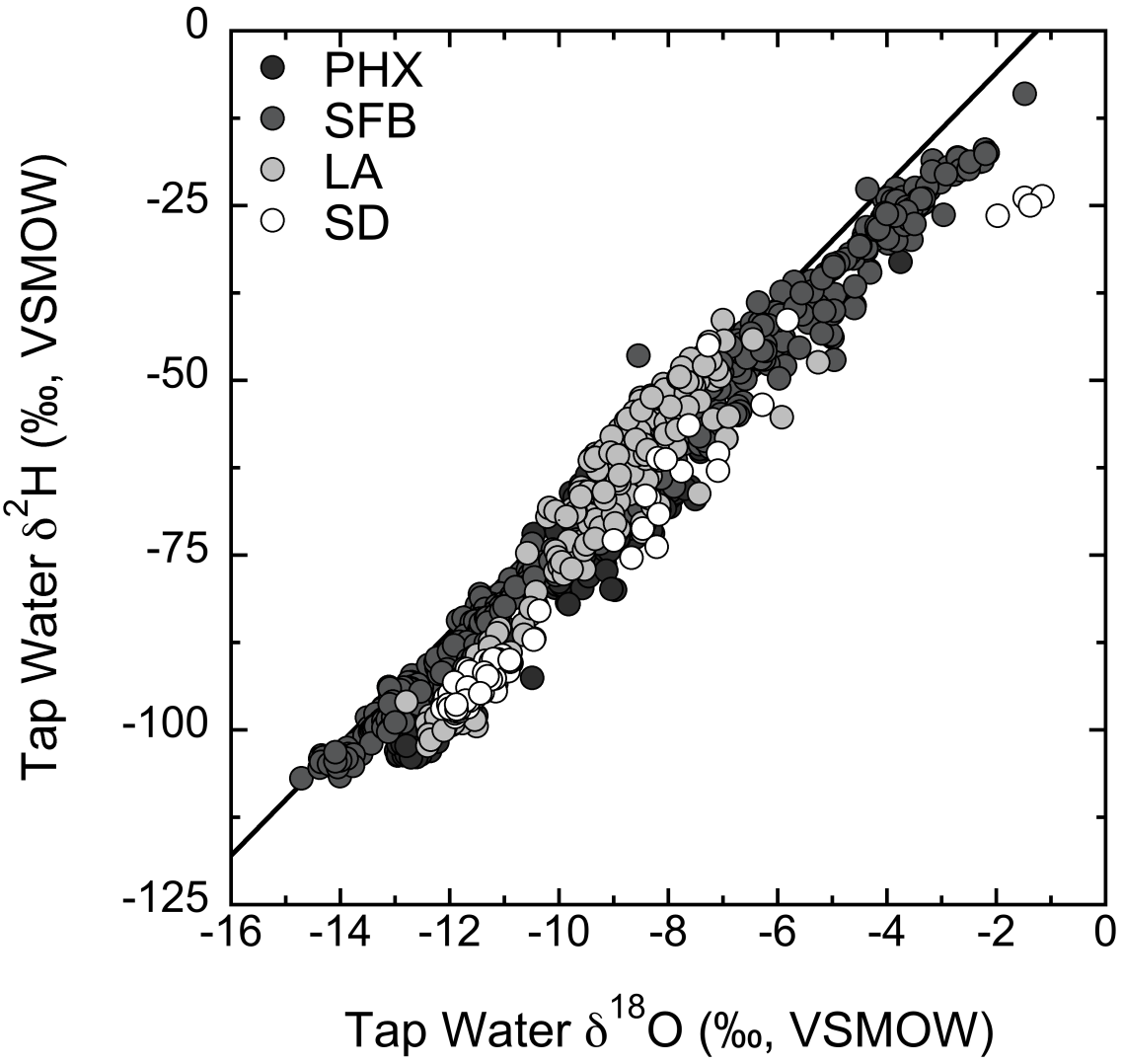

Figure 1. Cross-plot of the δ^2H and $\delta^{18}O$ values of tap water from the Phoenix-Mesa-Glendale (PHX), San Francisco-Oakland-Fremont and San Jose-Sunnyvale-Santa Clara (SFB), Los Angeles-Long Beach-Santa Ana and Riverside-San Bernardino-Ontario (LA), and San Diego-Carlsbad-San Marcos (SD) metropolitan areas.

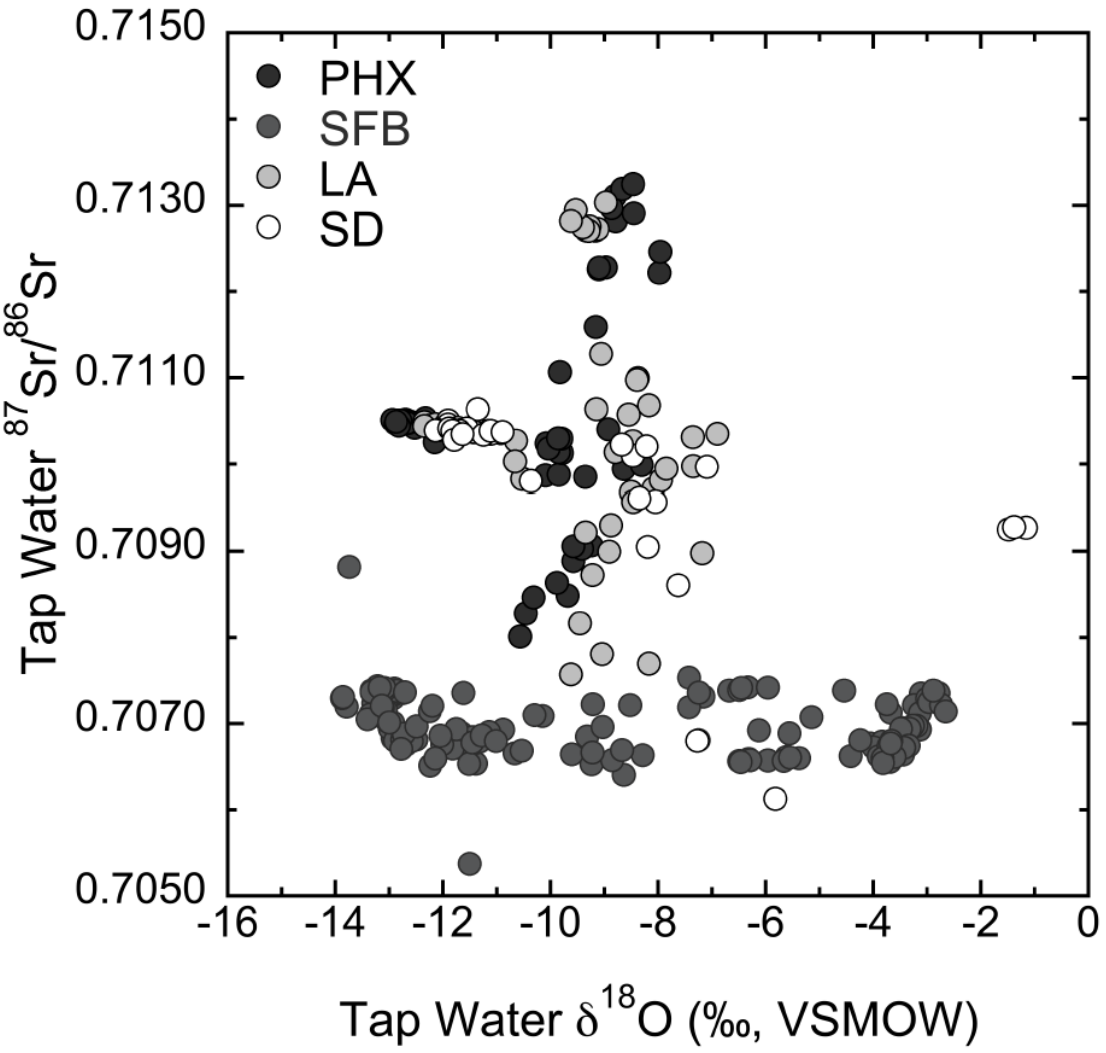

Figure 2. Cross-plot of the $^{87}Sr/^{86}Sr$ ratios and $\delta^{18}O$ values of tap water from the Phoenix-Mesa-Glendale (PHX), San Francisco-Oakland-Fremont and San Jose-Sunnyvale-Santa Clara (SFB), Los Angeles-Long Beach-Santa Ana and Riverside-San Bernardino-Ontario (LA), and San Diego-Carlsbad-San Marcos (SD) metropolitan areas.

Table 2. Summary statistics for the oxygen, hydrogen, and strontium isotope ratios from tap water samples collected in the Phoenix-Mesa-Glendale Metropolitan Area.

Date	Statistic	$\delta^{18}O$ (‰, VSMOW)	$\delta^{2}H$ (‰, VSMOW)	$^{87}Sr/^{86}Sr$
Spring 2014	Mean	-10.4	-81	0.71052
	SD	1.5	15	0.00138
	Range	5.0	44	0.00523
	Min	-13.0	-104	0.70802
	Max	-7.9	-60	0.71325
	Count	124	124	38
Fall 2014	Mean	-9.6	-76	0.71096
	SD	1.6	14	0.00152
	Range	9.0	69	0.00444
	Min	-12.8	-102	0.70847
	Max	-3.7	-33	0.71291
	Count	196	196	9

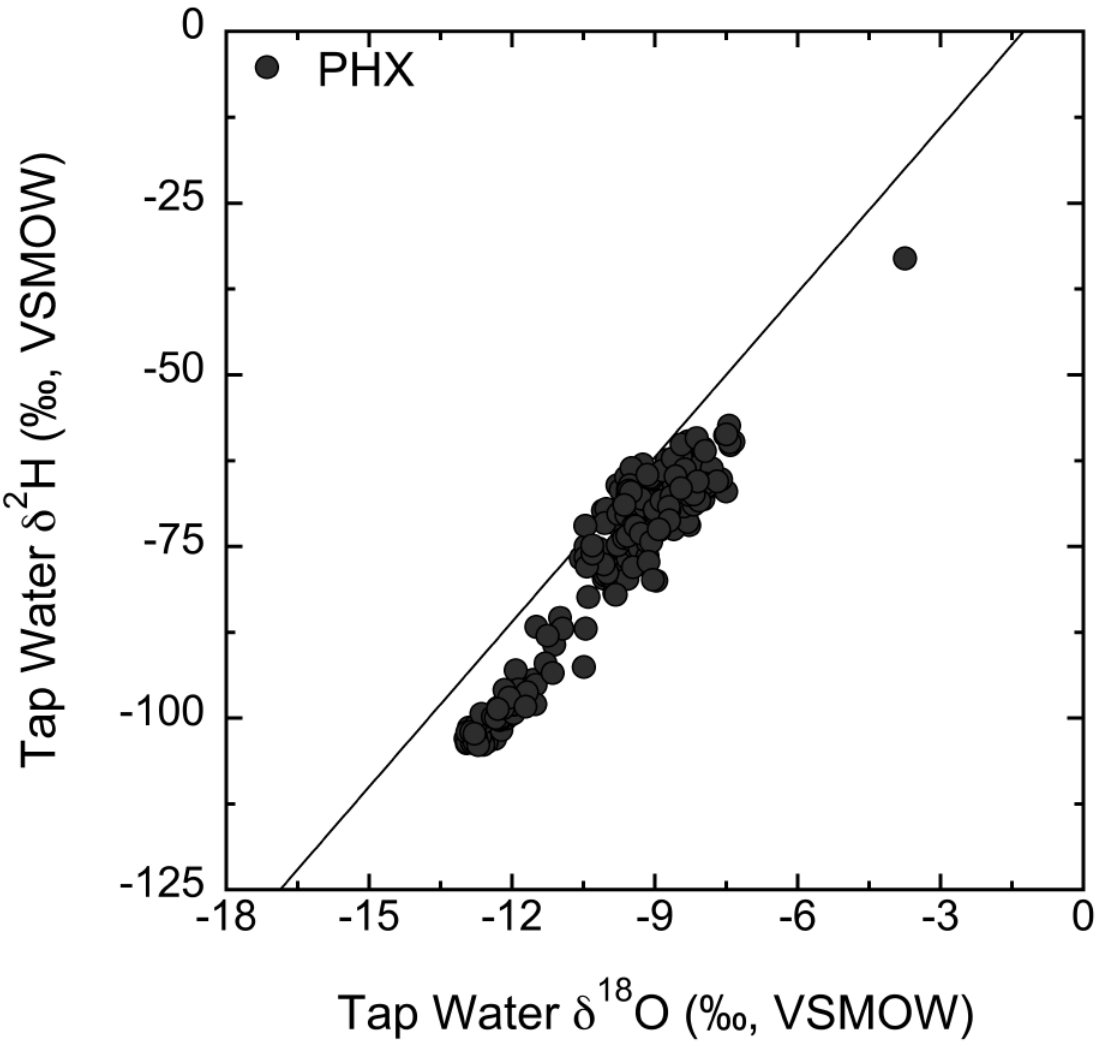

Figure 3. Cross-plot of the δ^2H and $\delta^{18}O$ values of tap water from the Phoenix-Mesa-Glendale metropolitan area. Meteoric water line is shown.

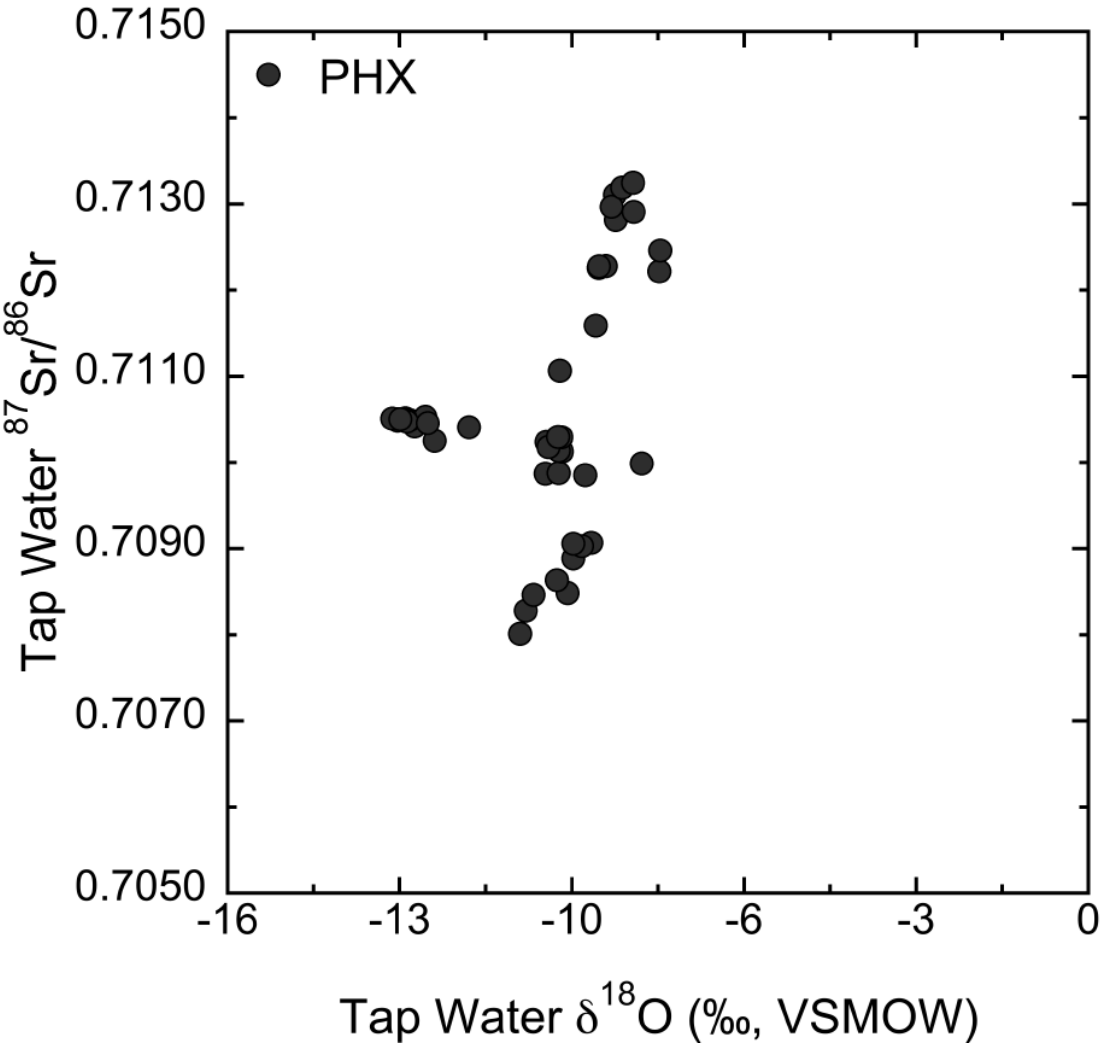

Figure 4. Cross-plot of the $^{87}Sr/^{86}Sr$ ratios and $\delta^{18}O$ values of tap water from the Phoenix-Mesa-Glendale metropolitan area.

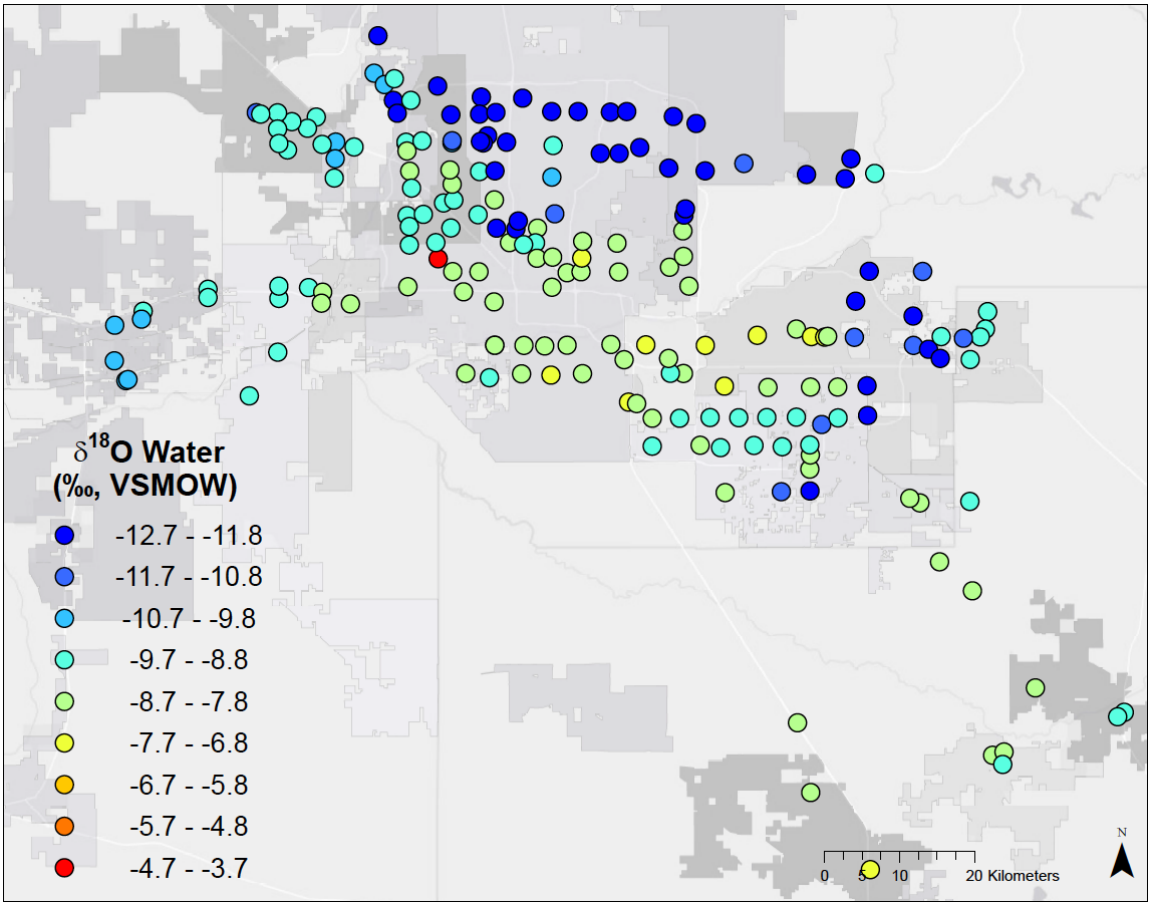

Figure 5. Spatial distribution of $\delta^{18}O$ values of tap water from the Phoenix-Mesa-Glendale metropolitan area collected in Fall 2014.

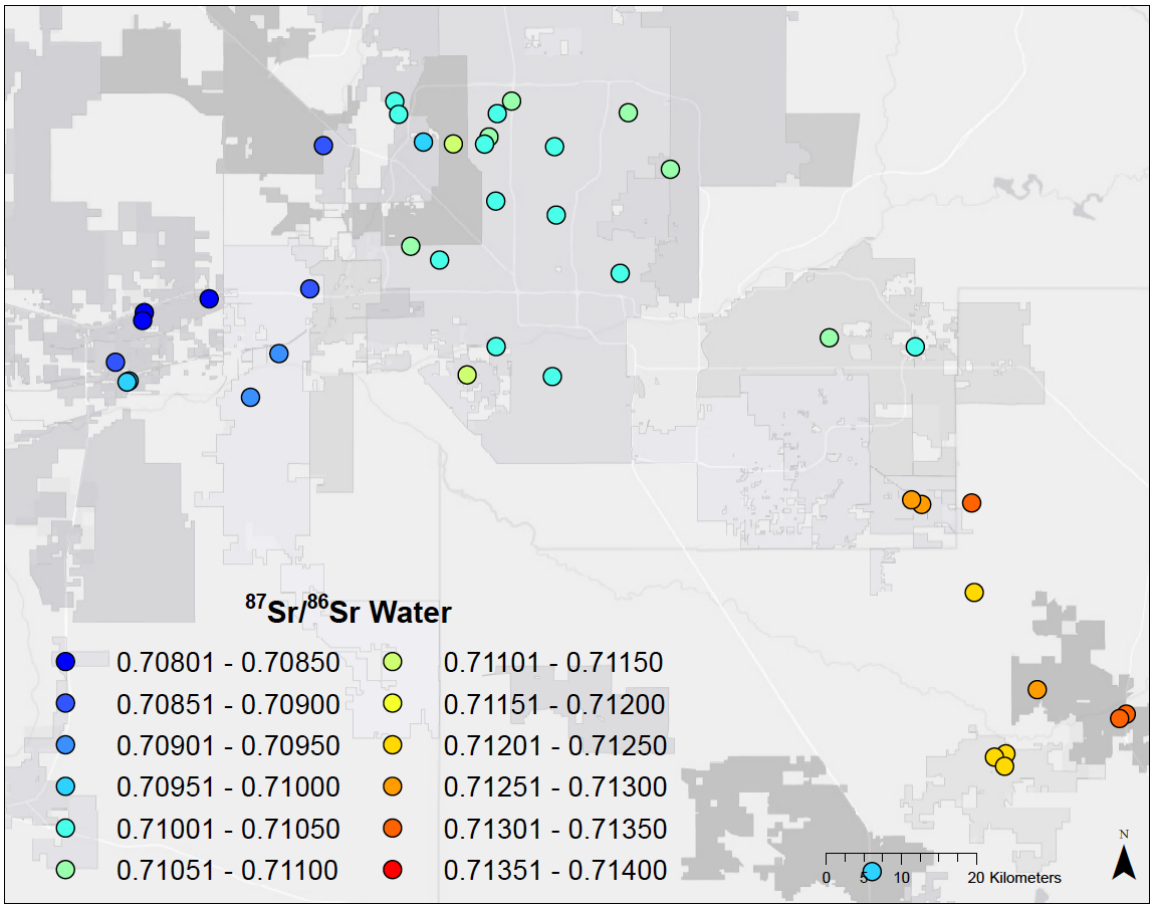

Figure 6. Spatial distribution of the $^{87}Sr/^{86}Sr$ ratios of tap water from the Phoenix-Mesa-Glendale metropolitan area collected in Fall 2014.

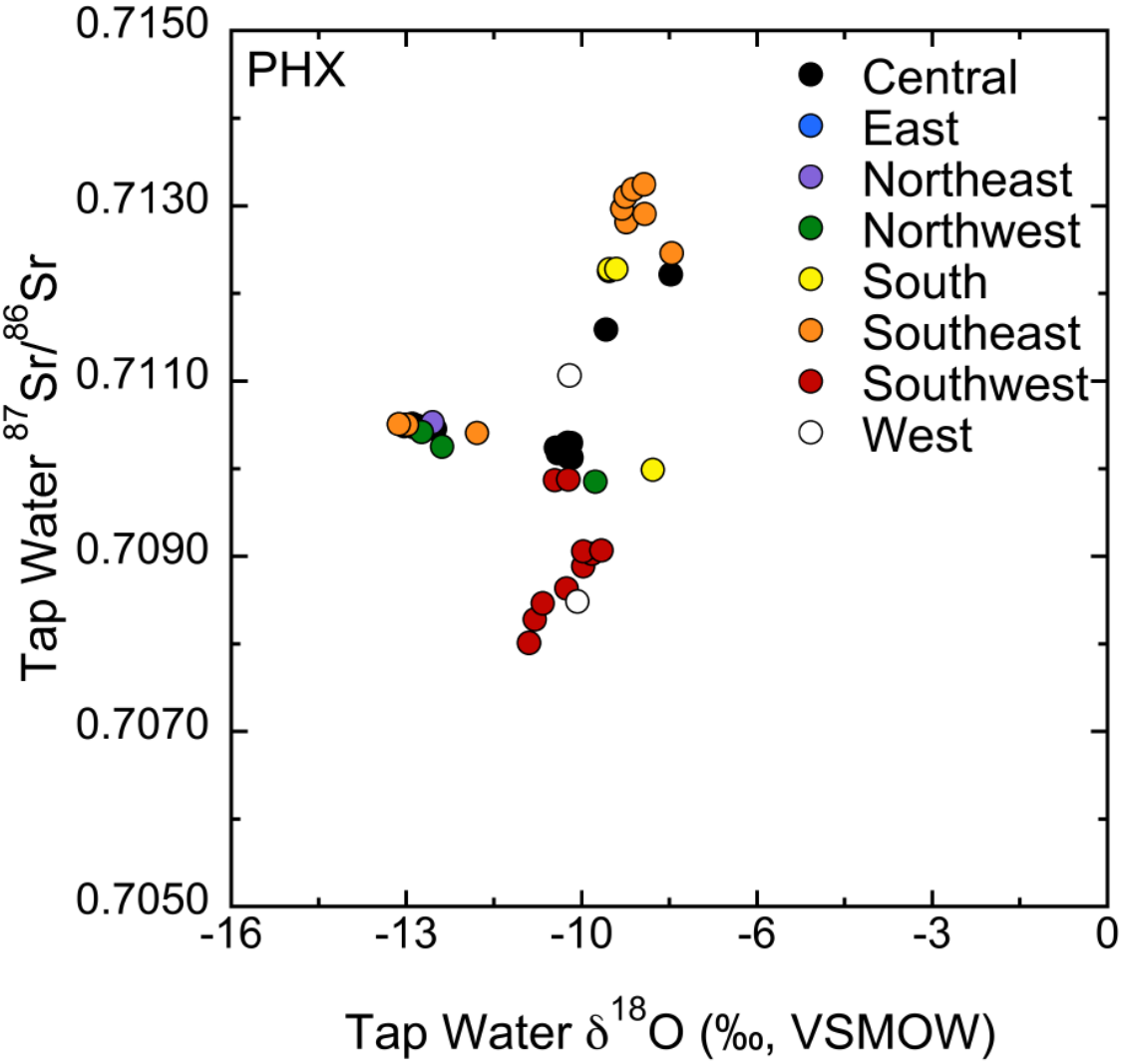

Figure 7. Cross-plot of the $^{87}Sr/^{86}Sr$ ratios and $\delta^{18}O$ values of tap water from the Phoenix-Mesa-Glendale metropolitan area. Colored symbols represent regions within the Phoenix-Mesa-Glendale metropolitan area.

Table 3. Cities in the Phoenix-Mesa-Glendale metropolitan area sampled and culinary water sources. Source information obtained from 2013/2014 water quality Consumer Confidence Reports.

Region	Metro Area	Geography	City	Water Sources				
Phoenix	Phoenix-Mesa-Glendale	Central	Phoenix	6	9	1		
Phoenix	Phoenix-Mesa-Glendale	East	Apache Junction	2	6			
Phoenix	Phoenix-Mesa-Glendale	East	Fountain Hills	6	1			
Phoenix	Phoenix-Mesa-Glendale	Northeast	Scottsdale	6	10	1		
Phoenix	Phoenix-Mesa-Glendale	Northwest	Peoria	6	1	9		
Phoenix	Phoenix-Mesa-Glendale	Northwest	Surprise - Agua Fria	6	3			
Phoenix	Phoenix-Mesa-Glendale	Northwest	Surprise - Other Districts	3				
Phoenix	Phoenix-Mesa-Glendale	South	Casa Grande	1				
Phoenix	Phoenix-Mesa-Glendale	South	Eloy	1				
Phoenix	Phoenix-Mesa-Glendale	Southeast	Chandler	1	6	7	8	9
Phoenix	Phoenix-Mesa-Glendale	Southeast	Florence	1				
Phoenix	Phoenix-Mesa-Glendale	Southeast	Gilbert	6	10			
Phoenix	Phoenix-Mesa-Glendale	Southeast	Mesa	10	6	1		
Phoenix	Phoenix-Mesa-Glendale	Southeast	Queen Creek	1				
Phoenix	Phoenix-Mesa-Glendale	Southeast	Tempe	10	6	11		
Phoenix	Phoenix-Mesa-Glendale	Southwest	Avondale	3				
Phoenix	Phoenix-Mesa-Glendale	Southwest	Buckeye	3	4			
Phoenix	Phoenix-Mesa-Glendale	Southwest	Goodyear	3				
Phoenix	Phoenix-Mesa-Glendale	West	El Mirage	5				
Phoenix	Phoenix-Mesa-Glendale	West	Glendale	6	10			

1. Groundwater; 2. Groundwater - Eastern Salt River Sub-Basin Aquifer; 3. Groundwater - West Salt River Valley Sub-Basin Aquifer; 4. Groundwater - Hassayampa Sub-Basin Aquifer; 5. Groundwater - Agua Fria Aquifer; 6. Colorado River - CAP; 7. Salt River; 8. Verde River; 9. Salt River Project - Wells; 10. Salt River Project; 11. Surface water sources stored as groundwater.

Table 4. Summary statistics for the oxygen, hydrogen, and strontium isotope ratios from tap water samples collected in the San Francisco-Oakland-Fremont and San Jose-Sunnyvale-Santa Clara Metropolitan Areas.

Date	Statistic	$\delta^{18}O$ (‰, VSMOW)	$\delta^{2}H$ (‰, VSMOW)	$^{87}Sr/^{86}Sr$
Winter 2013/2014	Mean	-10.1	-73	0.70690
	SD	3.3	26	0.00049
	Range	11.0	83	0.00344
	Min	-13.7	-102	0.70538
	Max	-2.8	-19	0.70882
	Count	59	59	32
Spring 2014	Mean	-9.5	-70	0.70704
	SD	3.6	27	0.00032
	Range	11.9	90	0.00103
	Min	-13.3	-99	0.70641
	Max	-1.5	-9	0.70744
	Count	204	204	64
Summer 2014	Mean	-8.6	-64	0.70708
	SD	3.5	27	0.00035
	Range	11.3	84	0.00089
	Min	-13.5	-101	0.70653
	Max	-2.2	-17	0.70742
	Count	85	85	13
Fall 2014	Mean	-9.4	-70	0.70700
	SD	3.7	28	0.00029
	Range	11.4	83	0.00100
	Min	-13.6	-101	0.70654
	Max	-2.2	-17	0.70754
	Count	101	101	14
Winter 2014/2015	Mean	-9.8	-72	0.70702
	SD	3.7	28	0.00030
	Range	11.4	81	0.00091
	Min	-14.4	-107	0.70652
	Max	-3.0	-25	0.70742
	Count	97	97	14
Spring 2015	Mean	-9.1	-68	0.70700
	SD	2.8	22	0.00028
	Range	8.7	69	0.00082
	Min	-13.2	-100	0.70660
	Max	-4.5	-31	0.70742
	Count	90	90	14
Summer 2015	Mean	-8.9	-67	–
	SD	3.1	24	–
	Range	9.9	78	–
	Min	-13.2	-100	–
	Max	-3.3	-23	–
	Count	88	88	0

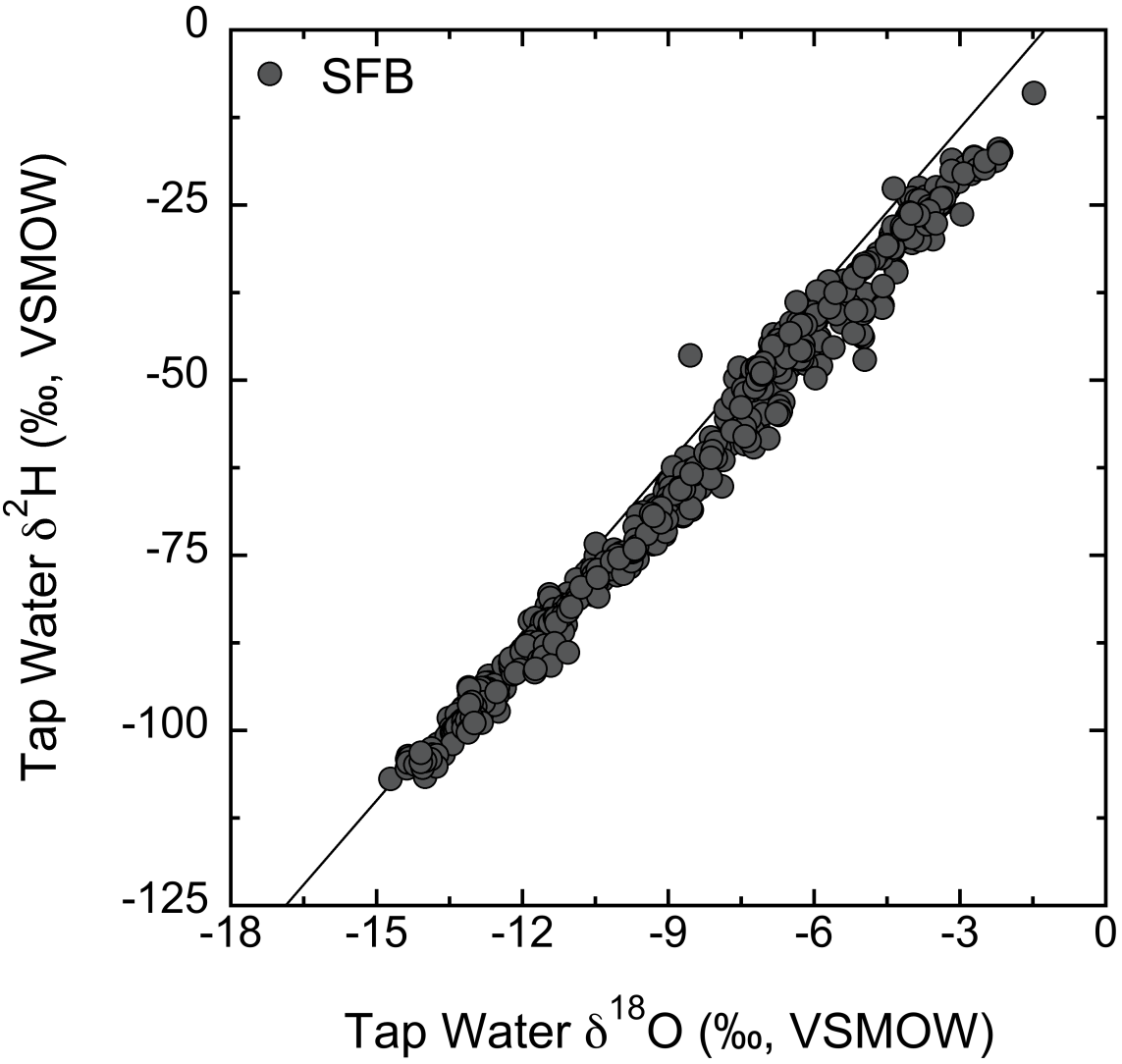

Figure 8. Cross-plot of the δ^2H and $\delta^{18}O$ values of tap water from the San Francisco-Oakland-Fremont and San Jose-Sunnyvale-Santa Clara metropolitan areas. Meteoric water line is shown.

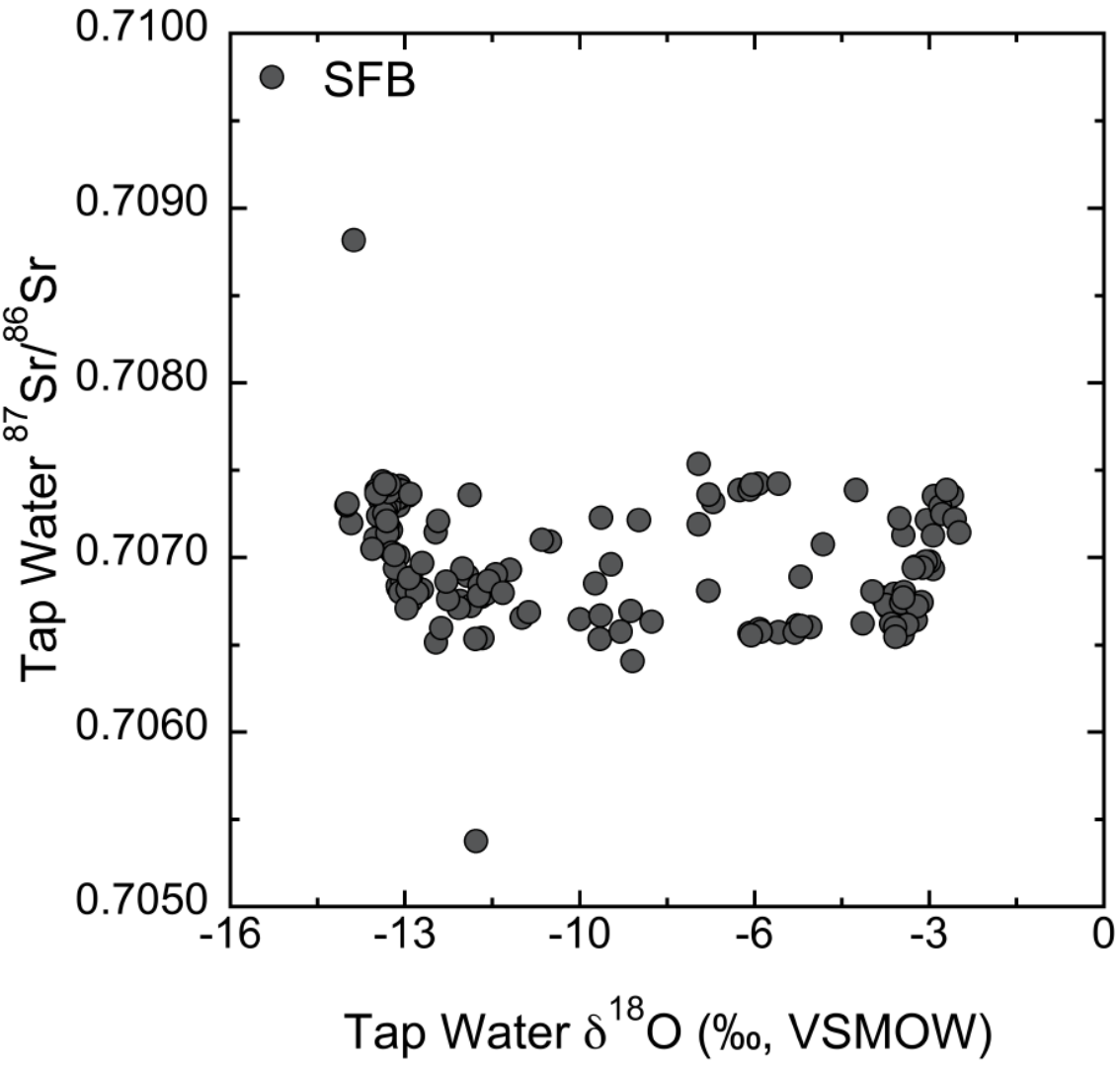

Figure 9. Cross-plot of the $^{87}Sr/^{86}Sr$ ratio and $\delta^{18}O$ values of tap water from the San Francisco-Oakland-Fremont and San Jose-Sunnyvale-Santa Clara metropolitan areas.

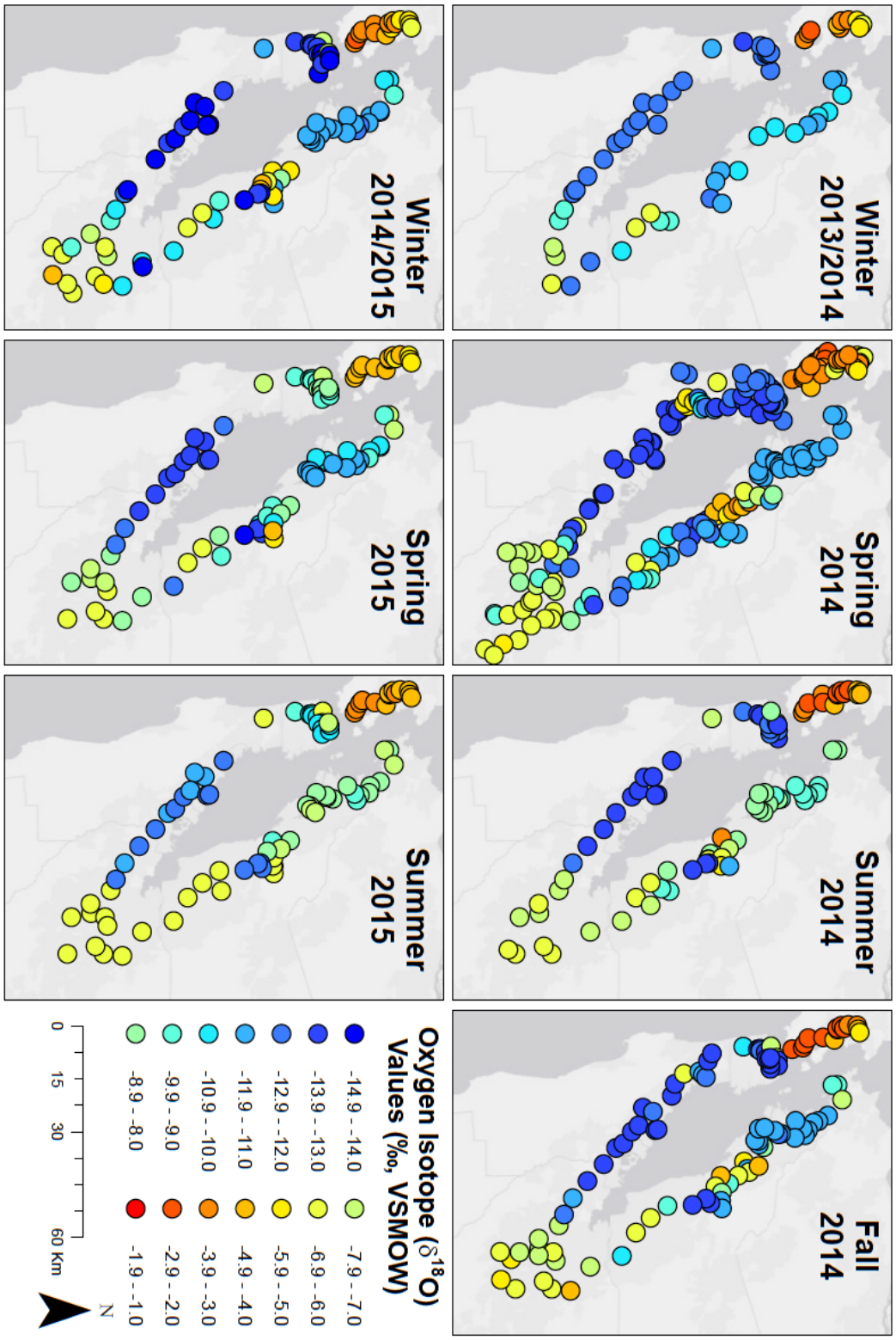

Figure 10. Spatial distribution of $\delta^{18}O$ values of tap water from the San Francisco-Oakland-Fremont and San Jose-Sunnyvale-Santa Clara metropolitan areas.

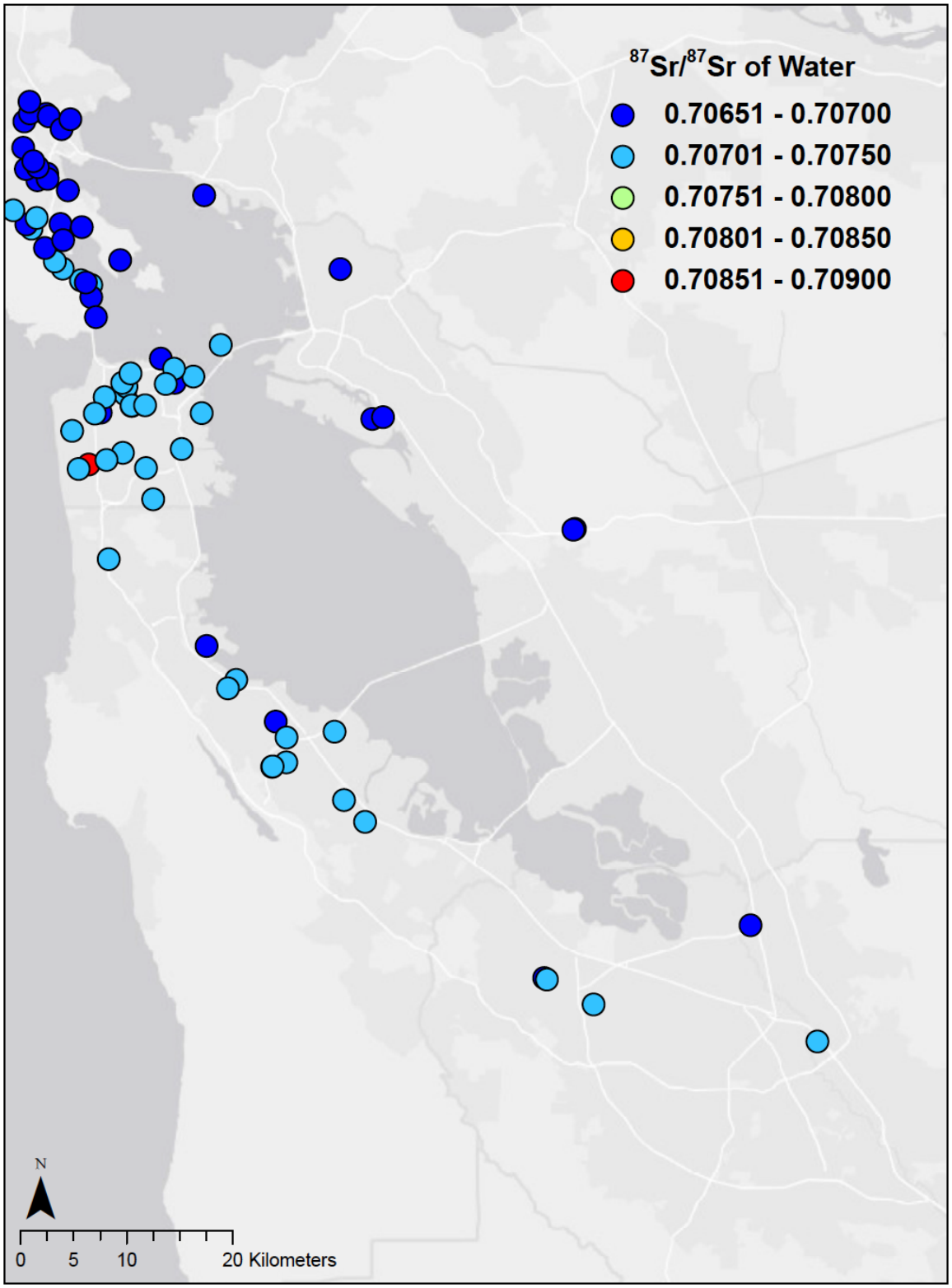

Figure 11. Spatial distribution of $^{87}Sr/^{86}Sr$ ratios of tap water from the San Francisco-Oakland-Fremont and San Jose-Sunnyvale-Santa Clara metropolitan areas during Spring 2014.

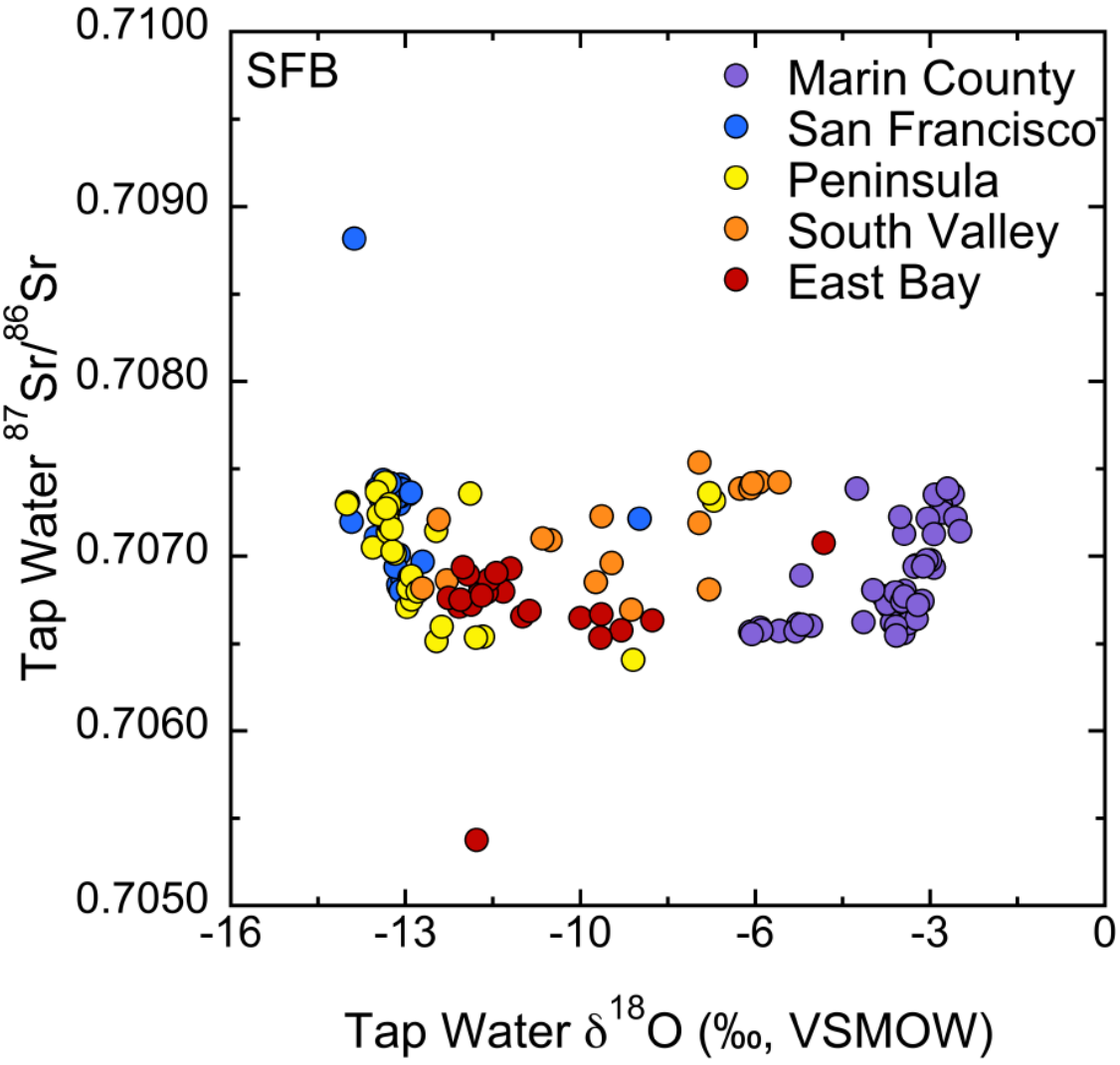

Figure 12. Cross-plot of the $^{87}Sr/^{86}Sr$ ratio and $\delta^{18}O$ values of tap water from the San Francisco-Oakland-Fremont and San Jose-Sunnyvale-Santa Clara metropolitan areas. Colored symbols represent regions in the larger SFB metro areas.

Table 5. Cities in the San Francisco-Oakland-Fremont metropolitan area sampled and culinary water sources. Source information obtained from 2013/2014 water quality Consumer Confidence Reports.

Region	Metro Area	Geography	City	Water Sources				
SFB	San Francisco-Oakland-Fremont	East Bay	Alameda	6	10			
SFB	San Francisco-Oakland-Fremont	East Bay	Albany	6	10			
SFB	San Francisco-Oakland-Fremont	East Bay	Berkeley	6	10			
SFB	San Francisco-Oakland-Fremont	East Bay	Castro Valley	1	6	9	10	
SFB	San Francisco-Oakland-Fremont	East Bay	El Cerrito	6	10			
SFB	San Francisco-Oakland-Fremont	East Bay	Emeryville	6	9	10		
SFB	San Francisco-Oakland-Fremont	East Bay	Fremont	1	2	3		
SFB	San Francisco-Oakland-Fremont	East Bay	Hayward	5	6	10		
SFB	San Francisco-Oakland-Fremont	East Bay	Newark	1	2	5		
SFB	San Francisco-Oakland-Fremont	East Bay	Oakland	6	10			
SFB	San Francisco-Oakland-Fremont	East Bay	Point Richmond	6	10			
SFB	San Francisco-Oakland-Fremont	East Bay	Richmond	6	10			
SFB	San Francisco-Oakland-Fremont	East Bay	Rockridge (Oakland)	6	10			
SFB	San Francisco-Oakland-Fremont	East Bay	San Leandro	6	10			
SFB	San Francisco-Oakland-Fremont	East Bay	Union City	1	2	5		
SFB	San Francisco-Oakland-Fremont	Marin County	Belvedere Tiburon	7	10			
SFB	San Francisco-Oakland-Fremont	Marin County	Corte Madera	7	10			
SFB	San Francisco-Oakland-Fremont	Marin County	Greenbrae	7	10			
SFB	San Francisco-Oakland-Fremont	Marin County	Lakespur	7	10			
SFB	San Francisco-Oakland-Fremont	Marin County	Marin City	7	10			
SFB	San Francisco-Oakland-Fremont	Marin County	Mill Valley	7	10			
SFB	San Francisco-Oakland-Fremont	Marin County	San Rafael	7	10			
SFB	San Francisco-Oakland-Fremont	Marin County	Sausalito	7	10			
SFB	San Francisco-Oakland-Fremont	Marin County	Tiburon	7	10			
SFB	San Francisco-Oakland-Fremont	Peninsula	Belmont	5	10			
SFB	San Francisco-Oakland-Fremont	Peninsula	Brisbane	5	10			
SFB	San Francisco-Oakland-Fremont	Peninsula	Burlingame	5				
SFB	San Francisco-Oakland-Fremont	Peninsula	Colma	5	10			
SFB	San Francisco-Oakland-Fremont	Peninsula	Daly City	1	5	10		
SFB	San Francisco-Oakland-Fremont	Peninsula	Millbrae	5	10			
SFB	San Francisco-Oakland-Fremont	Peninsula	Pacifica	5	10			
SFB	San Francisco-Oakland-Fremont	Peninsula	Redwood City	5	10			
SFB	San Francisco-Oakland-Fremont	Peninsula	San Bruno	1	5	10		
SFB	San Francisco-Oakland-Fremont	Peninsula	San Carlos	5	10			
SFB	San Francisco-Oakland-Fremont	Peninsula	San Mateo	5	10			
SFB	San Francisco-Oakland-Fremont	Peninsula	South San Francisco	1	5			
SFB	San Francisco-Oakland-Fremont	San Francisco	San Francisco	5	10			

1. Groundwater; 2. Feather River/California Aqueduct; 3. Colorado River; 4. Owens and Mono Basin/LA Aqueduct; 5. Tuolumne River/SFPUC; 6. Mokelumne River/EBMUD; 7. Russian and Eel Rivers; 8. Lake Berryessa/Putah Creek; 9. Central Valley Project/USBR; 10. Local Reservoirs/Streams; 11. Ocean Desalination.

Table 6. Cities in the San Jose-Sunnyvale-Santa Clara metropolitan area sampled and culinary water sources. Source information obtained from 2013/2014 water quality Consumer Confidence Reports.

Region	Metro Area	Geography	City	Water Sources				
SFB	San Jose-Sunnyvale-Santa Clara	South Valley	Campbell	1	2	5	9	10
SFB	San Jose-Sunnyvale-Santa Clara	South Valley	Cupertino	1	2	5	9	10
SFB	San Jose-Sunnyvale-Santa Clara	South Valley	Edenvale	1				
SFB	San Jose-Sunnyvale-Santa Clara	South Valley	Foster City	5				
SFB	San Jose-Sunnyvale-Santa Clara	South Valley	Gilroy	1				
SFB	San Jose-Sunnyvale-Santa Clara	South Valley	Los Altos	1	2			
SFB	San Jose-Sunnyvale-Santa Clara	South Valley	Los Gatos	1	2	5	9	10
SFB	San Jose-Sunnyvale-Santa Clara	South Valley	Menlo Park	5	10			
SFB	San Jose-Sunnyvale-Santa Clara	South Valley	Mountain View	1	2	5	9	10
SFB	San Jose-Sunnyvale-Santa Clara	South Valley	Palo Alto	5				
SFB	San Jose-Sunnyvale-Santa Clara	South Valley	San Jose	1	2	5	9	10
SFB	San Jose-Sunnyvale-Santa Clara	South Valley	Santa Clara	1	2	5	9	10
SFB	San Jose-Sunnyvale-Santa Clara	South Valley	Saratoga	1	2	5	9	10
SFB	San Jose-Sunnyvale-Santa Clara	South Valley	Sunnyvale	1	2	5	9	10
SFB	San Jose-Sunnyvale-Santa Clara	South Valley	Milpitas	2	5	9		

1. Groundwater; 2. Feather River/California Aqueduct; 3. Colorado River; 4. Owens and Mono Basin/LA Aqueduct; 5. Tuolumne River/SFPUC; 6. Mokelumne River/EBMUD; 7. Russian and Eel Rivers; 8. Lake Berryessa/Putah Creek; 9. Central Valley Project/USBR; 10. Local Reservoirs/Streams; 11. Ocean Desalination.

Table 7. Summary statistics for the oxygen, hydrogen, and strontium isotope ratios from tap water samples collected in the Los Angeles-Long Beach-Santa Ana and Riverside-San Bernardino-Ontario Metropolitan Areas.

Date	Statistic	$\delta^{18}O$ (‰, VSMOW)	$\delta^{2}H$ (‰, VSMOW)	$^{87}Sr/^{86}Sr$
Winter 2013/2014	Mean	-9.1	-61	0.71196
	SD	0.4	4	0.00126
	Range	1.3	15	0.00304
	Min	-9.4	-65	0.70972
	Max	-8.1	-50	0.71276
	Count	10	10	10
Spring 2014	Mean	-9.6	-70	0.70983
	SD	1.4	15	0.00142
	Range	5.5	59	0.00546
	Min	-12.4	-100	0.70758
	Max	-6.9	-41	0.71304
	Count	83	83	15
Fall 2014	Mean	-9.0	-66	0.71033
	SD	1.5	16	0.00128
	Range	7.1	58	0.00525
	Min	-12.4	-102	0.70770
	Max	-5.3	-44	0.71295
	Count	149	149	15

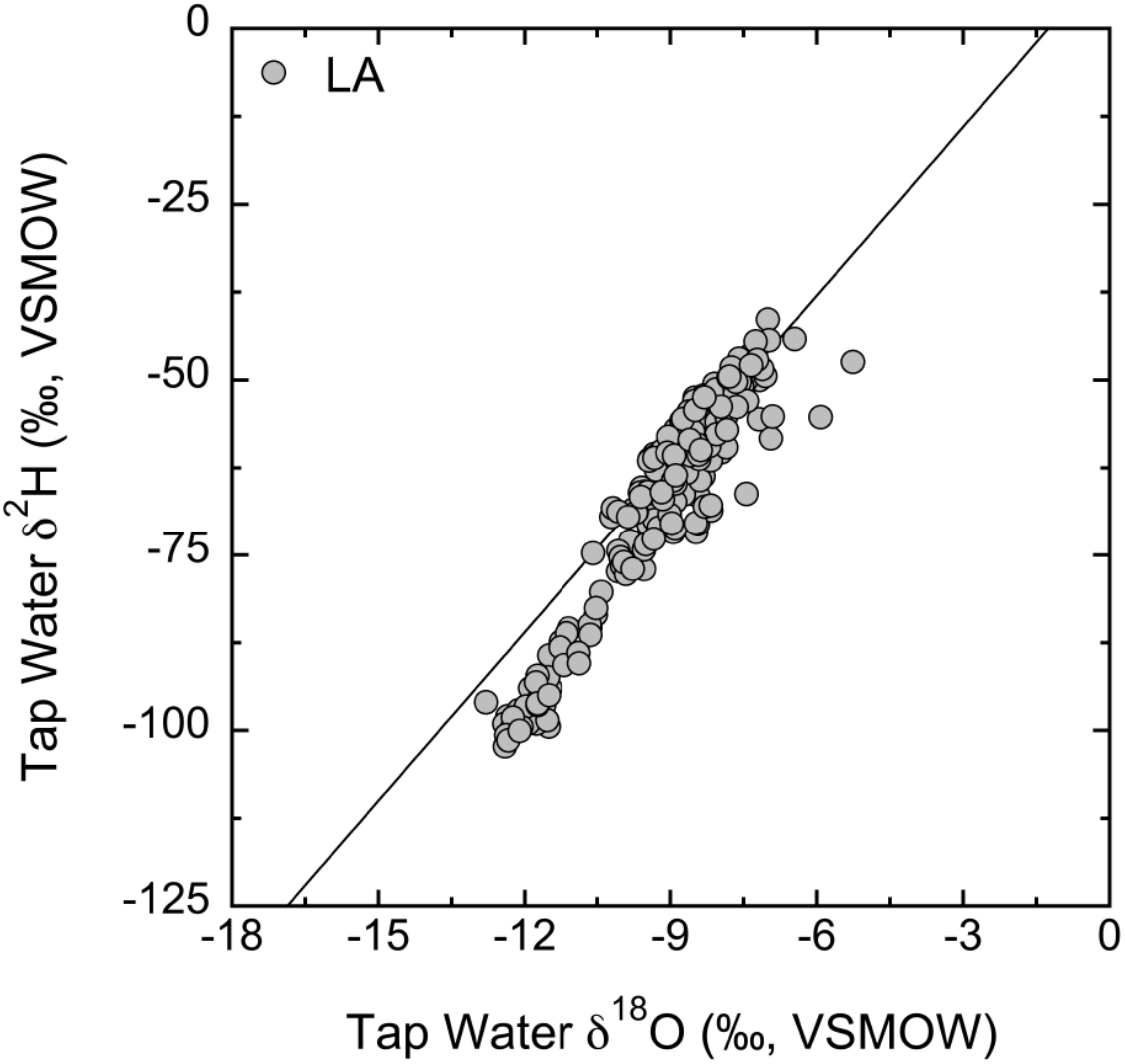

Figure 13. Cross-plot of the δ^2H and $\delta^{18}O$ values of tap water from the Los Angeles-Long Beach-Santa Ana and Riverside-San Bernardino-Ontario metropolitan areas. Meteoric water line is shown.

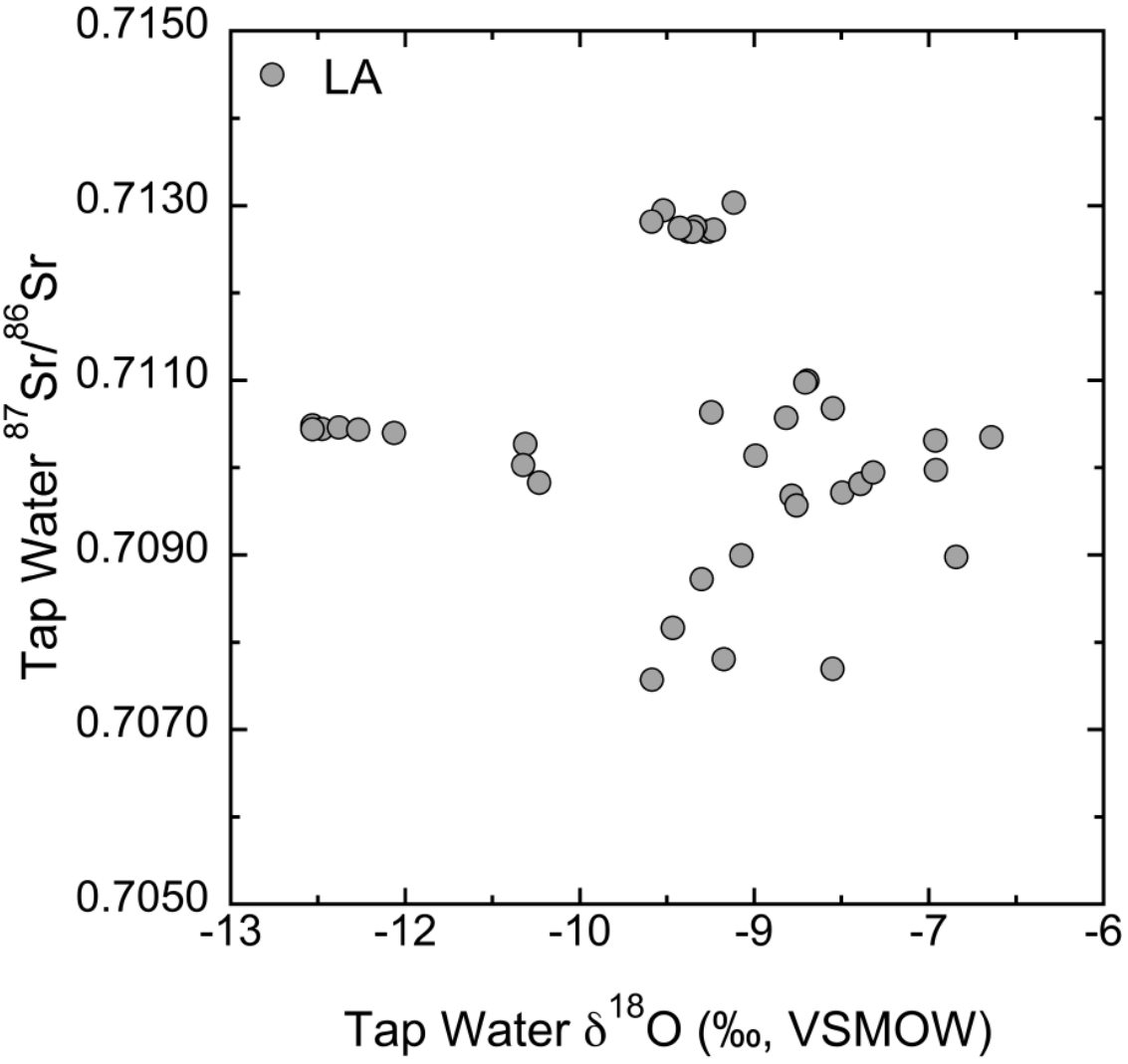

Figure 14. Cross-plot of the $^{87}Sr/^{86}Sr$ ratios and $\delta^{18}O$ values of tap water from the Los Angeles-Long Beach-Santa Ana and Riverside-San Bernardino-Ontario metropolitan areas.

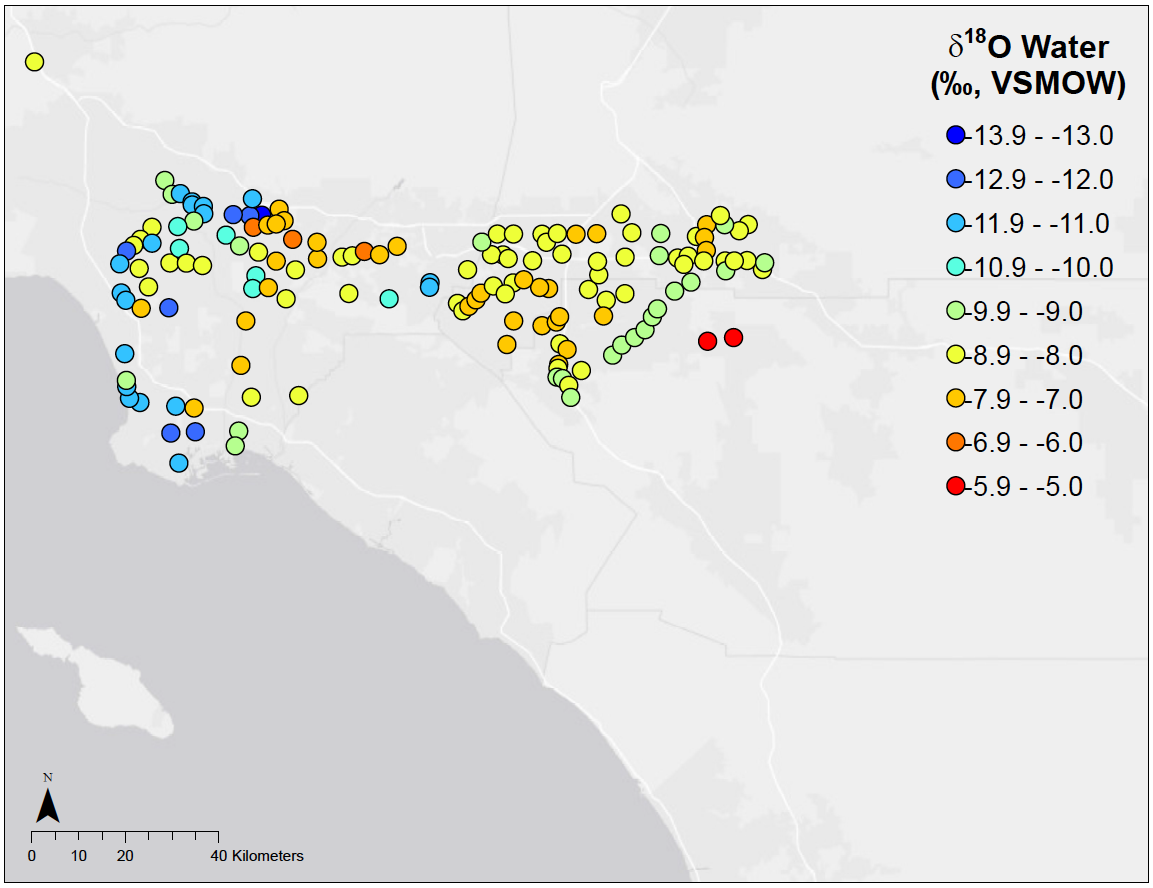

Figure 15. Spatial distribution of the $\delta^{18}O$ values of tap water from the Los Angeles-Long Beach-Santa Ana and Riverside-San Bernardino-Ontario metropolitan areas collected in Fall 2014.

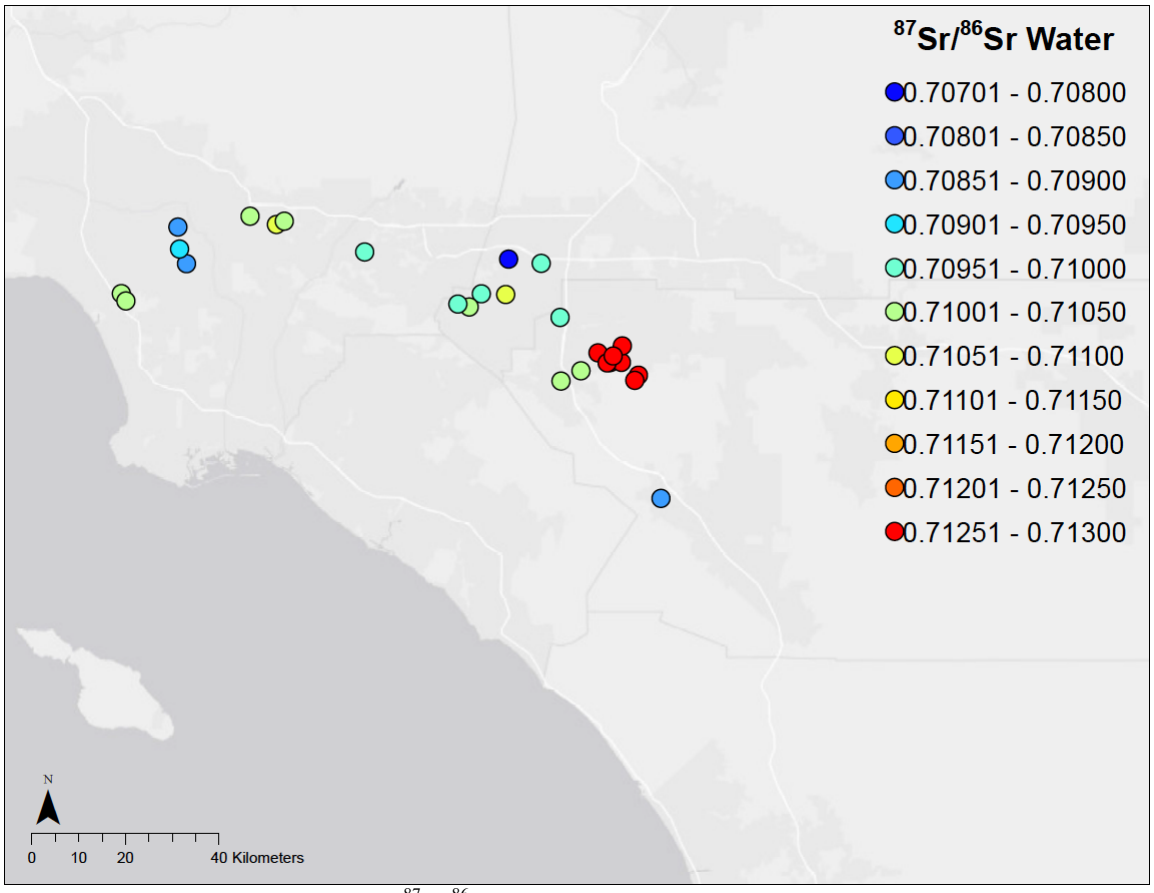

Figure 16. Spatial distribution of the $^{87}Sr/^{86}Sr$ ratios of tap water from the Los Angeles-Long Beach-Santa Ana and Riverside-San Bernardino-Ontario metropolitan areas collected in Winter 2013/2014, Spring 2014, and Fall 2014.

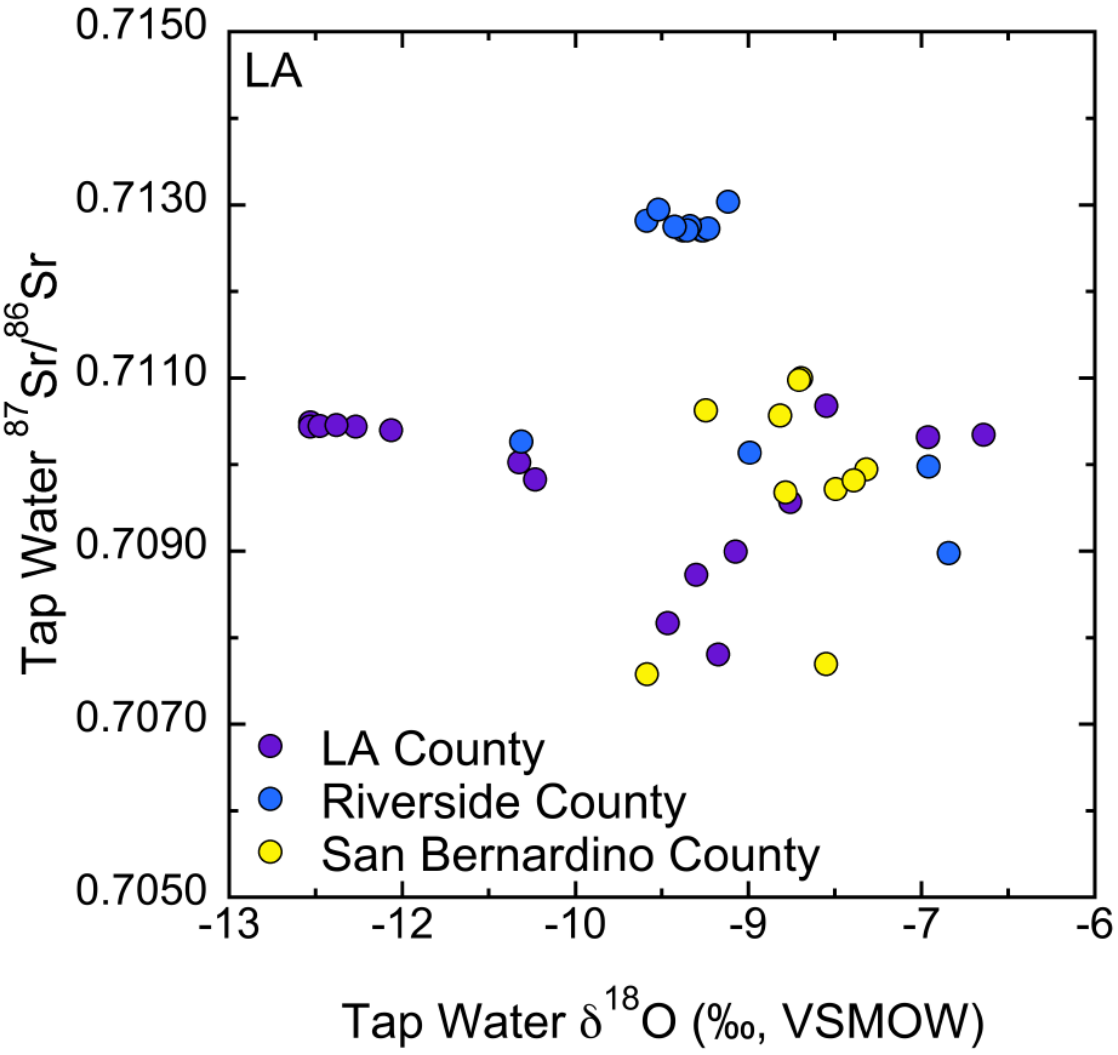

Figure 17. Cross-plot of the $^{87}Sr/^{86}Sr$ ratios and $\delta^{18}O$ values of tap water from the Los Angeles-Long Beach-Santa Ana and Riverside-San Bernardino-Ontario metropolitan areas. Colored symbols represent the three counties with in the larger LA metro area.

Table 8. Cities in the Los Angeles-Long Beach-Santa Ana metropolitan area sampled and culinary water sources. Source information obtained from 2013/2014 water quality Consumer Confidence Reports.

Region	Metro Area	Geography	City	Water Sources				
LA	Los Angeles-Long Beach-Santa Ana	LA County	Alhambra	1	2	3		
LA	Los Angeles-Long Beach-Santa Ana	LA County	Baldwin Park	1	2	3	10	
LA	Los Angeles-Long Beach-Santa Ana	LA County	Bell Gardens	1	2	3		
LA	Los Angeles-Long Beach-Santa Ana	LA County	Beverly Hills	2	3			
LA	Los Angeles-Long Beach-Santa Ana	LA County	Burbank	1	2	3		
LA	Los Angeles-Long Beach-Santa Ana	LA County	Carson	1	2	3		
LA	Los Angeles-Long Beach-Santa Ana	LA County	Cerritos	1	2	3		
LA	Los Angeles-Long Beach-Santa Ana	LA County	Claremont	1	2	3		
LA	Los Angeles-Long Beach-Santa Ana	LA County	Commerce	1	2	3		
LA	Los Angeles-Long Beach-Santa Ana	LA County	Covina	1	2	3	10	
LA	Los Angeles-Long Beach-Santa Ana	LA County	Culver City	1	2	3		
LA	Los Angeles-Long Beach-Santa Ana	LA County	Diamond Bar	2	3			
LA	Los Angeles-Long Beach-Santa Ana	LA County	El Monte	1	2	3		
LA	Los Angeles-Long Beach-Santa Ana	LA County	El Segundo	2	3			
LA	Los Angeles-Long Beach-Santa Ana	LA County	Glendale	1	2	3		
LA	Los Angeles-Long Beach-Santa Ana	LA County	Hermosa Beach	1	2	3		
LA	Los Angeles-Long Beach-Santa Ana	LA County	Lakewood	1	2	3		
LA	Los Angeles-Long Beach-Santa Ana	LA County	Lomita	1	2	3		
LA	Los Angeles-Long Beach-Santa Ana	LA County	Long Beach	1	2	3		
LA	Los Angeles-Long Beach-Santa Ana	LA County	Los Angeles	1	2	3	4	
LA	Los Angeles-Long Beach-Santa Ana	LA County	Manhattan Beach	1	2	3		
LA	Los Angeles-Long Beach-Santa Ana	LA County	Montebello	1	2	3		
LA	Los Angeles-Long Beach-Santa Ana	LA County	Monterey Park	1				
LA	Los Angeles-Long Beach-Santa Ana	LA County	Paramount	1	2	3		
LA	Los Angeles-Long Beach-Santa Ana	LA County	Pasadena	1	2	3	10	
LA	Los Angeles-Long Beach-Santa Ana	LA County	Pico Rivera	1				
LA	Los Angeles-Long Beach-Santa Ana	LA County	Pomona	1	2	10		
LA	Los Angeles-Long Beach-Santa Ana	LA County	Rancho Cucamonga	1	2	10		
LA	Los Angeles-Long Beach-Santa Ana	LA County	Redondo Beach	1	2	3		
LA	Los Angeles-Long Beach-Santa Ana	LA County	Rosemead	1	2	3		
LA	Los Angeles-Long Beach-Santa Ana	LA County	Rowland Heights	2	3			
LA	Los Angeles-Long Beach-Santa Ana	LA County	San Gabriel	1	2	3		
LA	Los Angeles-Long Beach-Santa Ana	LA County	San Marino	1	2	3		
LA	Los Angeles-Long Beach-Santa Ana	LA County	San Pedro	2	3			
LA	Los Angeles-Long Beach-Santa Ana	LA County	South El Monte	1	2	3		
LA	Los Angeles-Long Beach-Santa Ana	LA County	South Pasadena	1	2	3		
LA	Los Angeles-Long Beach-Santa Ana	LA County	Stevenson Ranch	1	2			
LA	Los Angeles-Long Beach-Santa Ana	LA County	Torrance	1	2	3		
LA	Los Angeles-Long Beach-Santa Ana	LA County	Valencia	1	2			
LA	Los Angeles-Long Beach-Santa Ana	LA County	West Covina	1	2	3	10	
LA	Los Angeles-Long Beach-Santa Ana	LA County	West Hollywood	2	3	4		
LA	Los Angeles-Long Beach-Santa Ana	LA County	Wilmington	1	2	3		

1. Groundwater; 2. Feather River/California Aqueduct; 3. Colorado River; 4. Owens and Mono Basin/LA Aqueduct; 5. Tuolumne River/SFPUC; 6. Mokelumne River/EBMUD; 7. Russian and Eel Rivers; 8. Lake Berryessa/Putah Creek; 9. Central Valley Project/USBR; 10. Local Reservoirs/Streams; 11. Ocean Desalination.

Table 9. Cities in the Riverside-San Bernardino-Ontario metropolitan area sampled and culinary water sources. Source information obtained from 2013/2014 water quality Consumer Confidence Reports.

Region	Metro Area	Geography	City	Water Sources				
LA	Riverside-San Bernardino-Ontario	Riverside County	Banning	1				
LA	Riverside-San Bernardino-Ontario	Riverside County	Cathedral City	1	2	3		
LA	Riverside-San Bernardino-Ontario	Riverside County	Corona	1	2	3	10	
LA	Riverside-San Bernardino-Ontario	Riverside County	Glen Avon	1	2	3		
LA	Riverside-San Bernardino-Ontario	Riverside County	Hemet	1	2	3	10	
LA	Riverside-San Bernardino-Ontario	Riverside County	Lake Elsinore	1	3	10		
LA	Riverside-San Bernardino-Ontario	Riverside County	Moreno Valley	1	2			
LA	Riverside-San Bernardino-Ontario	Riverside County	Murrieta	1	2	3	10	
LA	Riverside-San Bernardino-Ontario	Riverside County	Norco	1				
LA	Riverside-San Bernardino-Ontario	Riverside County	Perris	1	2	3		
LA	Riverside-San Bernardino-Ontario	Riverside County	Riverside	1				
LA	Riverside-San Bernardino-Ontario	Riverside County	San Jacinto	1	2	10		
LA	Riverside-San Bernardino-Ontario	Riverside County	Temecula	1	2	3	10	
LA	Riverside-San Bernardino-Ontario	San Bernadino County	Chino	1	2			
LA	Riverside-San Bernardino-Ontario	San Bernadino County	Chino Hills	1	2	3		
LA	Riverside-San Bernardino-Ontario	San Bernadino County	Colton	1				
LA	Riverside-San Bernardino-Ontario	San Bernadino County	Eastvale	1	2	3		
LA	Riverside-San Bernardino-Ontario	San Bernadino County	Fontana	1	2	10		
LA	Riverside-San Bernardino-Ontario	San Bernadino County	Grand Terrace	1	2			
LA	Riverside-San Bernardino-Ontario	San Bernadino County	Highland	1	2	10		
LA	Riverside-San Bernardino-Ontario	San Bernadino County	Loma Linda	1				
LA	Riverside-San Bernardino-Ontario	San Bernadino County	Montclair	1	2			
LA	Riverside-San Bernardino-Ontario	San Bernadino County	Ontario	1	2	3		
LA	Riverside-San Bernardino-Ontario	San Bernadino County	Redlands	1	2	10		
LA	Riverside-San Bernardino-Ontario	San Bernadino County	Rialto	1	2	10		
LA	Riverside-San Bernardino-Ontario	San Bernadino County	San Bernardino	1	2	10		
LA	Riverside-San Bernardino-Ontario	San Bernadino County	Upland	1	2	10		
LA	Riverside-San Bernardino-Ontario	San Bernadino County	Yermo	1				
LA	Riverside-San Bernardino-Ontario	San Bernadino County	Yucaipa	1	2	10		

1. Groundwater; 2. Feather River/California Aqueduct; 3. Colorado River; 4. Owens and Mono Basin/LA Aqueduct; 5. Tuolumne River/SFPUC; 6. Mokelumne River/EBMUD; 7. Russian and Eel Rivers; 8. Lake Berryessa/Putah Creek; 9. Central Valley Project/USBR; 10. Local Reservoirs/Streams; 11. Ocean Desalination.

Table 10. Summary statistics for the oxygen, hydrogen, and strontium isotope ratios from tap water samples collected in the San Diego-Carlsbad-San Marcos Metropolitan Area.

Date	Statistic	$\delta^{18}O$ (‰, VSMOW)	$\delta^{2}H$ (‰, VSMOW)	$^{87}Sr/^{86}Sr$
Winter 2013/2014	Mean	-10.5	-86	–
	SD	2.3	17	–
	Range	9.7	68	–
	Min	-11.7	-94	–
	Max	-2.0	-26	–
	Count	25	25	0
Spring 2014	Mean	-10.5	-85	0.70989
	SD	2.5	18	0.00098
	Range	11.0	74	0.00451
	Min	-12.1	-97	0.70613
	Max	-1.2	-24	0.71064
	Count	68	68	35

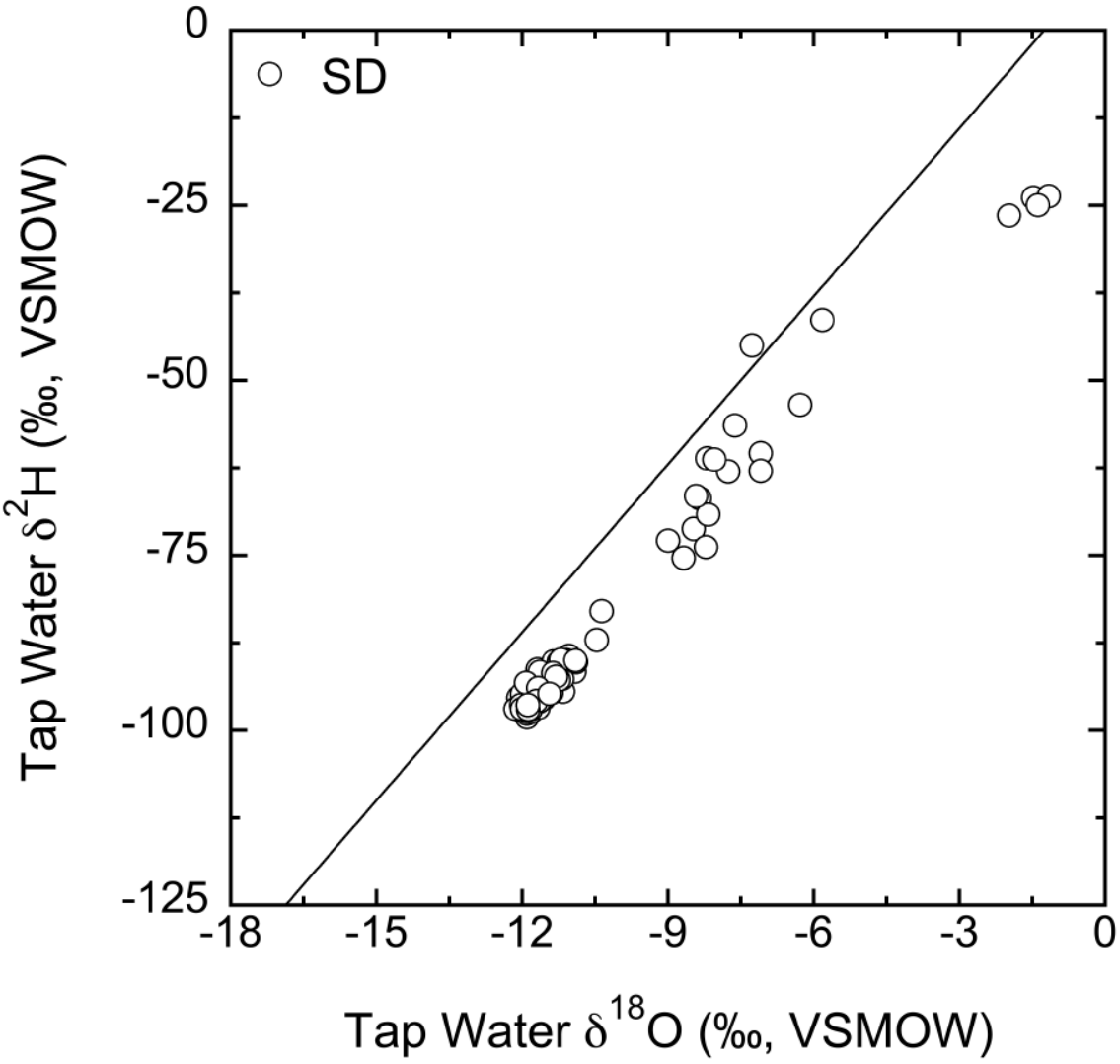

Figure 18. Cross-plot of the δ^2H and $\delta^{18}O$ values of tap water from the San Diego-Carlsbad-San Marcos metropolitan area. Meteoric water line is shown.

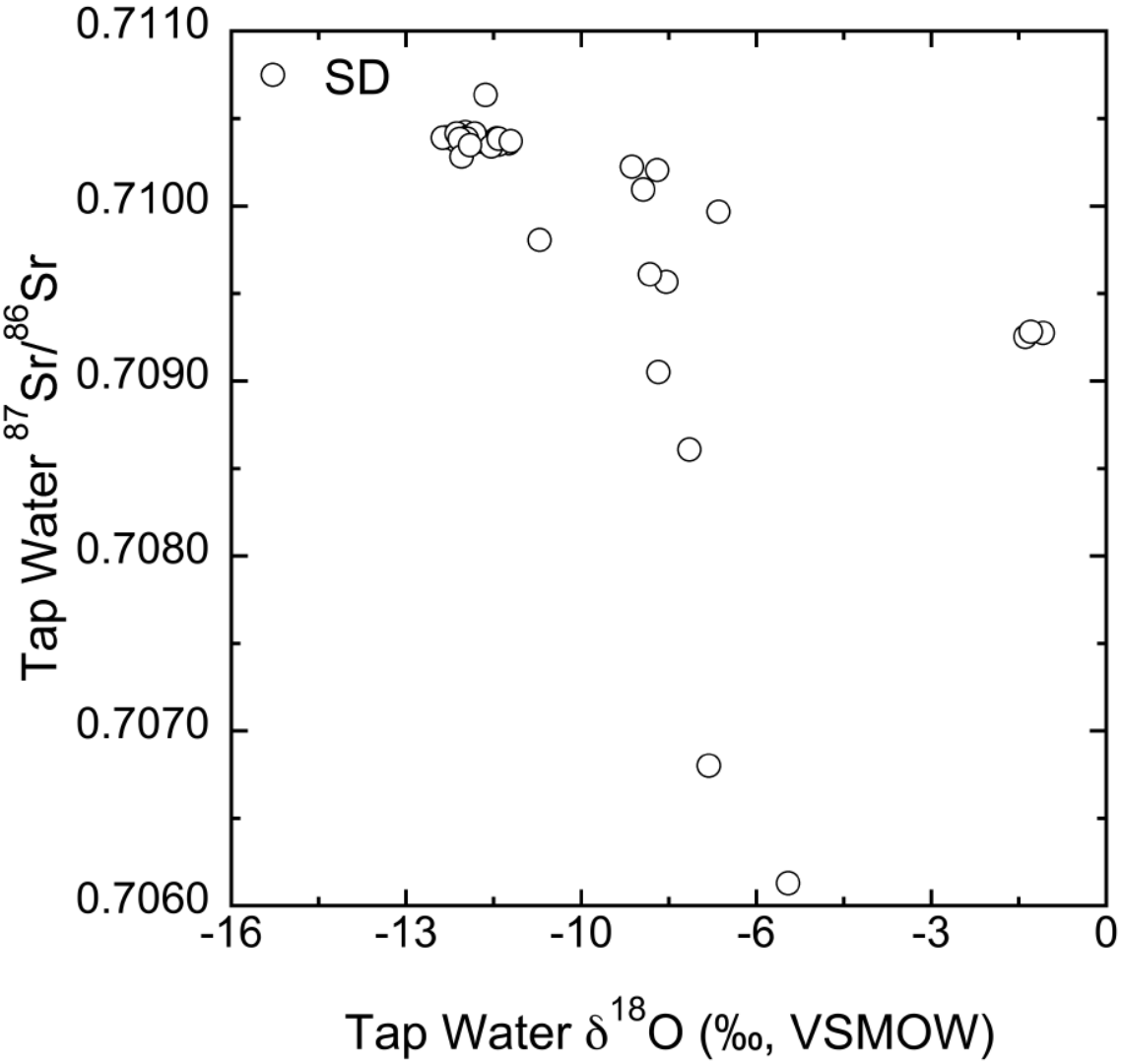

Figure 19. Cross-plot of the $^{87}Sr/^{86}Sr$ ratios and $\delta^{18}O$ values of tap water from the San Diego-Carlsbad-San Marcos metropolitan area.

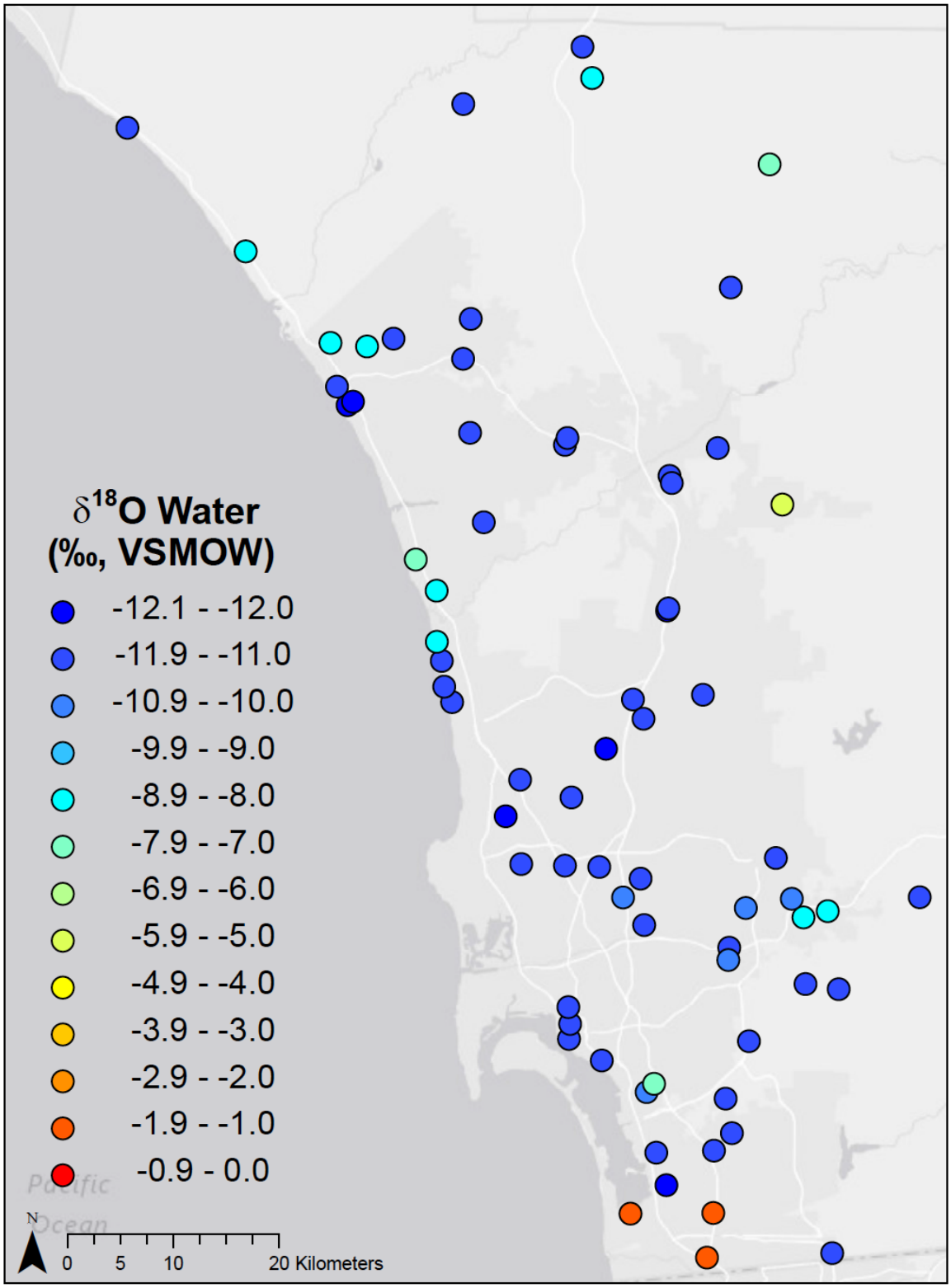

Figure 20. Spatial distribution of the $\delta^{18}O$ values of tap water from the San Diego-Carlsbad-San Marcos metropolitan area collected in Spring 2014.

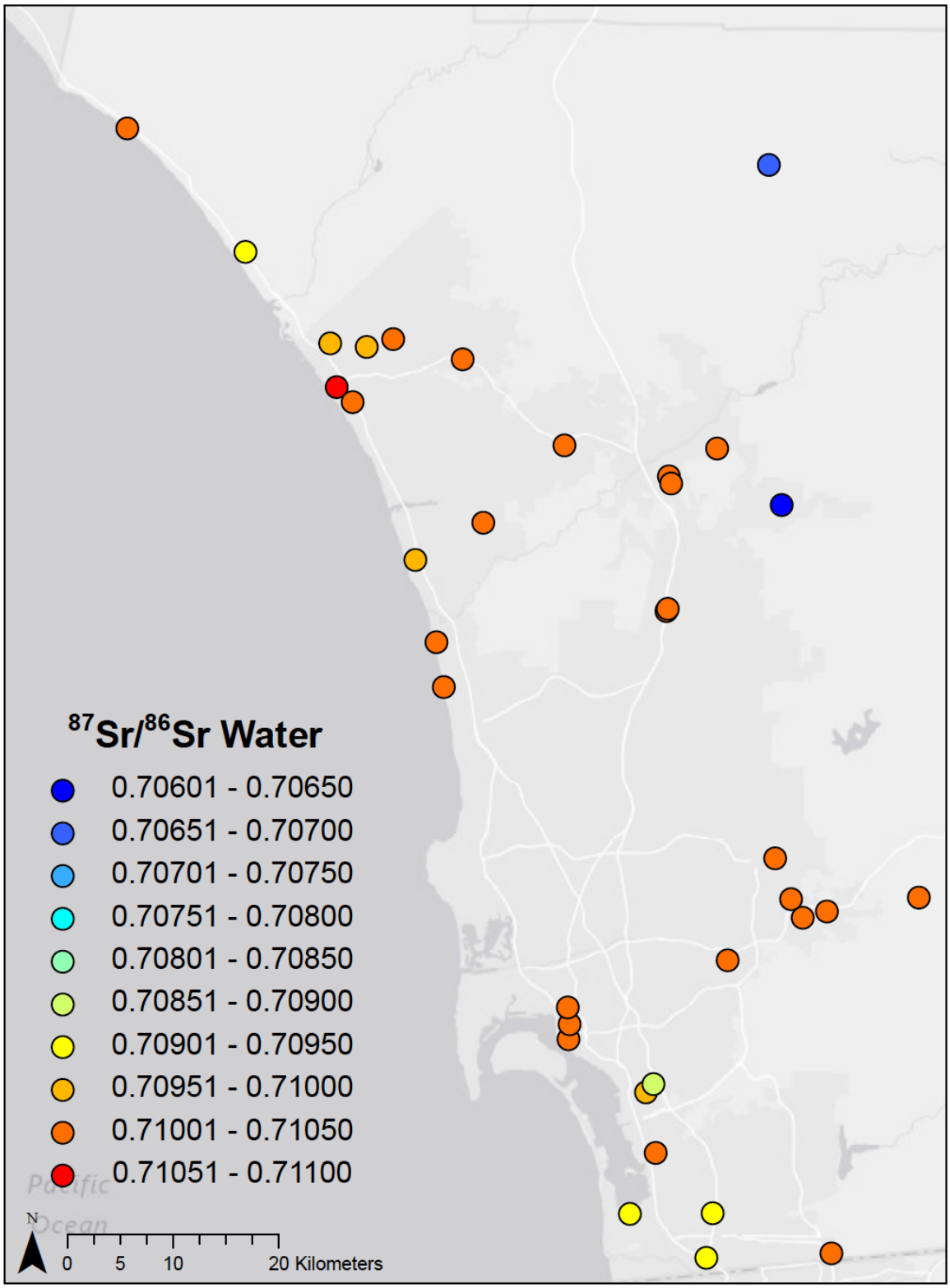

Figure 21. Spatial distribution of the $^{87}Sr/^{86}Sr$ ratios of tap water from the San Diego-Carlsbad-San Marcos metropolitan area in Spring 2014.

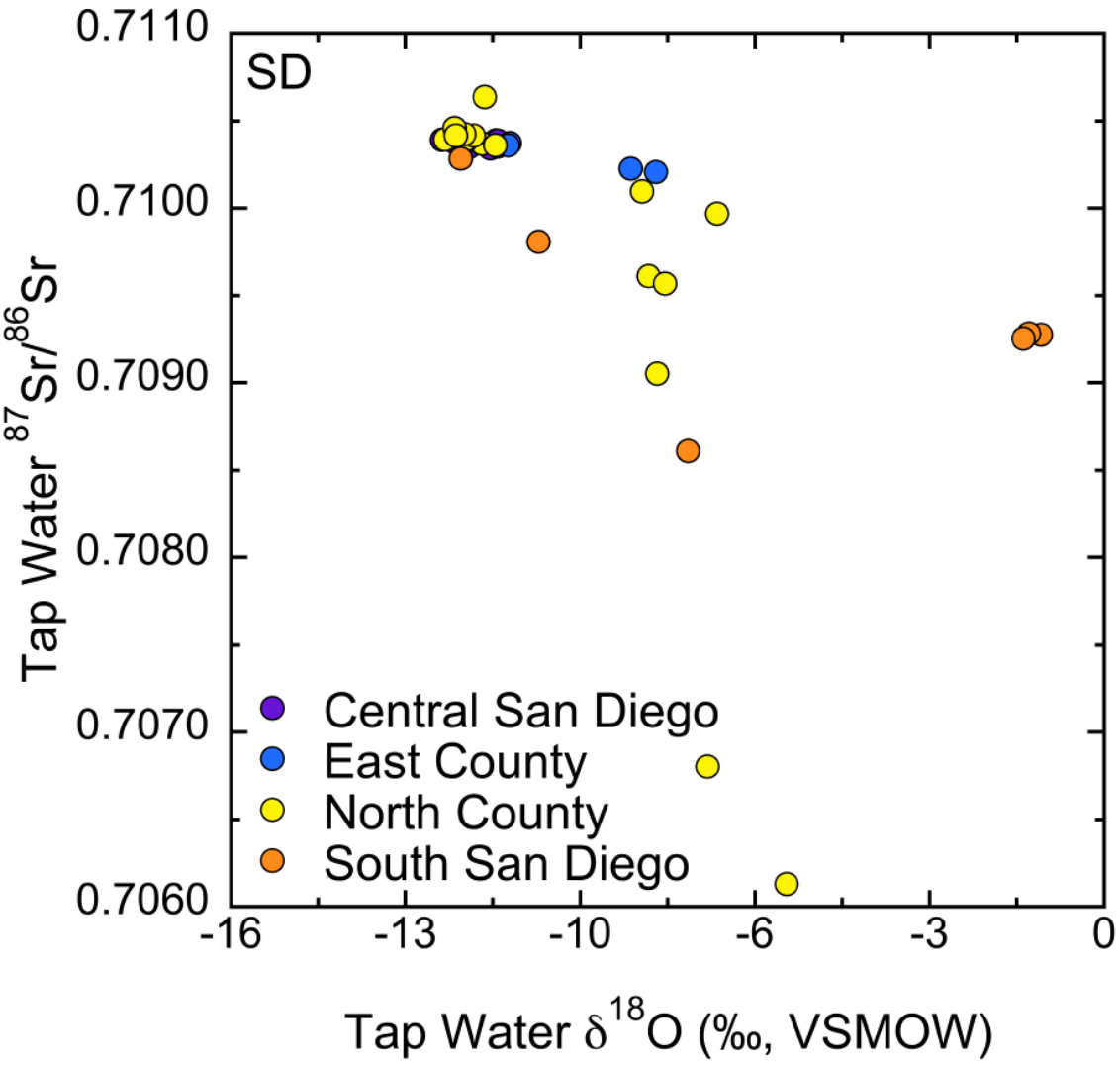

Figure 22. Cross-plot of the $^{87}Sr/^{86}Sr$ ratios and $\delta^{18}O$ values of tap water from the San Diego-Carlsbad-San Marcos metropolitan area. Regions of the San Diego-Carlsbad-San Marcos metropolitan area are represented with unique colored symbols.

Table 11. Cities in the San Diego-Carlsbad-San Marcos metropolitan area sampled and culinary water sources. Source information obtained from 2013/2014 water quality Consumer Confidence Reports.

Region	Metro Area	Geography	City	Water Sources				
SD	San Diego-Carlsbad-San Marcos	Central San Diego	Barrio Logan	2	3	10		
SD	San Diego-Carlsbad-San Marcos	Central San Diego	Bonita	2	3	10		
SD	San Diego-Carlsbad-San Marcos	Central San Diego	Clairemont Mesa	2	3	10		
SD	San Diego-Carlsbad-San Marcos	Central San Diego	Grantsville	2	3	10		
SD	San Diego-Carlsbad-San Marcos	Central San Diego	Kearney Mesa	2	3	10		
SD	San Diego-Carlsbad-San Marcos	Central San Diego	La Jolla	2	3	10		
SD	San Diego-Carlsbad-San Marcos	Central San Diego	Mira Mesa	2	3	10		
SD	San Diego-Carlsbad-San Marcos	Central San Diego	Miramar	2	3	10		
SD	San Diego-Carlsbad-San Marcos	Central San Diego	Rancho Penasquitos	2	3	10		
SD	San Diego-Carlsbad-San Marcos	Central San Diego	San Carlos	2	3	10		
SD	San Diego-Carlsbad-San Marcos	Central San Diego	San Diego	2	3	10		
SD	San Diego-Carlsbad-San Marcos	Central San Diego	Scripps Ranch	2	3	10		
SD	San Diego-Carlsbad-San Marcos	Central San Diego	Serra Mesa	2	3	10		
SD	San Diego-Carlsbad-San Marcos	Central San Diego	Sorrento Valley	2	3	10		
SD	San Diego-Carlsbad-San Marcos	Central San Diego	Tierra Santa	2	3	10		
SD	San Diego-Carlsbad-San Marcos	Central San Diego	University City	2	3	10		
SD	San Diego-Carlsbad-San Marcos	East County	Casa de Oro-Mount Helix	2	3	10		
SD	San Diego-Carlsbad-San Marcos	East County	El Cajon	2	3	10		
SD	San Diego-Carlsbad-San Marcos	East County	La Presa	2	3	10		
SD	San Diego-Carlsbad-San Marcos	East County	Rancho San Diego	2	3	10		
SD	San Diego-Carlsbad-San Marcos	East County	Santee	2	3			
SD	San Diego-Carlsbad-San Marcos	East County	Spring Valley	2	3	10		
SD	San Diego-Carlsbad-San Marcos	North County	Cardiff By The Sea	2	3	10		
SD	San Diego-Carlsbad-San Marcos	North County	Carlsbad	2	3			
SD	San Diego-Carlsbad-San Marcos	North County	Carmel Valley	2	3	10		
SD	San Diego-Carlsbad-San Marcos	North County	Del Mar	2	3	10		
SD	San Diego-Carlsbad-San Marcos	North County	Encinitas	2	3	10		
SD	San Diego-Carlsbad-San Marcos	North County	Escondido	2	3	10		
SD	San Diego-Carlsbad-San Marcos	North County	Fallbrook	2	3	10		
SD	San Diego-Carlsbad-San Marcos	North County	Oceanside	1	2	3	11	
SD	San Diego-Carlsbad-San Marcos	North County	Pauma Valley	1				
SD	San Diego-Carlsbad-San Marcos	North County	Poway	2	3	10		
SD	San Diego-Carlsbad-San Marcos	North County	San Marcos	2	3			
SD	San Diego-Carlsbad-San Marcos	North County	San Onofre	2	3	10		
SD	San Diego-Carlsbad-San Marcos	North County	Solana Beach	2	3	10		
SD	San Diego-Carlsbad-San Marcos	North County	Valley Center	2	3			
SD	San Diego-Carlsbad-San Marcos	North County	Vista	1	2	3	10	
SD	San Diego-Carlsbad-San Marcos	South San Diego	Chula Vista	2	3	10		
SD	San Diego-Carlsbad-San Marcos	South San Diego	Imperial Beach	2	3	10		
SD	San Diego-Carlsbad-San Marcos	South San Diego	National City	1	2	3	10	
SD	San Diego-Carlsbad-San Marcos	South San Diego	Otay Mesa West	2	3	10		
SD	San Diego-Carlsbad-San Marcos	South San Diego	San Ysidro	2	3	10		

1. Groundwater; 2. Feather River/California Aqueduct; 3. Colorado River; 4. Owens and Mono Basin/LA Aqueduct; 5. Tuolumne River/SFPUC; 6. Mokelumne River/EBMUD; 7. Russian and Eel Rivers; 8. Lake Berryessa/Putah Creek; 9. Central Valley Project/USBR; 10. Local Reservoirs/Streams; 11. Ocean Desalination.

Table 12. Summary statistics for the oxygen, hydrogen, and strontium isotope ratios from hair samples collected in the Phoenix-Mesa-Glendale Metropolitan Area.

Date	Statistic	$\delta^{18}O$ (‰, VSMOW)	$\delta^{2}H$ (‰, VSMOW)	$^{87}Sr/^{86}Sr$
Spring 2014	Mean	11.9	-84	0.71022
	SD	1.0	5	0.00064
	Range	4.1	18	0.00274
	Min	9.6	-96	0.70877
	Max	13.7	-77	0.71150
	Count	17	17	17
Fall 2014	Mean	12.0	-86	0.71137
	SD	1.0	6	0.00144
	Range	4.1	26	0.00485
	Min	9.3	-103	0.70849
	Max	13.4	-77	0.71334
	Count	18	18	18

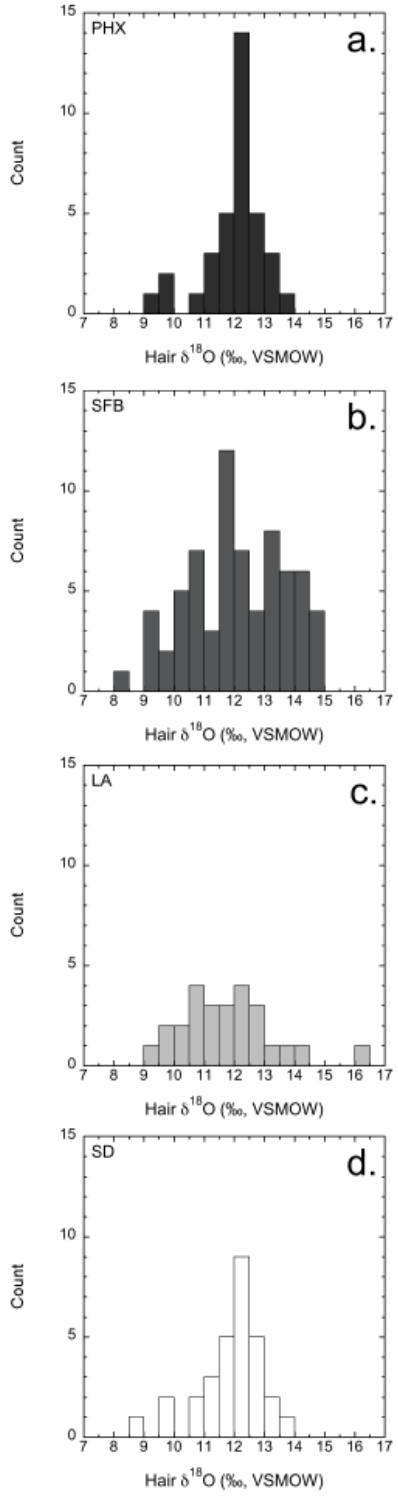

Figure 23. Histogram of the $\delta^{18}O$ values of hair from the Phoenix-Mesa-Glendale (PHX, panel a), San Francisco-Oakland-Fremont and San Jose-Sunnyvale-Santa Clara (SFB, panel b), Los Angeles-Long Beach-Santa Ana and Riverside-San Bernardino-Ontario (LA, panel c), and San Diego-Carlsbad-San Marcos (SD, panel d) metropolitan areas.

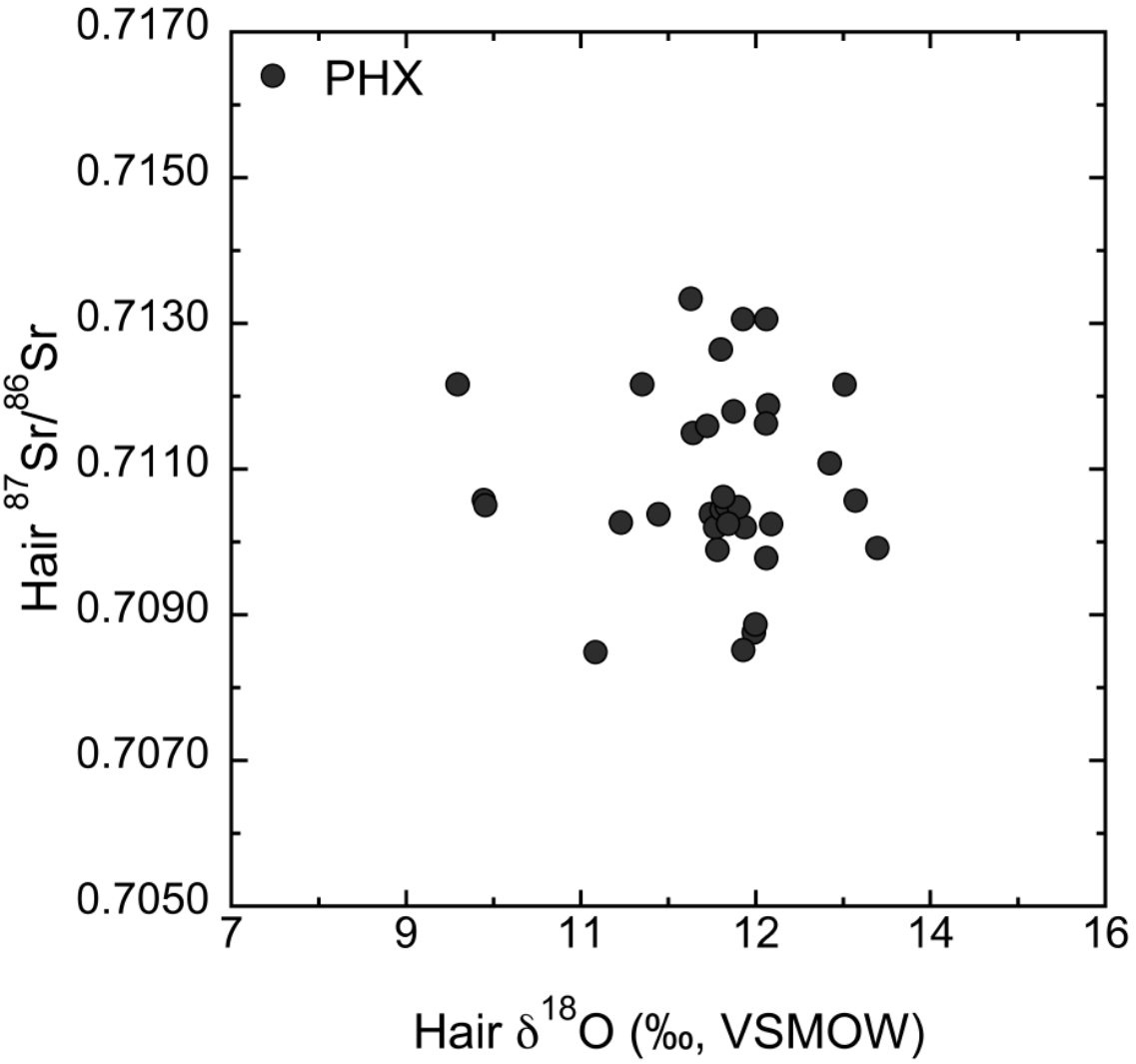

Figure 24. Cross-plot of the $^{87}Sr/^{86}Sr$ ratios and $\delta^{18}O$ values of hair from the Phoenix-Mesa-Glendale metropolitan area.

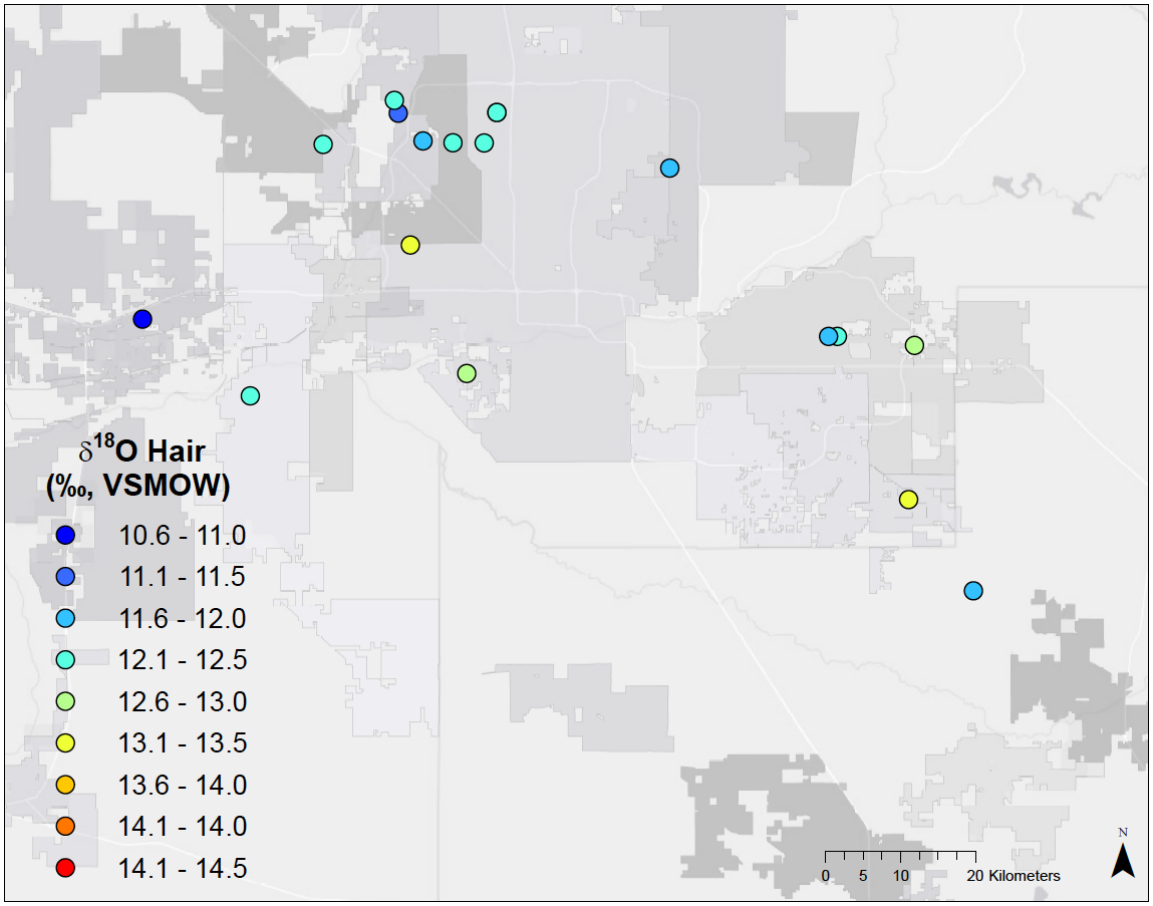

Figure 25. Spatial distribution of the $\delta^{18}O$ values of hair from the Phoenix-Mesa-Glendale metropolitan area.

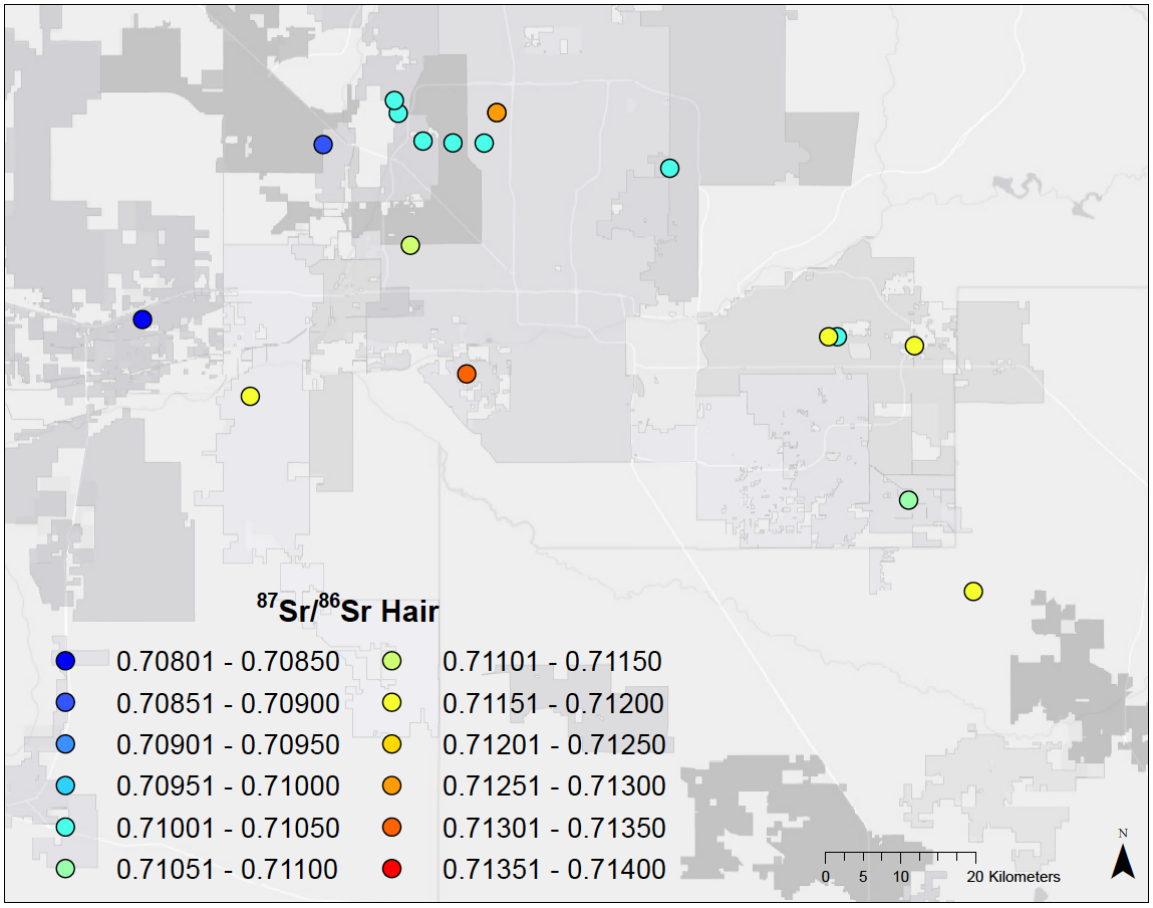

Figure 26. Spatial distribution of the $^{87}Sr/^{86}Sr$ ratios of hair from the Phoenix-Mesa-Glendale metropolitan area.

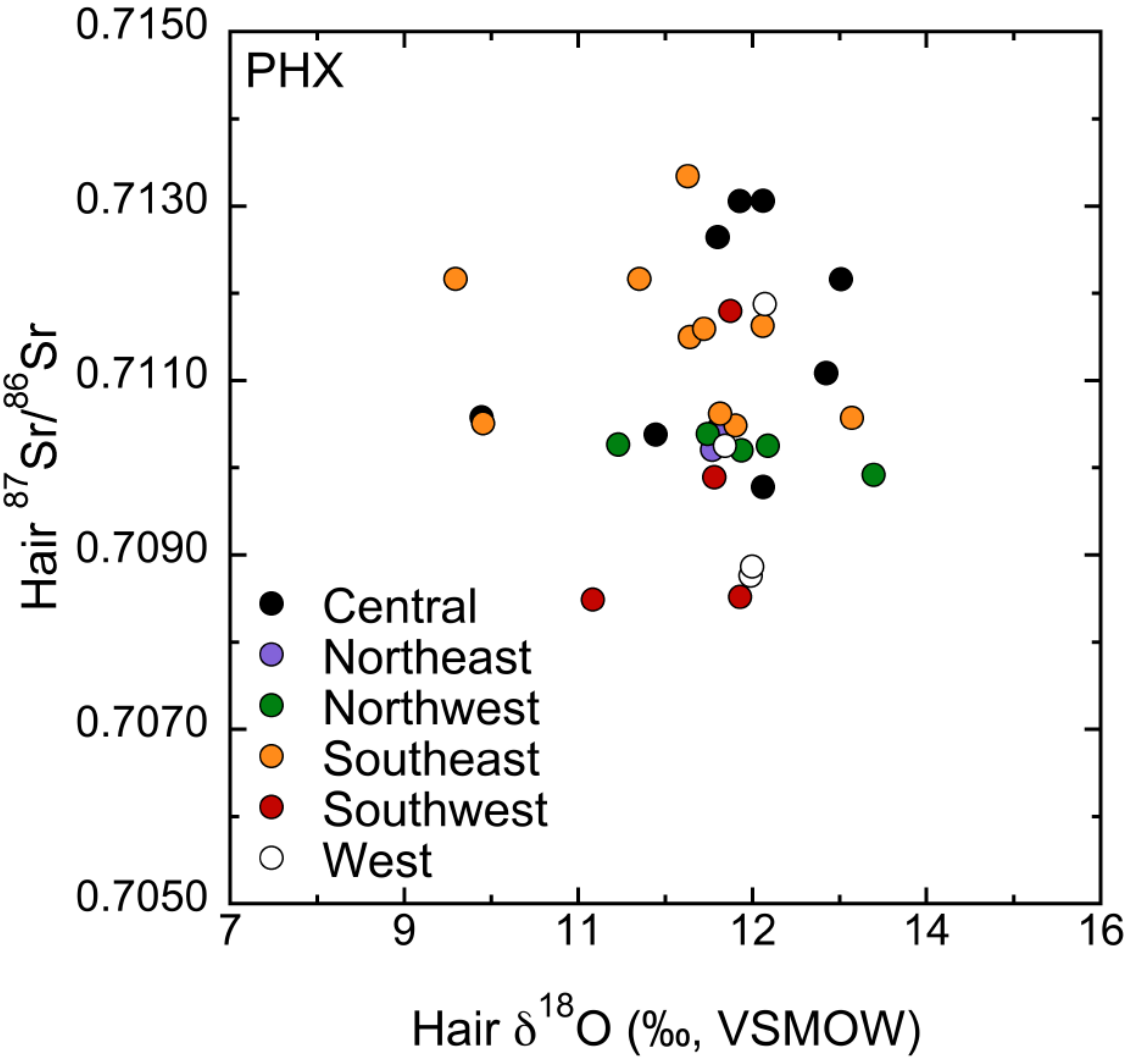

Figure 27. Cross-plot of the $^{87}Sr/^{86}Sr$ ratios and $\delta^{18}O$ values of hair from the Phoenix-Mesa-Glendale metropolitan area. Colored symbols represent regions within the Phoenix-Mesa-Glendale metropolitan area.

Table 13. Summary statistics for the oxygen, hydrogen, and strontium isotope ratios from hair samples collected in the San Francisco-Oakland-Fremont and San Jose-Sunnyvale-Santa Clara Metropolitan Areas.

Date	Statistic	$\delta^{18}O$ (‰, VSMOW)	$\delta^{2}H$ (‰, VSMOW)	$^{87}Sr/^{86}Sr$
Winter 2013/2014	Mean	11.5	-82	0.70737
	SD	2.0	12	0.00042
	Range	5.9	35	0.00151
	Min	8.3	-100	0.70671
	Max	14.3	-65	0.70822
	Count	12	12	12
Spring 2014	Mean	12.2	-79	0.70743
	SD	1.5	7	0.00055
	Range	5.8	33	0.00263
	Min	9.0	-101	0.70660
	Max	14.8	-67	0.70923
	Count	57	57	57

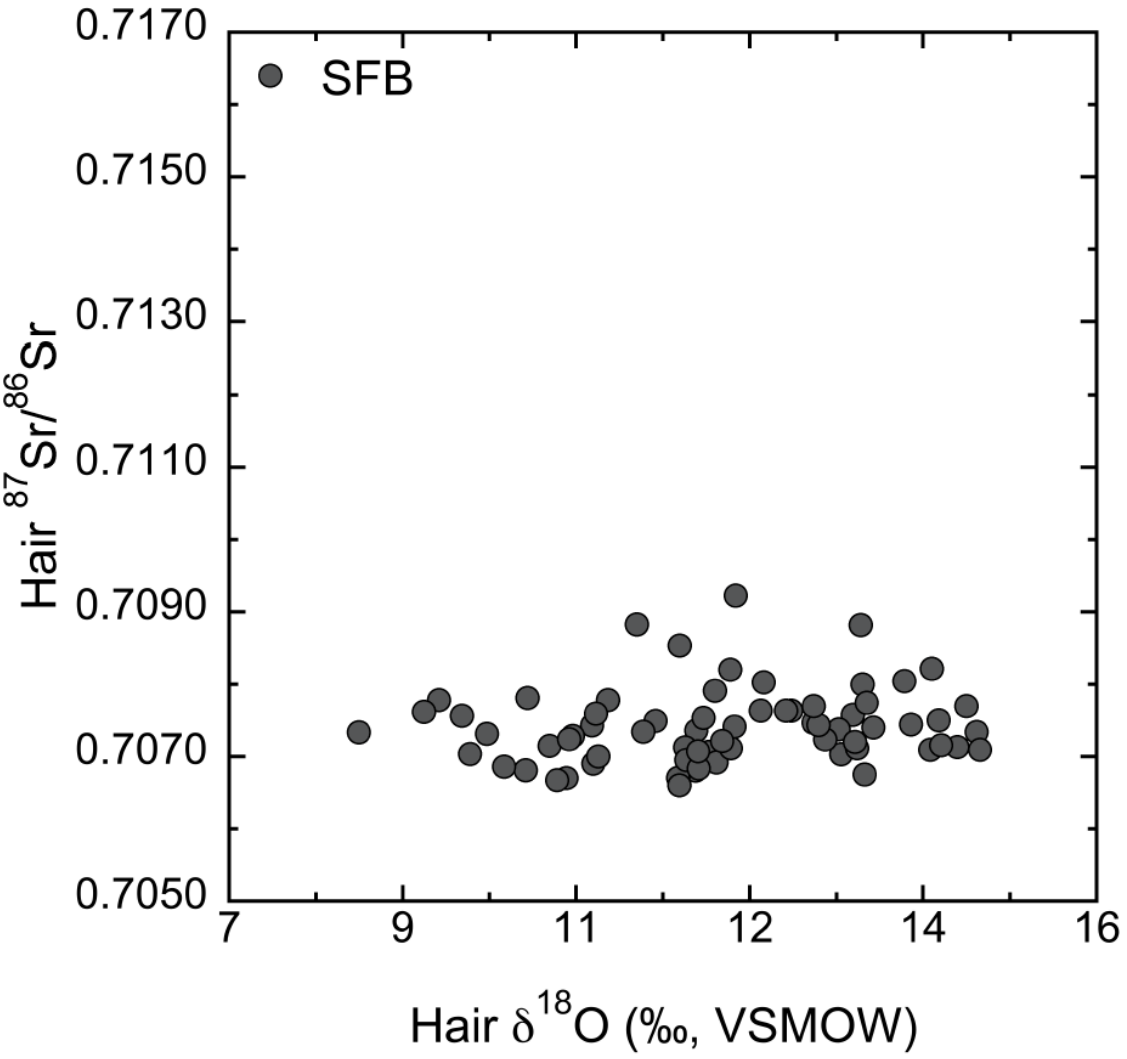

Figure 28. Cross-plot of the $^{87}Sr/^{86}Sr$ ratio and $\delta^{18}O$ values of hair from the San Francisco-Oakland-Fremont and San Jose-Sunnyvale-Santa Clara metropolitan areas.

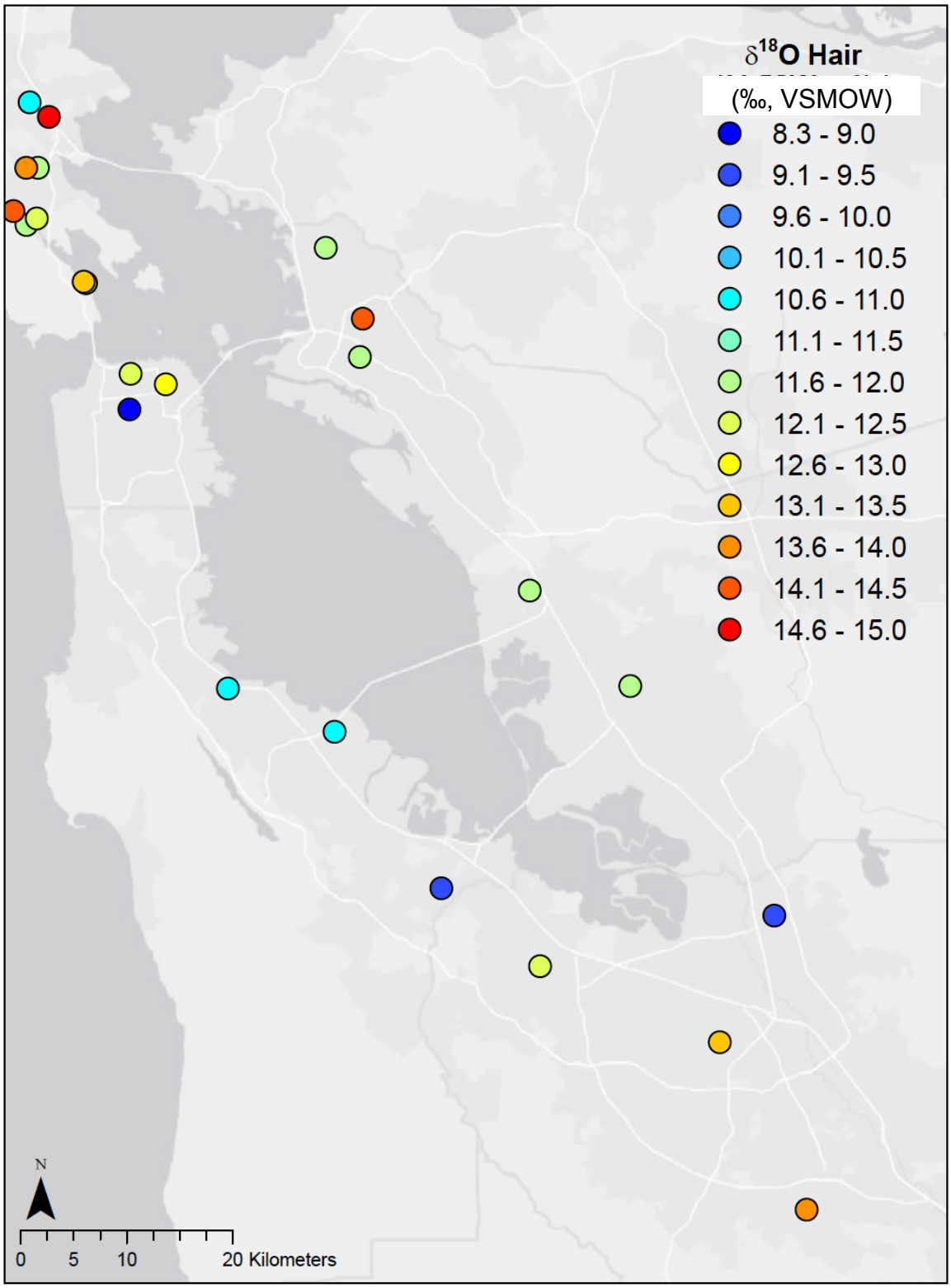

Figure 29. Spatial distribution of the $\delta^{18}O$ values of hair from the San Francisco-Oakland-Fremont and San Jose-Sunnyvale-Santa Clara metropolitan areas.

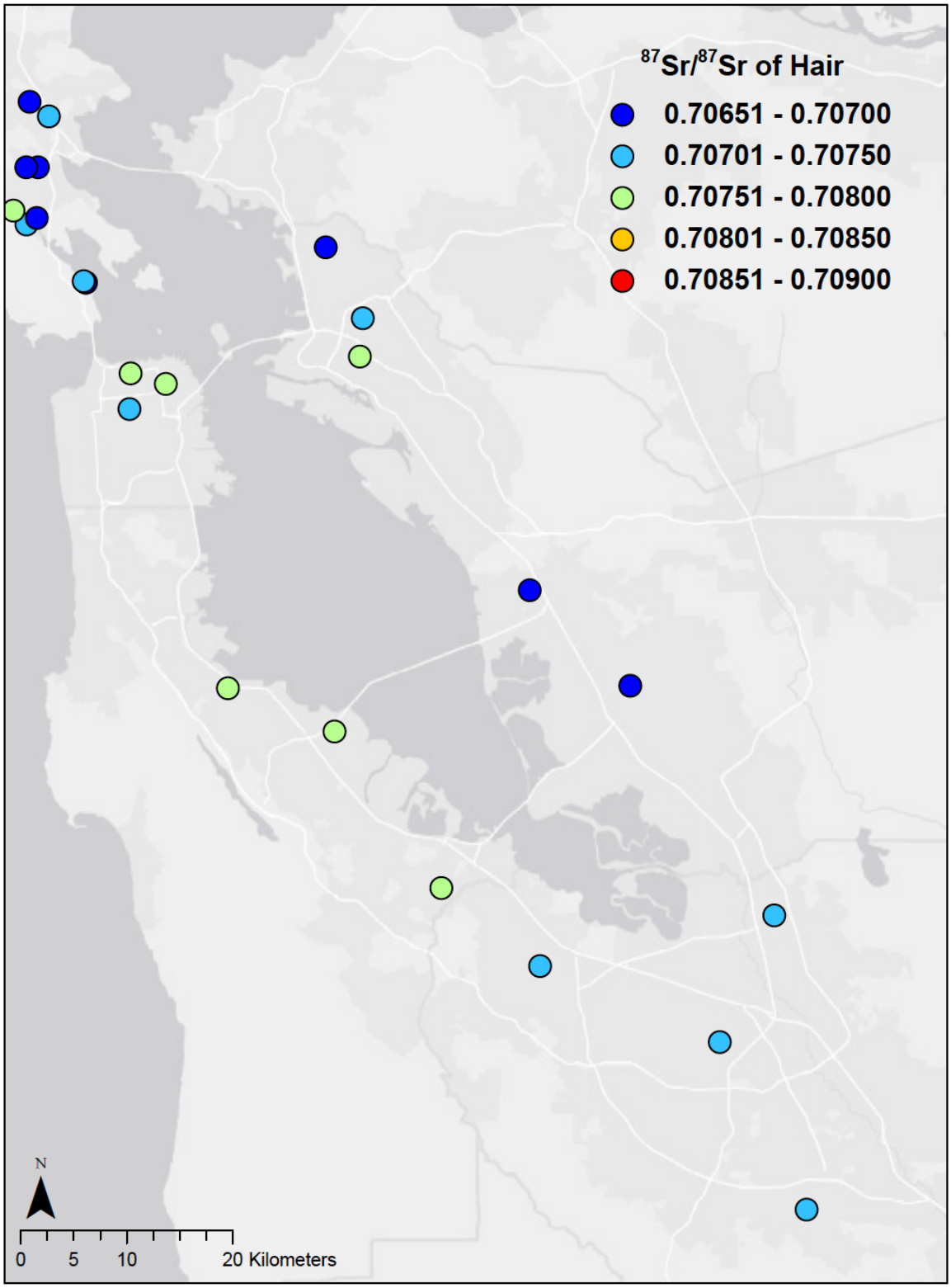

Figure 30. Spatial distribution of the $^{87}Sr/^{86}Sr$ ratio of hair from the San Francisco-Oakland-Fremont and San Jose-Sunnyvale-Santa Clara metropolitan areas.

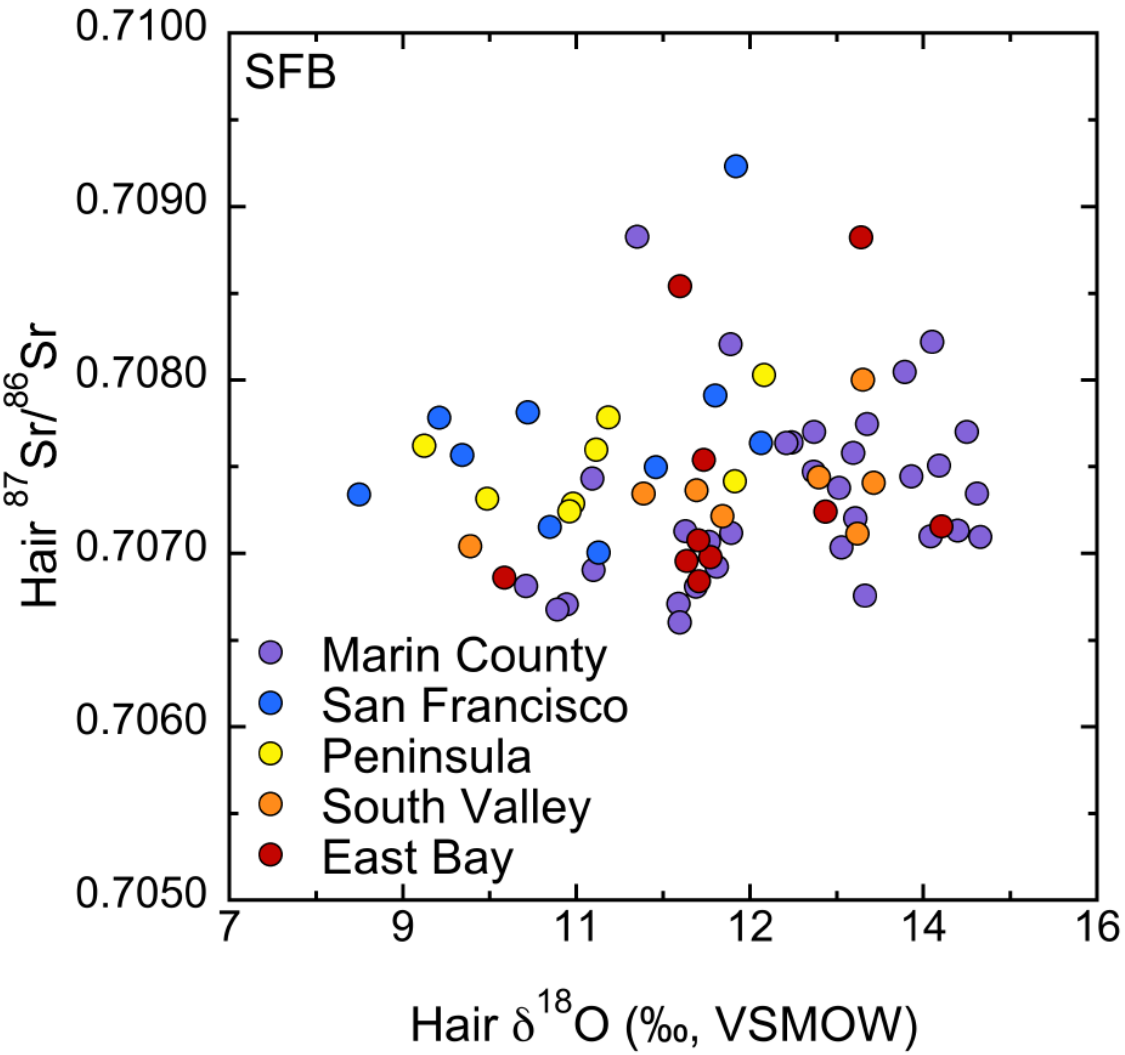

Figure 31. Cross-plot of the $^{87}Sr/^{86}Sr$ ratio and $\delta^{18}O$ values of hair from the San Francisco-Oakland-Fremont and San Jose-Sunnyvale-Santa Clara metropolitan areas. Colored symbols represent regions within the larger SFB metro areas.

Table 14. Summary statistics for the oxygen, hydrogen, and strontium isotope ratios from hair samples collected in the Los Angeles-Long Beach-Santa Ana and Riverside-San Bernardino-Ontario Metropolitan Areas.

Date	Statistic	$\delta^{18}O$ (‰, VSMOW)	$\delta^{2}H$ (‰, VSMOW)	$^{87}Sr/^{86}Sr$
Spring 2014	Mean	11.6	-84	0.70884
	SD	1.7	7	0.00068
	Range	7.4	27	0.00096
	Min	9.0	-98	0.70836
	Max	16.4	-70	0.70932
	Count	18	18	2
Fall 2014	Mean	12.1	-78	–
	SD	1.3	7	–
	Range	3.3	20	–
	Min	10.8	-89	–
	Max	14.1	-68	–
	Count	8	8	0

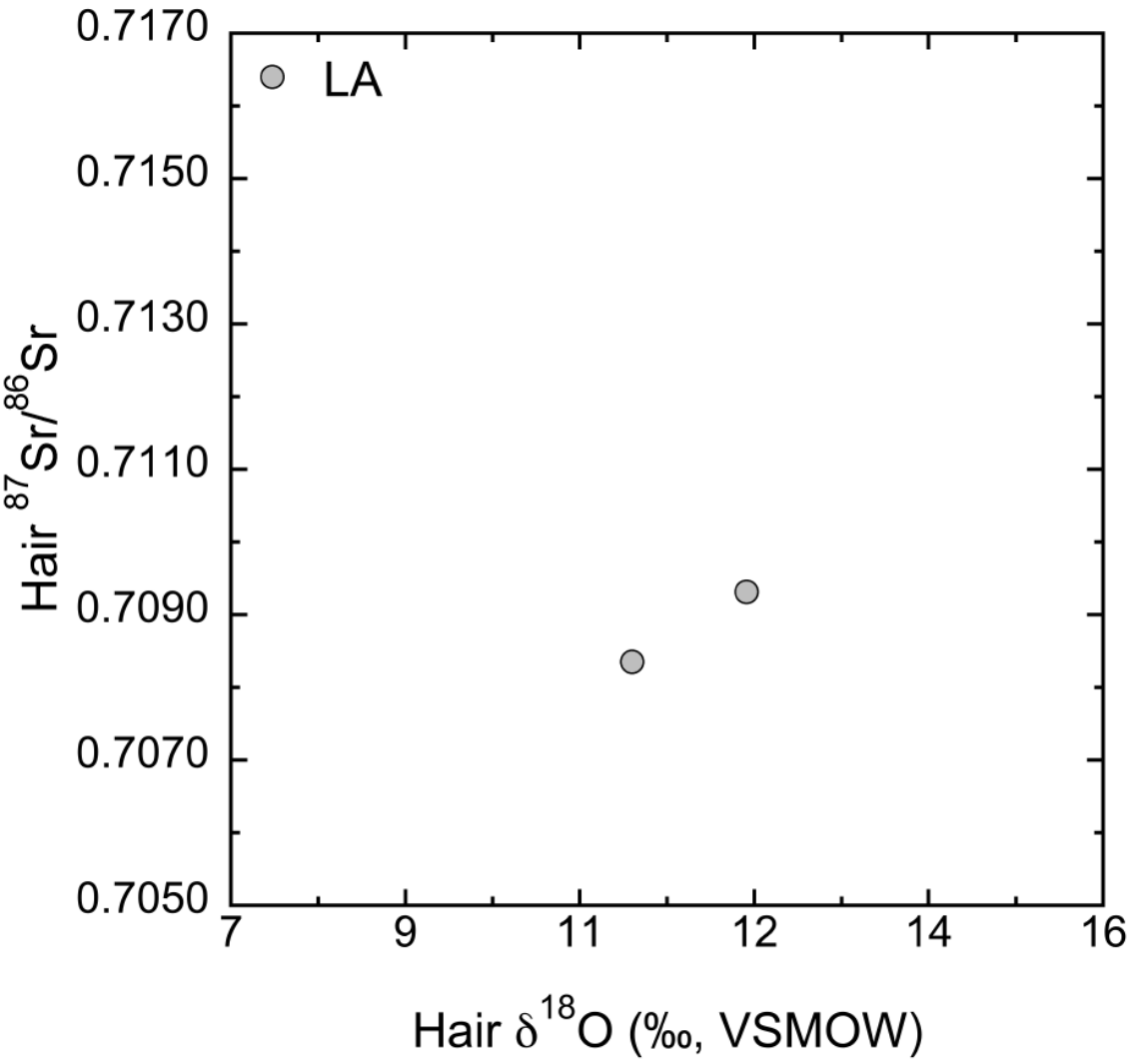

Figure 32. Cross-plot of the $^{87}Sr/^{86}Sr$ ratios and $\delta^{18}O$ values of hair from the Los Angeles-Long Beach-Santa Ana and Riverside-San Bernardino-Ontario metropolitan areas.

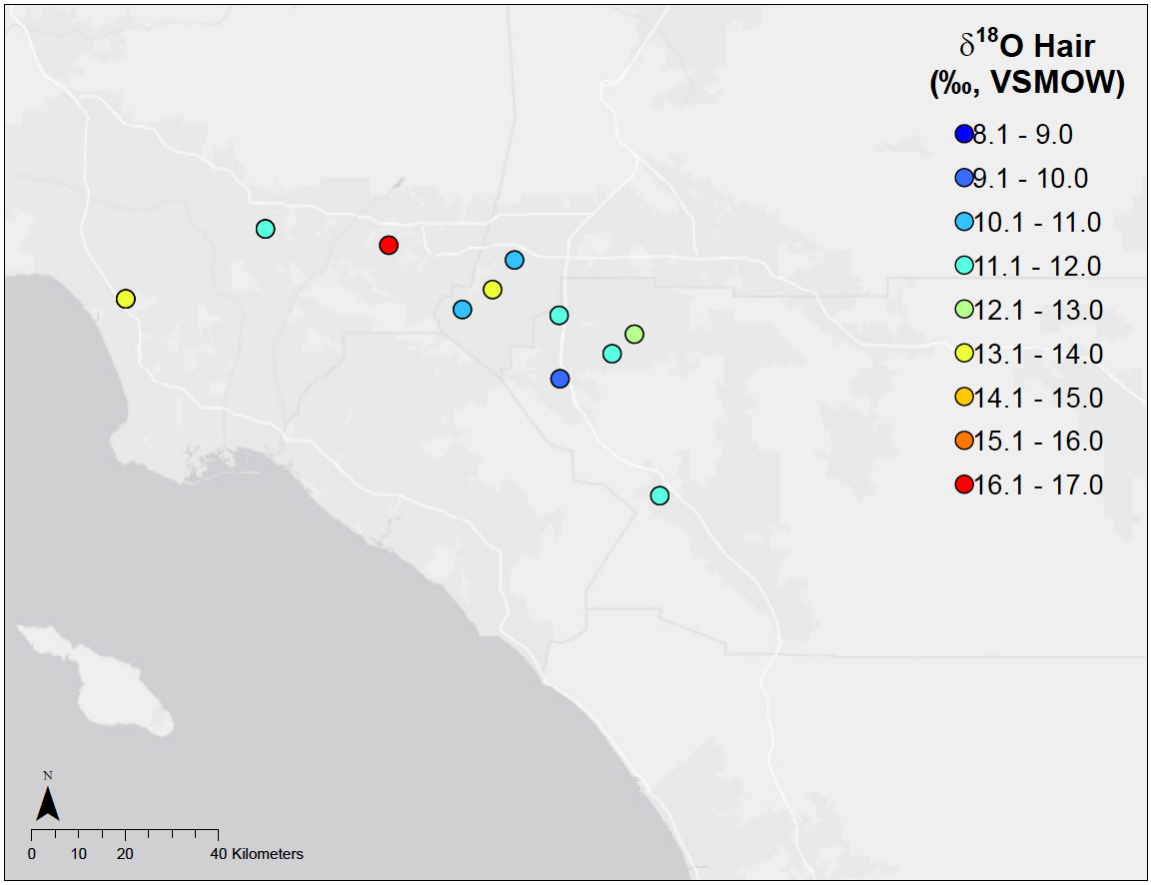

Figure 33. Spatial distribution of the $\delta^{18}O$ values of hair from the Los Angeles-Long Beach-Santa Ana and Riverside-San Bernardino-Ontario metropolitan areas.

Table 15. Summary statistics for the oxygen, hydrogen, and strontium isotope ratios from hair samples collected in the San Diego-Carlsbad-San Marcos Metropolitan Area.

Date	Statistic	$\delta^{18}O$ (‰, VSMOW)	$\delta^{2}H$ (‰, VSMOW)	$^{87}Sr/^{86}Sr$
Spring 2014	Mean	11.9	-82	0.71020
	SD	1.1	7	0.00022
	Range	5.4	27	0.00085
	Min	8.6	-97	0.70954
	Max	14.0	-69	0.71039
	Count	30	30	30

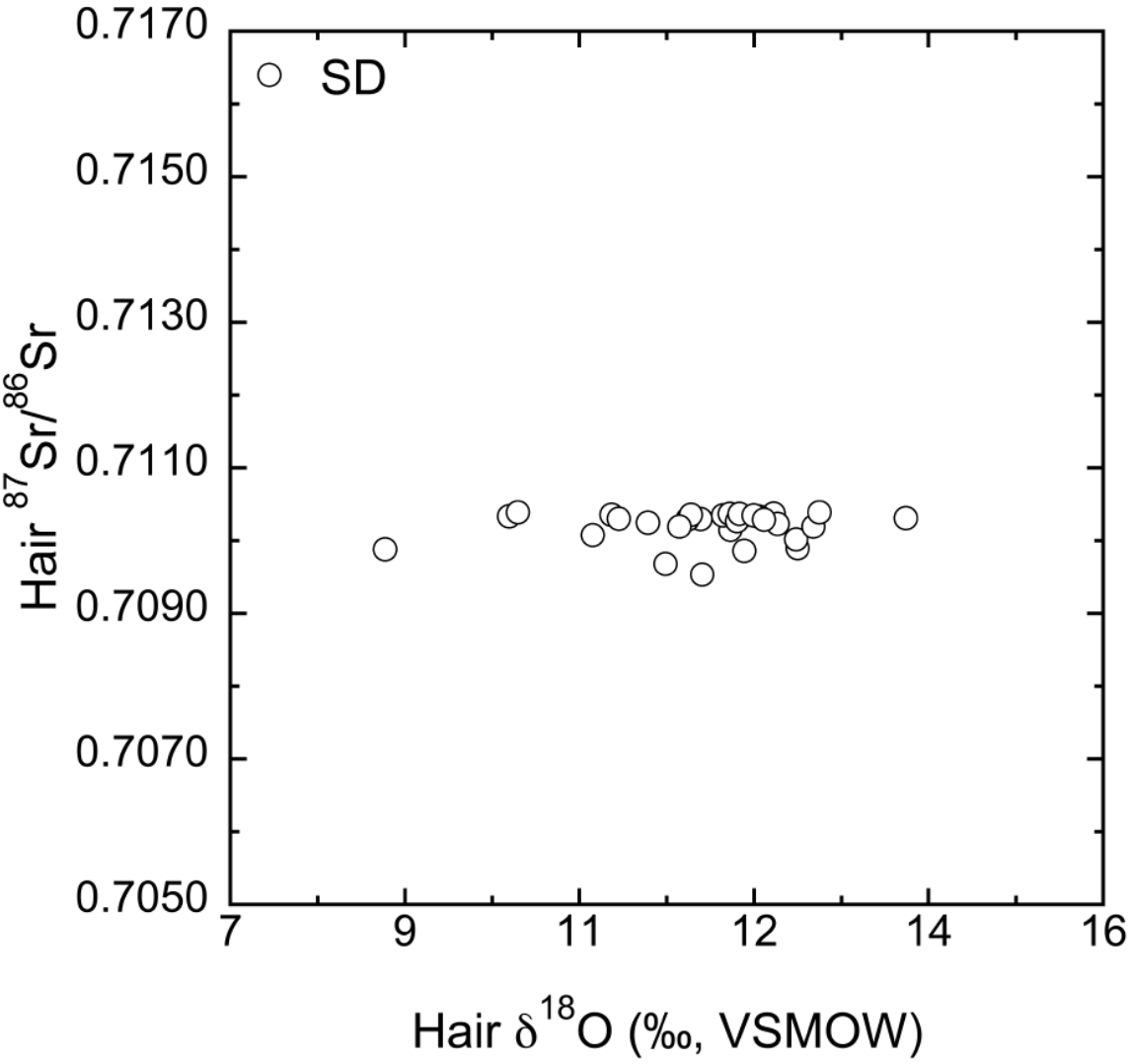

Figure 34. Cross-plot of the $^{87}Sr/^{86}Sr$ ratios and $\delta^{18}O$ values of hair from the San Diego-Carlsbad-San Marcos metropolitan area.

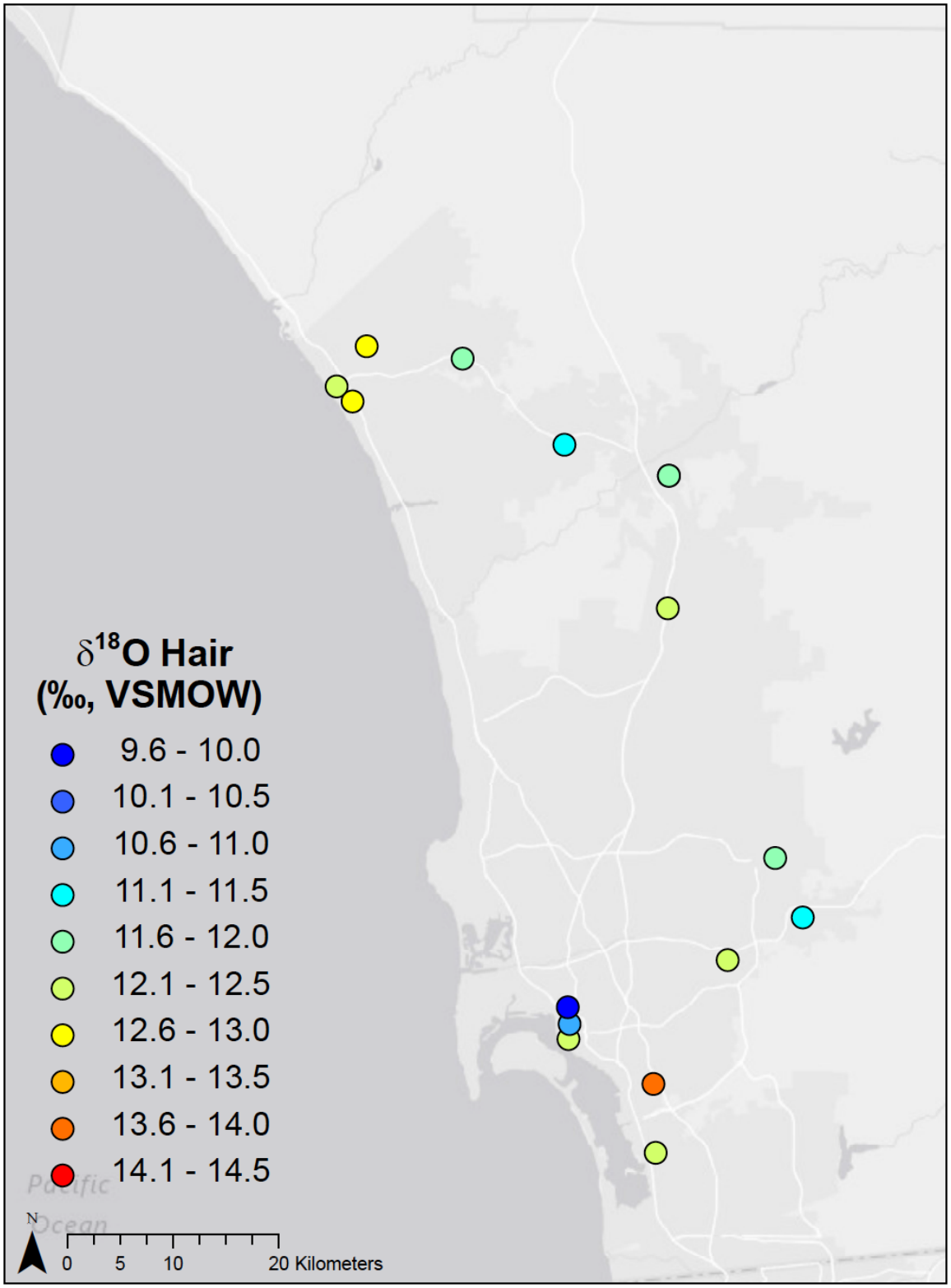

Figure 35. Spatial distribution of the $\delta^{18}O$ values of hair from the San Diego-Carlsbad-San Marcos metropolitan area.

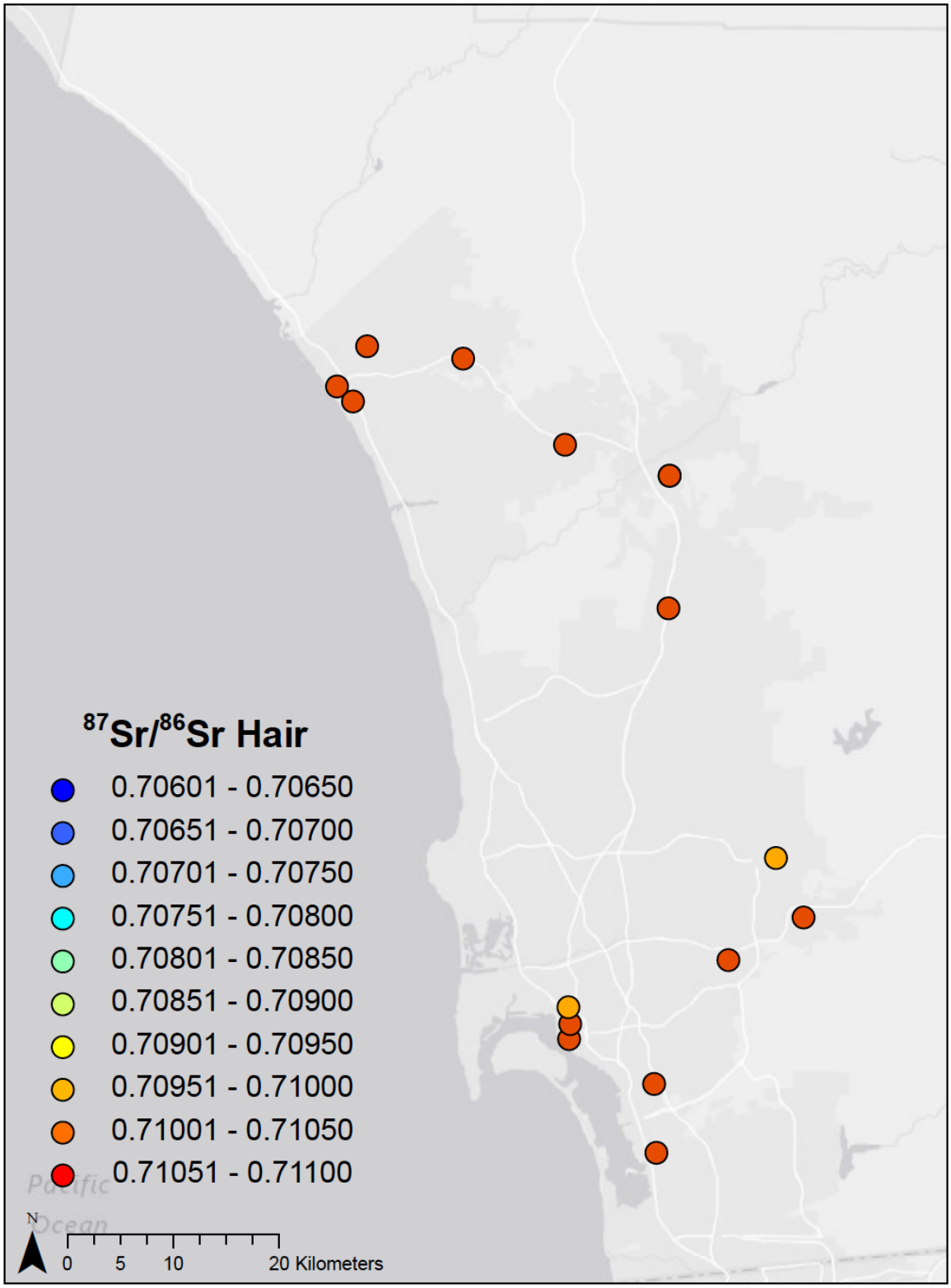

Figure 36. Spatial distribution of the $^{87}Sr/^{86}Sr$ ratios of hair from the San Diego-Carlsbad-San Marcos metropolitan area.

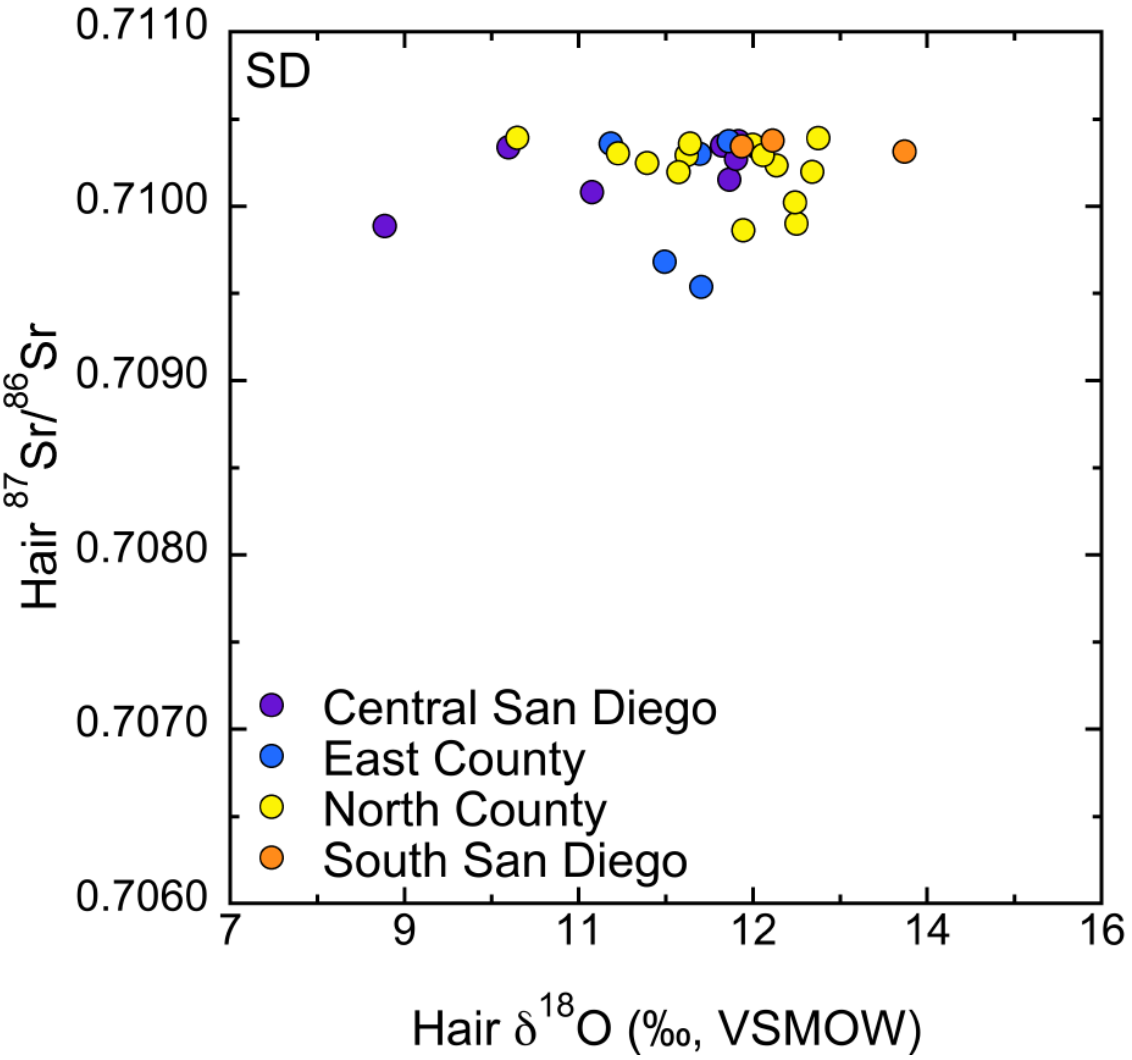

Figure 37. Cross-plot of the $^{87}Sr/^{86}Sr$ ratios and $\delta^{18}O$ values of hair from the San Diego-Carlsbad-San Marcos metropolitan area. Regions within the San Diego-Carlsbad-San Marcos metropolitan area are noted with colored symbols.

Table 16. Summary statistics for the oxygen, hydrogen, and strontium isotope ratios from water samples collected in the Salt Lake Valley Metropolitan Area.

Date	Statistic	$\delta^{18}O$ (‰, VSMOW)	$\delta^{2}H$ (‰, VSMOW)	$^{87}Sr/^{86}Sr$
Fall 2013	Mean	-16.1	-120	0.71098
	SD	0.6	3	0.00120
	Range	3.3	18	0.00484
	Min	-17.3	-127	0.70978
	Max	-14.0	-109	0.71462
	Count	42	42	42
Winter 2014	Mean	-16.1	-121	0.71077
	SD	1.2	6	0.00149
	Range	6.7	33	0.00556
	Min	-17.9	-128	0.70840
	Max	-11.2	-95	0.71395
	Count	142	142	57
Spring 2014	Mean	-15.9	-119	0.71093
	SD	1.0	5	0.00151
	Range	6.3	29	0.00586
	Min	-17.3	-125	0.70854
	Max	-11.0	-95	0.71440
	Count	64	64	64
Summer 2014	Mean	-15.7	-119	0.71082
	SD	0.8	4	0.00086
	Range	5.4	28	0.00358
	Min	-16.8	-124	0.70951
	Max	-11.5	-96	0.71309
	Count	41	41	41
Summer 2014	Mean	-15.7	-119	0.71054
	SD	0.7	4	0.00100
	Range	5.4	29	0.00546
	Min	-17.2	-128	0.70895
	Max	-11.8	-99	0.71441
	Count	55	55	55
Fall 2014	Mean	-15.7	-120	0.71070
	SD	0.5	3	0.00148
	Range	3.2	18	0.00718
	Min	-17.2	-129	0.70856
	Max	-14.0	-111	0.71573
	Count	39	39	39
Winter 2015	Mean	-15.9	-120	0.71046
	SD	0.4	2	0.00117
	Range	2.6	13	0.00619
	Min	-17.1	-128	0.70865
	Max	-14.6	-115	0.71484
	Count	39	39	39
Spring 2015	Mean	-15.5	-118	0.71102
	SD	0.8	4	0.00148
	Range	5.7	32	0.00655
	Min	-17.2	-130	0.70887
	Max	-11.5	-97	0.71542
	Count	55	55	55

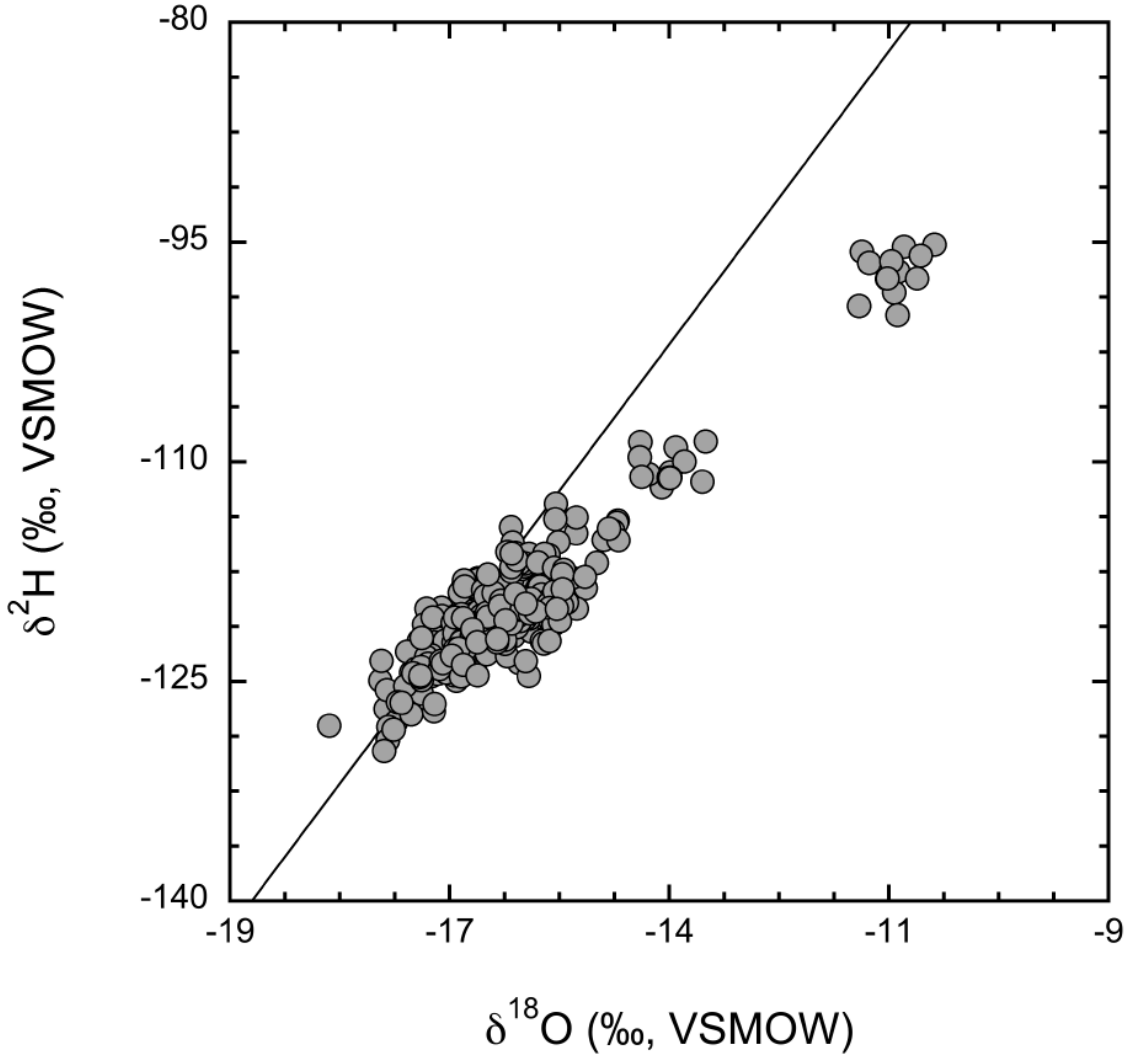

Figure 38. Cross-plot of the δ^2H and $\delta^{18}O$ values of tap water from the Salt Lake City metropolitan area. Meteoric water line is shown.

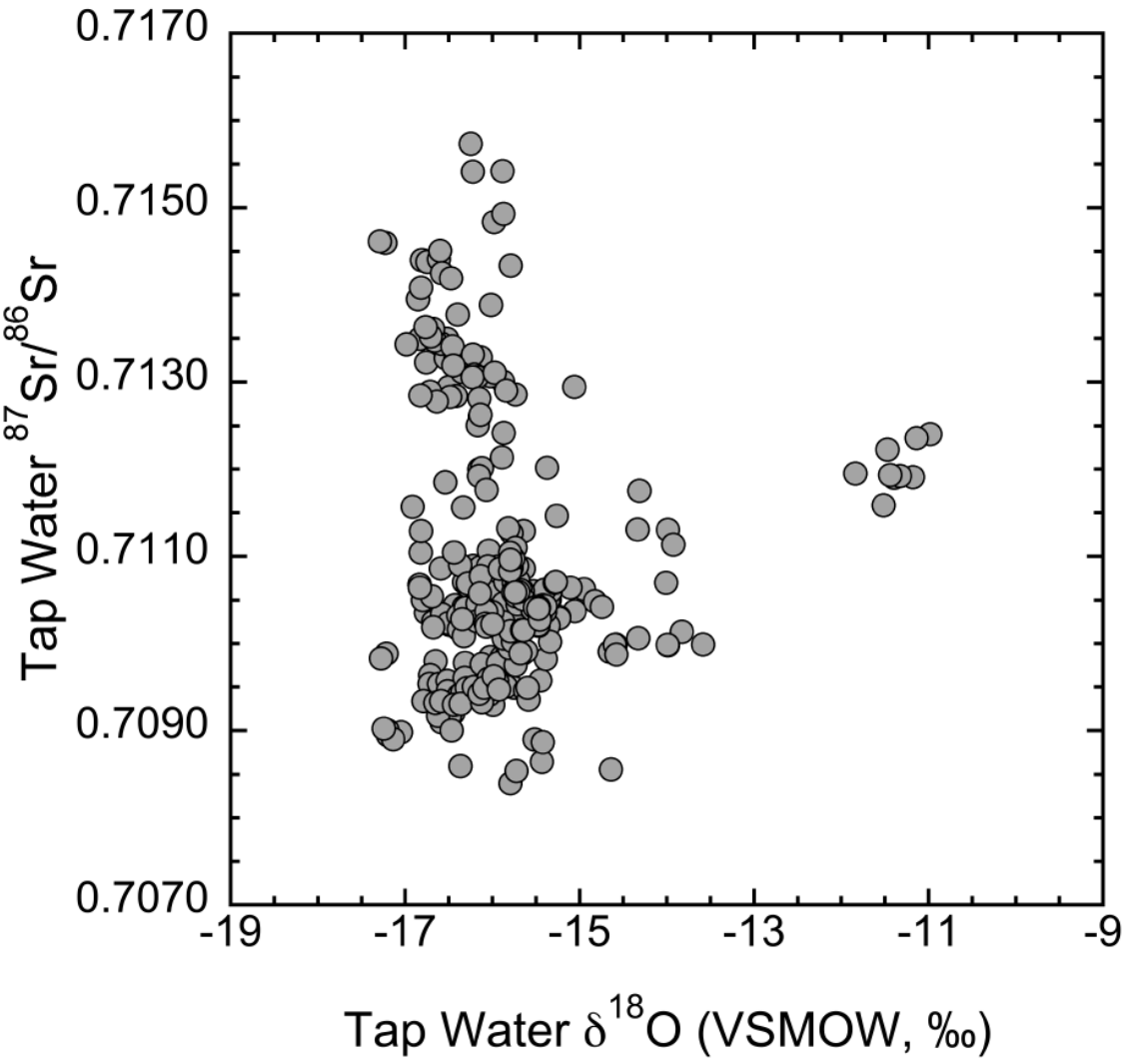

Figure 39. Cross-plot of the $^{87}Sr/^{86}Sr$ ratios and $\delta^{18}O$ values of tap water from the Salt Lake City metropolitan area.

Table 17. Water Districts in the Salt Lake City metropolitan area sampled and culinary water sources. Source information obtained from 2013/2014 water quality Consumer Confidence Reports.

Region	Metro Area	Geography	Water District	Water Sources				
Salt Lake Valley	Salt Lake City	Central	Granger-Hunter Improvement District	1	2*			
Salt Lake Valley	Salt Lake City	Central	Kearns Improvement District	1	2*			
Salt Lake Valley	Salt Lake City	Central	Midvale City Water System	1*	2			
Salt Lake Valley	Salt Lake City	Central	Murray City Water System	1				
Salt Lake Valley	Salt Lake City	Central	Taylorsville-Bennion Water Improvement District	1*	2			
Salt Lake Valley	Salt Lake City	Central	West Jordan City Water	1	2*			
Salt Lake Valley	Salt Lake City	North	Salt Lake City Corporation Culinary Water	1*	2	3		
Salt Lake Valley	Salt Lake City	South	Bluffdale Water System	2				
Salt Lake Valley	Salt Lake City	South	City of South Jordan	2				
Salt Lake Valley	Salt Lake City	South	Draper Irrigation Company (Water Pro)	2				
Salt Lake Valley	Salt Lake City	South	Riverton City Water System	1	2			
Salt Lake Valley	Salt Lake City	South	Sandy City Corporation Water	1*	2	3		
Salt Lake Valley	Salt Lake City	South	White City Water Improvement District	1				
Salt Lake Valley	Salt Lake City	West	Magna Water Improvement District	1	2*			

1. Groundwater; 2. Jordan Valley Conservation District; 3. Metro SLC

* Indicates source that contributes greater than 75%

Table 18. Summary statistics for the oxygen, hydrogen, and strontium isotope ratios from hair samples collected in the Salt Lake Valley Metropolitan Area.

Date	Statistic	$\delta^{18}O$ (‰, VSMOW)	$\delta^{2}H$ (‰, VSMOW)	$^{87}Sr/^{86}Sr$
Winter 2014	Mean	9.3	-102	0.71053
	SD	1.4	9	0.00109
	Range	4.9	34	0.00367
	Min	6.9	-122	0.70945
	Max	11.8	-88	0.71312
	Count	23	23	12
Spring 2014	Mean	9.8	-94	0.71096
	SD	1.7	11	0.00100
	Range	6.2	41	0.00301
	Min	6.5	-114	0.70941
	Max	12.7	-73	0.71241
	Count	11	11	11
Summer 2014	Mean	9.5	-98	0.71063
	SD	1.3	8	0.00091
	Range	6.0	40	0.00455
	Min	6.0	-120	0.70944
	Max	12.0	-80	0.71399
	Count	48	48	48
Spring 2015	Mean	9.1	-98	–
	SD	1.2	8	–
	Range	6.1	44	–
	Min	6.2	-128	–
	Max	12.3	-85	–
	Count	48	48	0

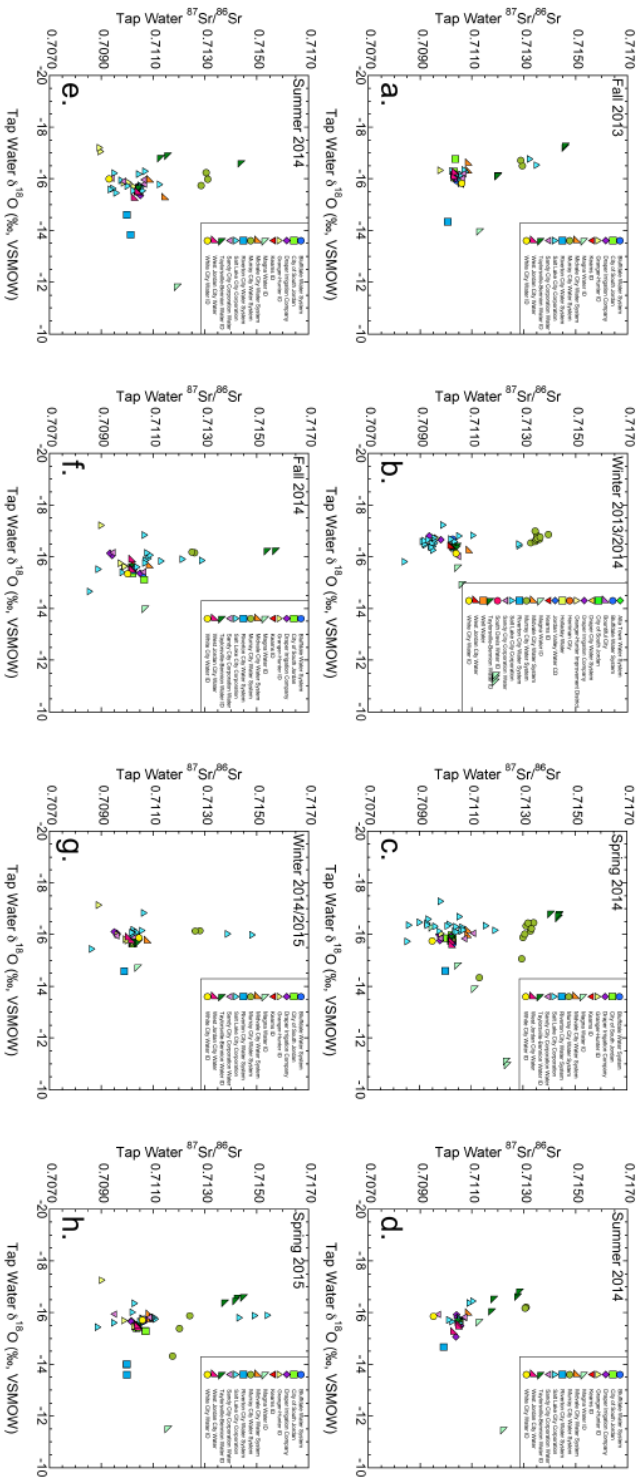

Figure 40. Cross-plots of the $^{87}Sr/^{86}Sr$ ratios and $\delta^{18}O$ values of tap water from the Salt Lake City metropolitan area. Each plot shows data from the stated season. Colored symbols represent the water management districts.

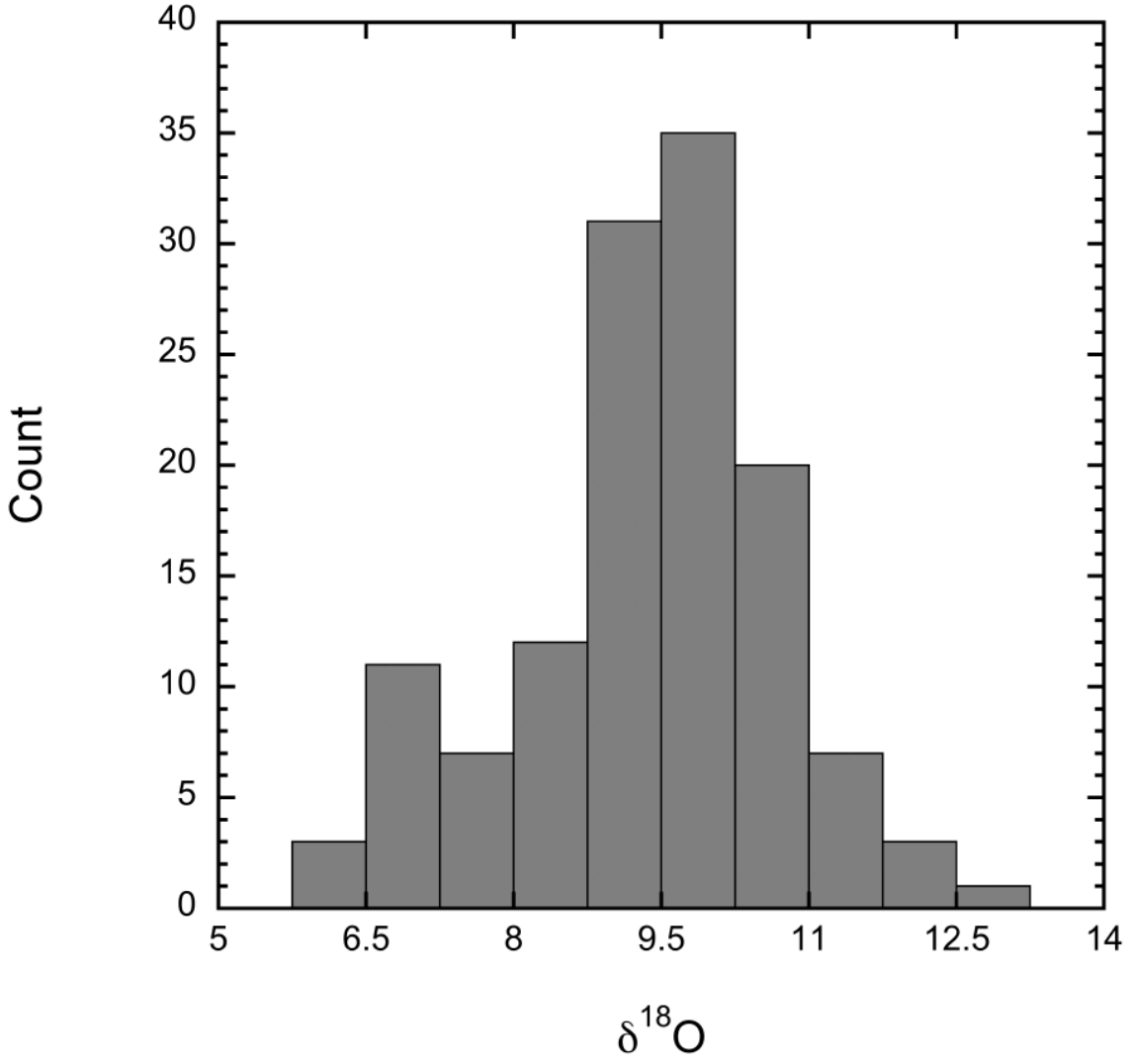

Figure 41. Histogram of the $\delta^{18}O$ values of hair collected in the Salt Lake City metropolitan area.

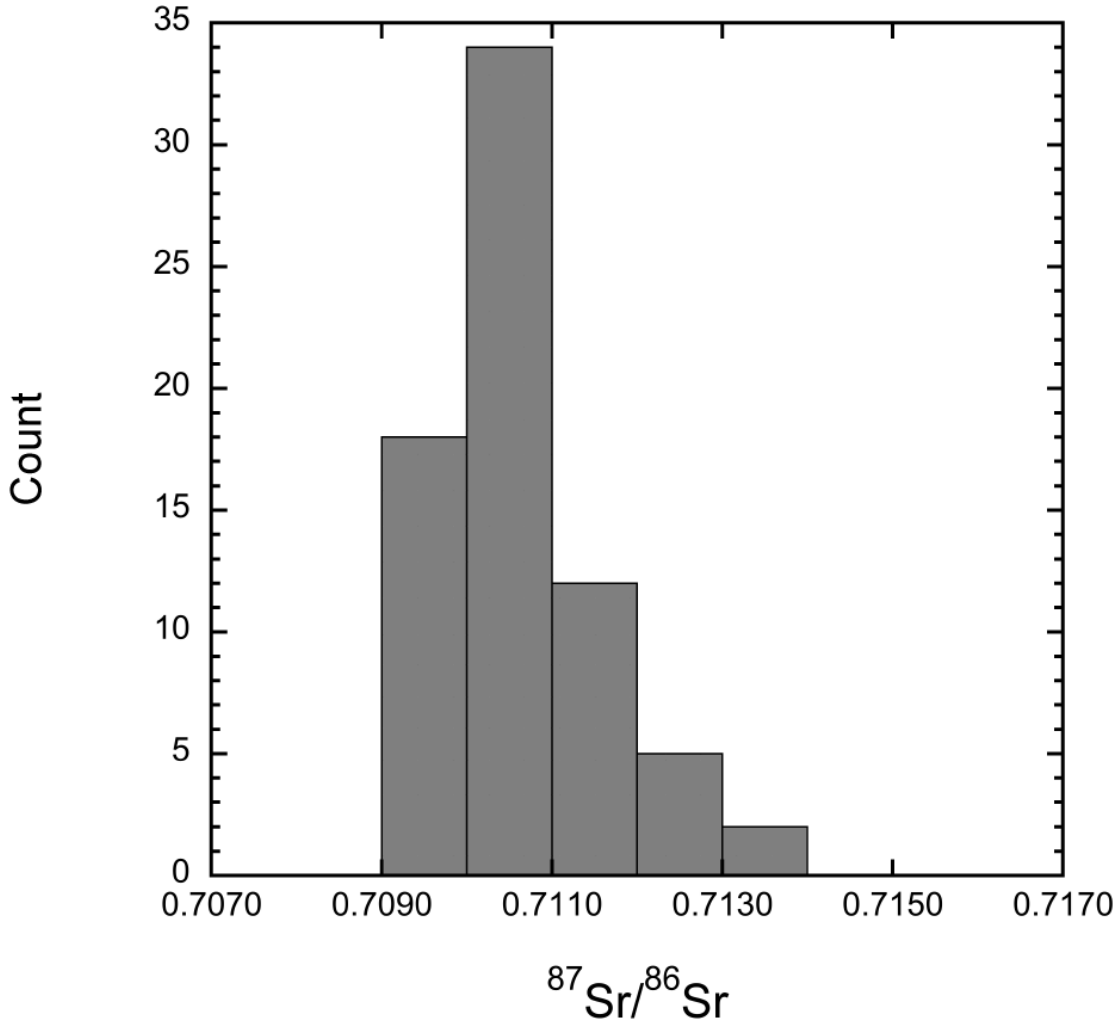

Figure 42. Histogram of the $^{87}Sr/^{86}Sr$ ratios of hair collected in the Salt Lake City metropolitan area.

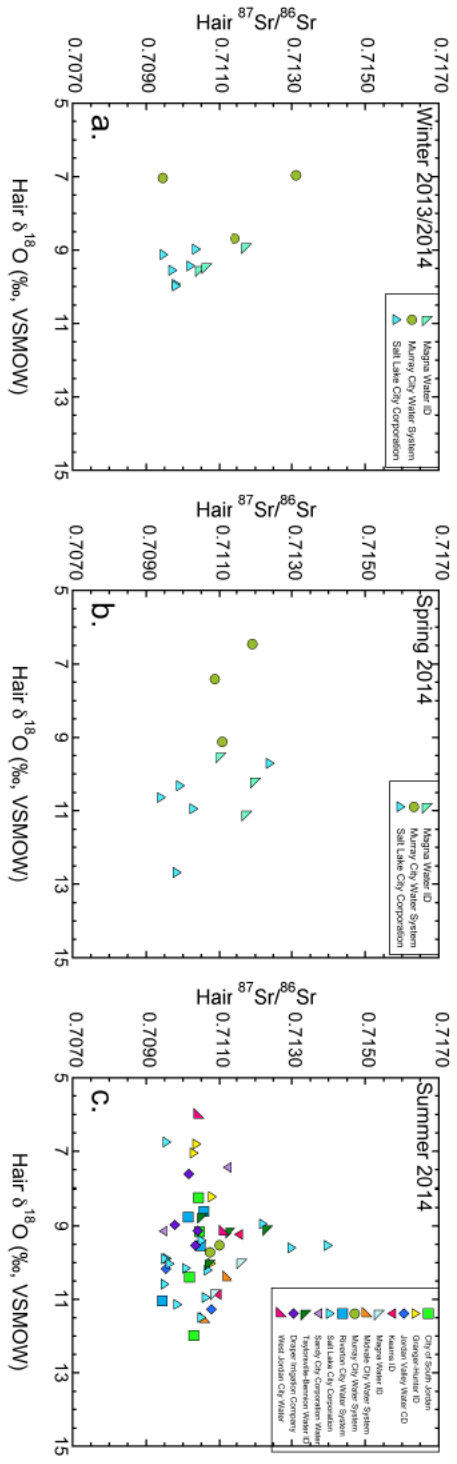

Figure 43. Cross-plots of the $^{87}Sr/^{86}Sr$ ratios and $\delta^{18}O$ values of hair from the Salt Lake City metropolitan area. Each plot shows data from the stated date. Colored symbols represent the water management districts.

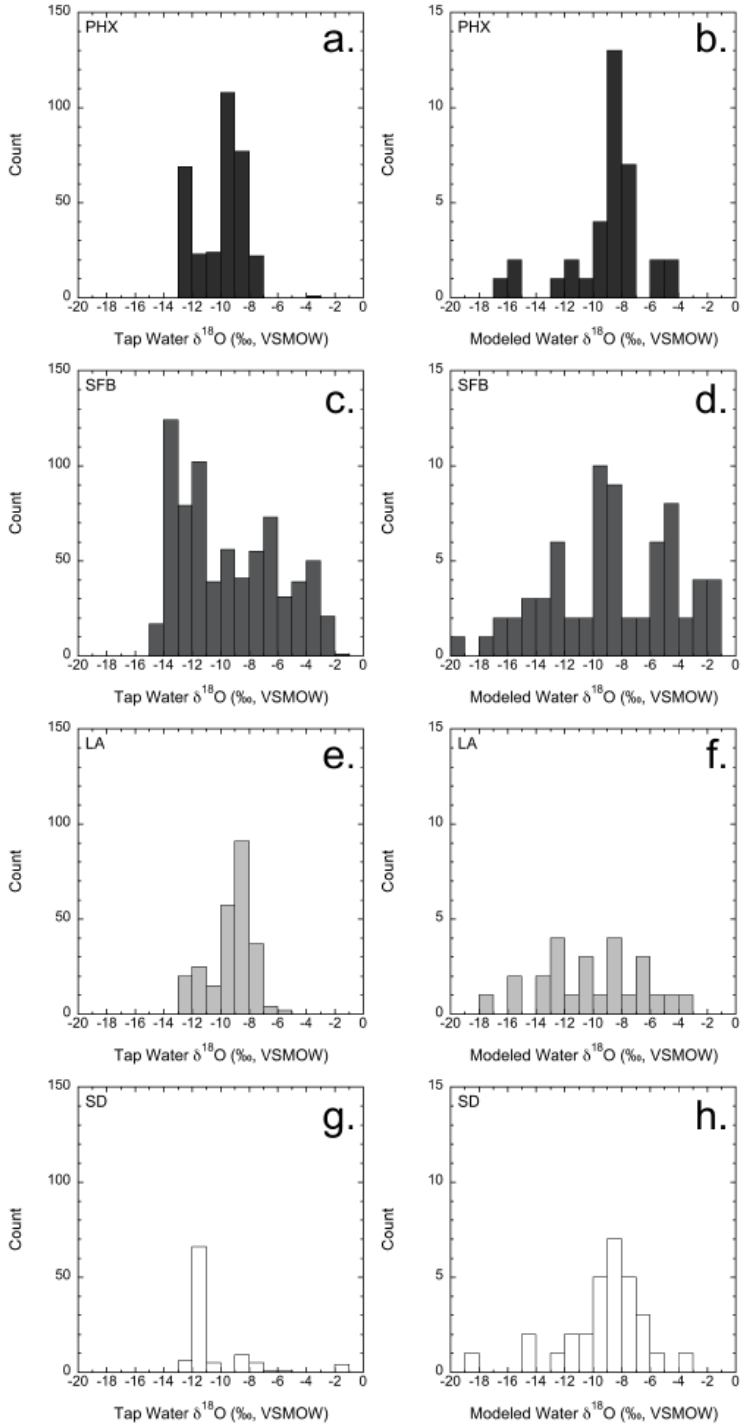

Figure 44. Histograms of the measured (left) and modeled (right) $\delta^{18}O$ values of tap water from the Phoenix-Mesa-Glendale (PHX, panels a and b)), San Francisco-Oakland-Fremont and San Jose-Sunnyvale-Santa Clara (SFB, panels c and d), Los Angeles-Long Beach-Santa Ana and Riverside-San Bernardino-Ontario (LA, panels e and f), and San Diego-Carlsbad-San Marcos (SD, panels g and h) metropolitan areas.

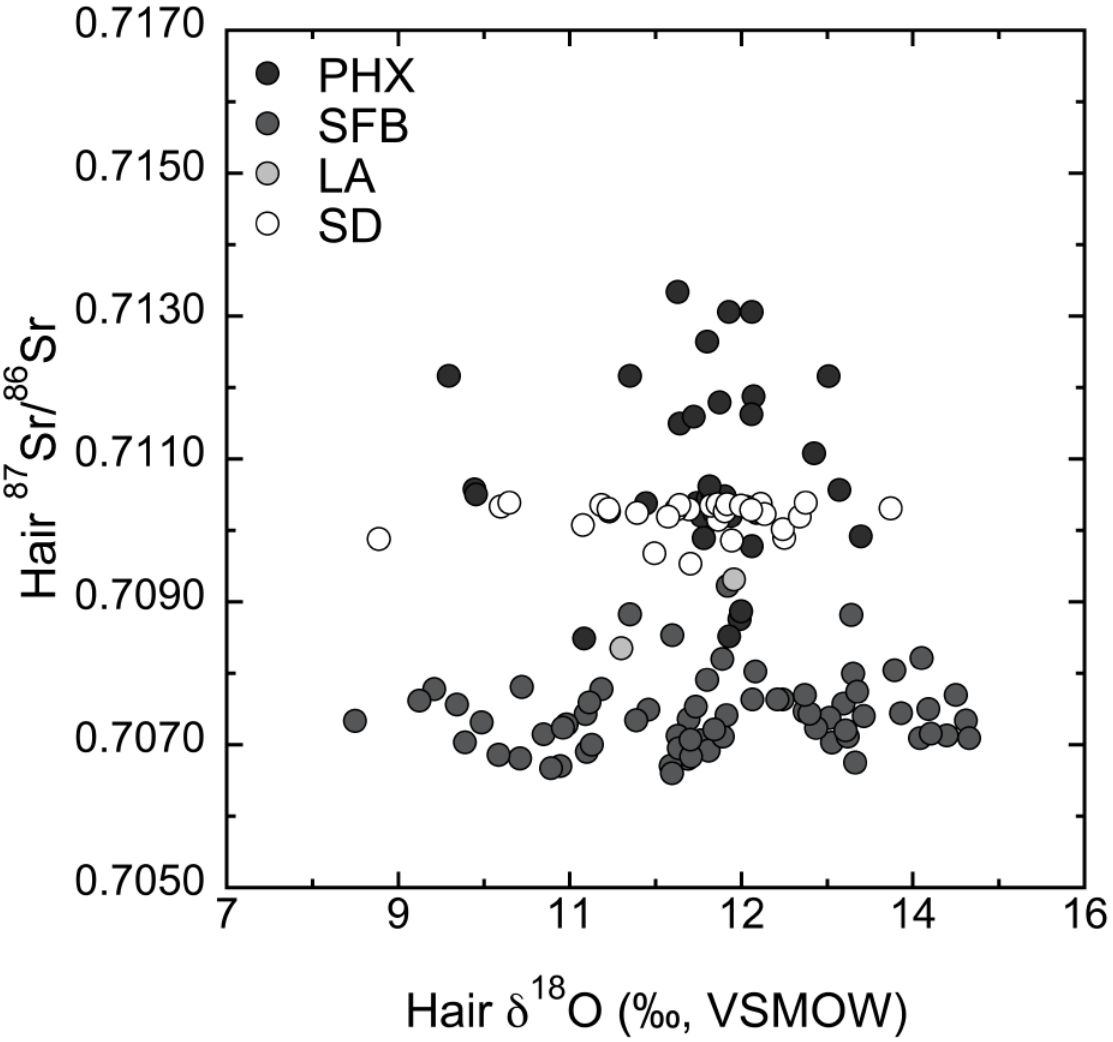

Figure 45. Cross-plot of the $^{87}Sr/^{86}Sr$ ratios and $\delta^{18}O$ values of hair from the Phoenix-Mesa-Glendale (PHX), San Francisco-Oakland-Fremont and San Jose-Sunnyvale-Santa Clara (SFB), Los Angeles-Long Beach-Santa Ana and Riverside-San Bernardino-Ontario (LA), and San Diego-Carlsbad-San Marcos (SD) metropolitan areas.

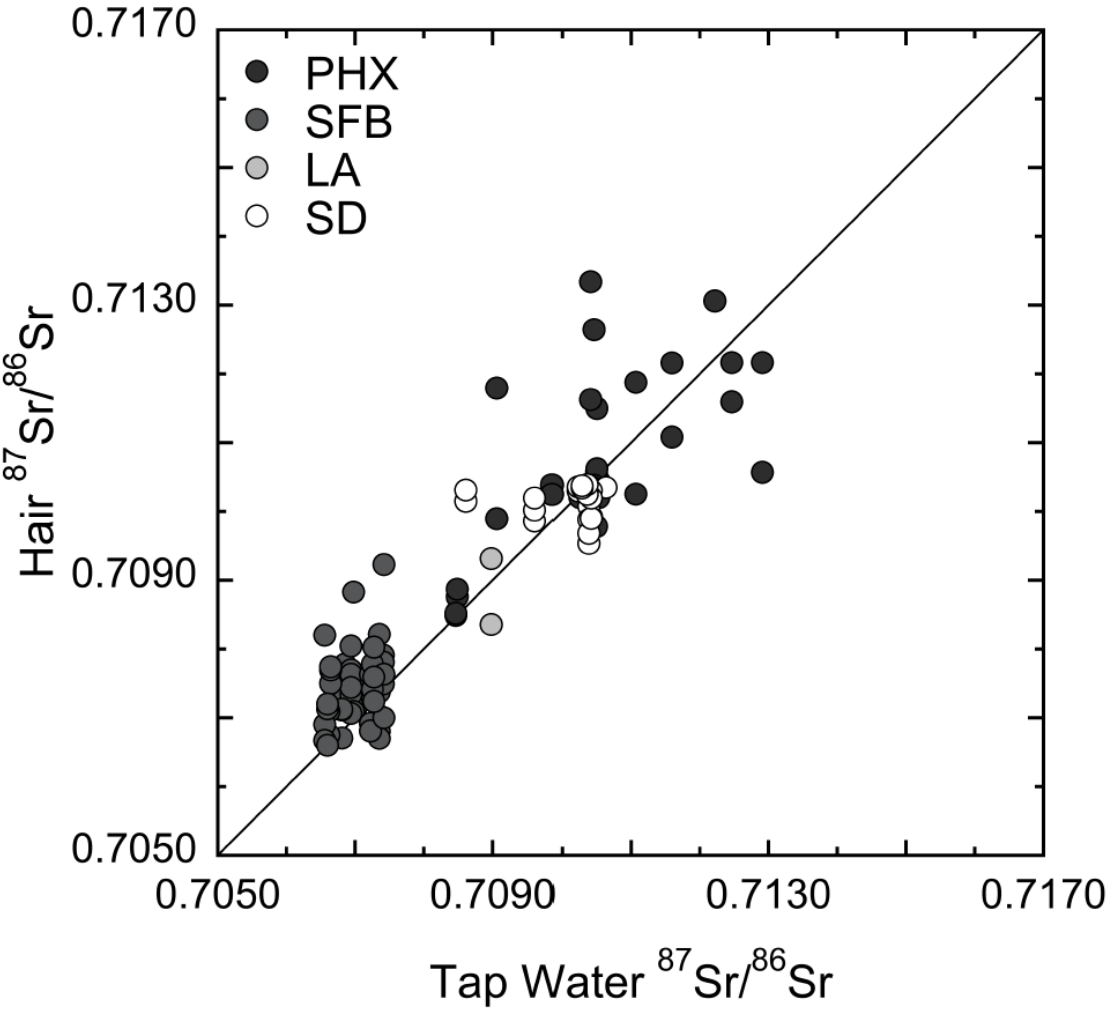

Figure 46. Cross-plot of the $^{87}Sr/^{86}Sr$ ratios of hair and tap water from the Phoenix-Mesa-Glendale (PHX), San Francisco-Oakland-Fremont and San Jose-Sunnyvale-Santa Clara (SFB), Los Angeles-Long Beach-Santa Ana and Riverside-San Bernardino-Ontario (LA), and San Diego-Carlsbad-San Marcos (SD) metropolitan areas.

References

Beard, B. L., and C. M. Johnson. 2000. Strontium isotope composition of skeletal material can determine the birth place and geographic mobility of humans and animals. Journal of Forensic Sciences **45**:1049-1061.

Bentley, R. A., T. D. Price, J. Luning, D. Gronenborn, J. Wahl, and P. D. Fullagar. 2002. Prehistoric Migration in Europe: Strontium Isotope Analysis of Early Neolithic Skeletons. Current Anthropology **43**:799-804.

Britton, K., V. Grimes, J. Dau, and M. P. Richards. 2009. Reconstructing faunal migrations using intra-tooth sampling and strontium and oxygen isotope analyses: a case study of modern caribou (Rangifer tarandus granti). Journal of Archaeological Science **36**:1163-1172.

Chenery, C., G. Muldner, J. Evans, H. Eckardt, and M. Lewis. 2010. Strontium and stable isotope evidence for diet and mobility in Roman Gloucester, UK. Journal of Archaeological Science **37**:150-163.

Chittleborough, G. 1980. A chemist's view of the analysis of human hair for trace elements. Science of the Total Environment **14**:53-75.

Druyan, M. E., D. Bass, R. Puchyr, K. Urek, D. Quig, E. Harmon, and W. Marquardt. 1998. Determination of reference ranges for elements in human scalp hair. Biological Trace Element Research **62**:183-198.

English, N. B., J. L. Betancourt, J. S. Dean, and J. Quade. 2001. Strontium isotopes reveal distant sources of architectural timber in Chaco Canyon, New Mexico. Proceedings of the National Academy of Science **95**:11891-11896.

Faure, G. 1977. Principles of Isotope Geology. 2nd edition. Wiley, New York.

Franke, B. M., S. Koslitz, F. Micaux, U. Piantini, V. Maury, E. Pfammater, S. Wunderli, G. Gremaud, J.-O. Bosset, R. Hadorn, and M. Kreuzer. 2007. Tracing the geographic origin of poultry meat and dried beef with oxygen and strontium isotope ratios. European Food Research and Technology.

Gellein, K., S. Lierhagen, P. S. Brevik, M. Teigen, P. Kaur, T. Singh, T. P. Flaten, and T. Syversen. 2008. Trace Element Profiles in Single Strands of Human Hair Determined by HR-ICP-MS. Biological Trace Element Research **123**:250-260.

Juarez, C. A. 2008. Strontium and Geolocation, the Pathway to Identification for Deceased Undocumented Mexican Border-Crossers: A Preliminary Report. Journal of Forensic Sciences **53**:46-49.

Knudson, K., J., S. R. Williams, R. Osborn, K. Forgey, and P. R. Williams. 2009. The geographic origins of Nasca trophy heads using strontium, oxygen, and carbon isotope data. Journal of Anthropological Archaeology **28**:244-257.

Lewis, M. E., and G. N. Rutty. 2003. The endangered child: the personal identification of children in forensic anthropology. Forensic Anthropology **43**:201-209.

Montgomery, J., J. A. Evans, and G. Wildman. 2006. 87Sr/86Sr isotope composition of bottled British mineral waters for environmental and forensic purposes. Applied Geochemistry **21**:1626-1634.

Nehlich, O., J. Montgomery, J. Evans, S. Schade-Lindig, S. L. Pichler, M. P. Richards, and K. W. Alt. 2009. Mobility or migration: a case study from the Neolithic settlement of Nieder-Morlen (Hessen, Germany). Journal of Archaeological Science **36**:1791-1799.

Perry, M. A., D. Coleman, and N. Delhopital. 2008. Mobility and Exile at 2nd Century A.D. Khirbet edh-Dharih: Strontium Isotope Analysis of Human Migration in Western Jordan. Geoarchaeology **23**:528-549.

Price, T. D., J. H. Burton, and J. B. Stoltman. 2007. Place of Origin of Prehistoric Inhabitants of Aztalan, Jefferson Co., Wisconsin. American Antiquity **72**:524-538.

Radloff, F. G. T., L. Mucina, W. J. Bond, and P. J. le Roux. 2010. Strontium isotope analyses of large herbivore habitat use in the Cape Fynbos region of South Africa. Oecologia **164**:567-578.

Rauch, E., S. Rummel, C. Lehn, and A. Buttner. 2007. Origin assignment of unidentified corpses by use of stable isotope ratios of light (bio-) and heavy (geo-) elements—A case report. Forensic Science International **168**:215-218.

Reynolds, A. C., J. L. Betancourt, J. Quade, P. J. Patchett, J. S. Dean, and J. Stein. 2005. 87Sr/86Sr sourcing of ponderosa pine used in Anasazi great house construction at Chaco Canyon, New Mexico. Journal of Archaeological Science **32**:1061-1075.

Richards, M., K. Harvarti, V. Grimes, C. Smith, T. Smith, J.-J. Hublin, P. Karkanas, and E. Panagopoulou. 2008. Strontium isotope evidence of Neanderthal mobility at the site of Lakonis, Greece using laser-ablation PIMMS. Journal of Archaeological Science **35**:1251-1256.

Rodrigues, C. I., C. Maguas, and T. Prohaska. 2010. Strontium and oxygen isotope fingerprinting of green coffee beans and its potential to proof authenticity of coffee. European Food Research and Technology.

Rosner, M. 2010. Geochemical and instrumental fundamentals for accurate and precise strontium isotope data of food samples: Comment on ‘‘Determination of the strontium isotope ratio by ICP-MS ginseng as a tracer of regional origin” (Choi et al., 2008). Food Chemistry **121**:918-921.

Sellick, M. J., T. K. Kyser, M. B. Wunder, D. Chipley, and D. R. Norris. 2009. Geographic Variation of Strontium and Hydrogen Isotopes in Avian Tissue: Implications for Tracking Migration and Dispersal. PLoS ONE **4**:e4735.

Voerkelius, S., G. D. Lorenz, S. Rummel, C. R. Quetel, G. Heiss, M. Baxter, C. Brach-Papa, P. Deters-Itzelsberger, S. Hoelzl, J. Hoogewerff, E. Ponzevera, M. Van Bocxstaele, and H. Ueckermann. 2010. Strontium isotopic signatures of natural mineral waters, the reference to a simple geological map and its potential for authentication of food. Food Chemistry **118**:933-940.

von Carnap-Bornheim, C., M.-L. Nosch, G. Grupe, A.-M. Mekota, and M. M. Schweissing. 2007. Stable strontium isotopic ratios from archaeological organic remains from the Thorsberg peat bog. Rapid Communications in Mass Spectrometry **21**:1541-1545.

West, J. B., J. M. Hurley, F. O. Dudas, and J. R. Ehleringer. 2009. The Stable Isotope Ratios of Marijuana. II. Strontium Isotopes Relate to Geographic Origin. Journal of Forensic Sciences **54**:1261-1269.